NORTHWESTERN UNIVERSITY

Requirement of the Caspase-3 Homologue DrICE in *Drosophila* Tracheal Size Control

A DISSERTATION

SUBMITTED TO THE GRADUATE SCHOOL
IN PARTIAL FULFILLMENT OF THE REQUIREMENTS

for the degree of

DOCTOR OF PHILOSOPHY

Field of Interdisciplinary Biological Sciences (IBiS)

By

Saoirse S. McSharry

EVANSTON, ILLINOIS

June 2019

ABSTRACT

Requirement of the Caspase-3 Homologue DrICE in *Drosophila* Tracheal Size Control

Saoirse S. McSharry

Proper size control of organs and tissues is critical to their function, and it is necessary for the millions of precisely sized tubes that make up those organs— for example, excessive cell growth can lead to devastating diseases such as Polycystic Kidney Disease. The regulation of tube growth is therefore essential to organismal health. Many key molecular pathways are known to control aspects of growth through managing a desirable balance between cell division and cell death. In this work, I describe a novel feature of this management whereby a protein known for executing cell death, DrICE, is required for the proper lengthening of an epithelial tube in *Drosophila*, the trachea, but it does so without causing apoptosis.

In Chapter 2, I describe a novel mechanism by which DrICE, a component of cell death machinery, is required for proper tracheal size control in the fruit fly *Drosophila melanogaster*. Although well known for its role in apoptosis, DrICE, an executioner caspase, has a non-apoptotic function that is required for elongation of the epithelial tubes of the *Drosophila* tracheal system. I show that DrICE acts downstream of the Hippo Network to regulate endocytic trafficking of at least seven cell polarity, cell junction and apical extracellular matrix proteins involved in tracheal tube size control. I further show that tracheal cells are competent to undergo apoptosis, even though developmentally-regulated DrICE function rarely kills tracheal cells. My results reveal a novel developmental role for caspases, a previously unidentified pool of DrICE that colocalizes with endocytic markers, and a mechanism by which the Hippo Network controls endocytic trafficking. Given published reports of *in vitro* regulation of endocytosis by mammalian caspases during apoptosis, I propose that caspase-mediated regulation of endocytic trafficking is an evolutionarily conserved function of caspases that can be deployed during morphogenesis.

In Chapter 3, I explore the results of the candidate approach for caspase substrate identification, in which I probed the Sterol Regulatory Element Binding Protein (SREBP) as a potential tracheal-elongating substrate of DrICE. A series of epistasis experiments with new transgenic and CRISPR alleles of dSREBP shows that DrICE may cleave and activate dSREBP in the trachea. I show that overexpression of the canonical S2P-processed form of dSREBP is lethal to tracheal cells, and that our new CRISPR-mediated loss-of-function allele, $dSREBP^{\Delta ORF}$, causes dramatic synthetic lethality when combined with $yorkie^{B5}$ and $DrICE^{17}$ mutant alleles. I also demonstrate that $dSREBP^{\Delta ORF}$ has the same epistatic relationships with septate junction loss-of-function alleles as $DrICE^{17}$, which is consistent with a model in which there is interplay between dSREBP and DrICE. The exact molecular mechanism of the relationship between DrICE and lipid levels is complex and remains to be elucidated. Clarifying this relationship, however, could have important consequences for our understanding of the interactions between lipid metabolism, apoptosis, and disease.

ACKNOWLEDGEMENTS

I would like to thank my advisor, **Greg Beitel** for providing six years of mentorship in the forms of optimism ("Trust your data!"), enthusiasm ("YOUZZA!"), crazy anecdotes, dad jokes, and gentle guidance. Greg, your inquisitive nature, precisely-calculated experimental philosophy, and generous support are what drew me to your lab in the first place, and you have always been an inspiration to me. You helped me grow as a scientist, and I'll always be grateful to you for everything from your cheerful disposition, to coming with me to conferences, to your boundless patience with me as I learned. To the members of my thesis committee, **Rich Carthew**, **Laura Lackner, Eric Weiss**, and **Shelby Blythe**: thank you for your brilliant ideas and recommendations, and more importantly for your encouragement. In the times when none of my experiments seemed to work, I would have given up in frustration were it not for your guidance, strength, and reassurance. Thank you all for guiding me through this wild process!

I would also like to thank my *extremely*-soon-to-be husband, **Ed Goncz**, for his seemingly endless supply of patience, support, sandwiches, and board games to help me through this similarly endless endeavor. I remember years ago, at his defense, Kyle remarked how he wouldn't have been able to graduate without his wife—he would come home at the end of his days and say, "that's it, I just can't do this anymore," and she would look right back at him and said "yes you can!", which gave him the strength and courage to carry on. I could not possibly identify more. I always dreamed of getting a PhD, and despite my years of tech experience before I started, nothing could have prepared me for how challenging it would be. I would have never made it here without your support. Through your sense of humor, kindness, positivity, trust in me, love, and delicious cooking, you helped me discover and foster my own strength and resilience. It's because of you that I was able to follow through on my dream— thank you, from the bottom of my heart. I would also like to thank my in-laws **Ed, Julie, Paula, AJ, Caleb, and Lauren** for their love and support.

And to my *incredibly* strong, loving, and compassionate friends, with many of whom I crossed paths at Northwestern University, **Dr. Amanda Bayer, Josh Schubring, Dr. Lauren Kraft, Dr. Aaron Peters, Amy and Alex Escatel**: I'm sorry for drinking so much of your wine.

Dedicated to my mentors, especially:

Dr. Sundram Sujakumar

&

Dr. Gene Kim,

who made me believe I could be a scientist.

TABLE OF CONTENTS

LIST OF TABLES AND FIGURES

CHAPTER 3:
Sterol Regulatory Element Binding Protein as a putative target of DrICE

APPENDICES

CHAPTER 1: INTRODUCTION TO TUBE SIZE CONTROL

I. Impact of size control on human disease

Size of the body is no mere accident.

–D'Arcy Thompson, On Growth and Form. 1917

It's hard to imagine that we are each derived from a single cell: a fertilized egg, measuring a mere 0.1mm, or 0.004 inches, in diameter. Through the marvelous processes of embryonic development, childhood, and adolescence, humans grow multiple orders of magnitude such that the average man is 1,700 mm, or roughly 70 inches, tall. Though this remodeling is extensive, it is robust in its precision; human size consistently falls within a bell curve, with our bodily proportions remaining intact. This is a truly miraculous occurrence! How do our bodies inherently possess the ability to grow by multiple orders of magnitude— beginning from the size of a fertilized egg to the predictable size of an adult— and then stop growing? Furthermore, how has evolution directed the development of all multicellular organisms such that the proportions of the body plan are maintained, with each organ reaching only the size that ensures optimal function?

Near the turn of the century, mathematicians and biologists like D'Arcy Thompson asked similar questions about the mechanisms by which organismal size and shape were determined. Just a few decades before Thompson's *On Growth and Form*, Charles Darwin had published *On the Origin of Species* in 1859, and implied that the sizes of animals—among other properties— could be determined by natural selection. Although many people expressed incredulity or even took umbrage at the implication that humans shared common ancestry with animals, we now know that Darwin was correct. Indeed, innovative technological advances of the 20th century have given rise to a massive spike in human knowledge that has permitted modern scientists to probe the natural world for answers.

The spike in research and experimentation of the 20th century gave rise to massive discoveries about body plans in evolution. For example, in 1995, Ed Lewis, Christiane Nüsslein-Volhard and Eric Wieschaus were awarded the Nobel Prize in Physiology or Medicine for their identification and classification of the *Homeobox*, or *Hox*, genes, which give rise to the "master regulator" transcription factors that ultimately specify the common body plan of all animals. This elegant evolutionary wonder explains why all species have tops and bottoms, heads and feet, and so on. What the *Hox* genes fail to explain, however, is what drives the specificity of tissue size within that body plan. This curiosity—uncovering the molecular mechanisms of tissue size— is not only worthwhile for waxing philosophical at cocktail parties, but because we now know that failure of proper cell and tissue growth underlie many intractable human diseases.

One particular problem in understanding organismal size control is the regulation of tube dimensions. Many organs are comprised of networks of epithelial tubes that are essential for the exchange of nutrients, gases, and waste between the environment and the body. For example, the nephrons of the kidney enable blood filtration, while the bronchi of the lung facilitate respiration. It is absolutely necessary that these tubes are precisely sized. [6] Without proper control of biological tube size, organ and vascular function can be devastated, which can lead to debilitating diseases such as polycystic kidney disease (PKD), cerebral cavernous malformations (CCM), ischemia, renal cysts & diabetes syndrome, and others. [7-10]

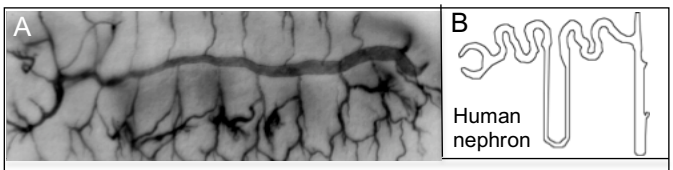

Figure 1.1 The *Drosophila* trachea as a model for morphogenesis and maintenance of epithelial tubes. (A) In *Drosophila*, epithelial tubes of characteristic sizes form a network in a late-stage embryo[3]. (B) Schematic of human nephron from the kidney, which, like the trachea, has precisely regulated tube dimensions.

In this introductory chapter, I describe Polycystic Kidney Disease, an example of a disease of tube size control in humans, and I give examples of how model organisms *Drosophila* and *C. elegans* have contributed to our knowledge of the molecular mechanisms that govern tube size. Because this project was predicated on evidence from the Beitel lab published in 2014 that indicated that the notorious growth-controlling Hippo Network may play a role in size control of the *Drosophila* tracheal system, this chapter will

next delve into the details of known complex mechanisms of Hippo Network-mediated growth control which may ultimately act upstream of tracheal size control. (Figure 1.1)

In Chapter 2, I report the characterization of the caspase DrICE as a modifier of intracellular trafficking in the trachea as it acts downstream of the Hippo Network. I begin by providing additional background on caspase function as it relates to cell death and to newly discovered non-apoptotic processes. This chapter will then offer a detailed description of my experiments showing that DrICE controls tracheal elongation downstream of the Hippo Network, that it is necessary and sufficient for tracheal elongation, and also necessary for tracheal cell death. I also provide evidence that DrICE localizes to discrete cytosolic punctae enriched at the apical surface where it associates with compartments marked by Clathrin, and furthermore that DrICE alters trafficking of select yet diverse tracheal size determining cargo. Finally, I expand upon my published findings to describe a putative mechanism by which DrICE is involved in endocytosis through an interaction with Clathrin adaptor protein Adaptin (AP47).

In Chapter 3, I explore the results of the candidate approach for caspase substrate identification, in which I investigated the Sterol Regulatory Element Binding Protein (SREBP) as a potential tracheal-elongating substrate of DrICE. A series of epistasis experiments with new transgenic and CRISPR alleles of dSREBP shows that DrICE may cleave and activate dSREBP in the trachea, which supports evidence at the organismal level presented by Amarneh et al in 2009.[11] I show that overexpression of the canonical S2P-processed form of dSREBP is lethal in tracheal cells, and that our new CRISPR-mediated loss-of-function allele, $dSREBP^{\Delta ORF}$, causes dramatic synthetic lethality when combined with $yorkie^{B5}$ and $DrICE^{17}$ mutant alleles. I also demonstrate that $dSREBP^{\Delta ORF}$ has the same epistatic relationships with septate junction loss-of-function alleles as $DrICE^{17}$, which supports a model in which there is interplay between dSREBP and DrICE functions. The exact molecular mechanism of the relationship between the DrICE and lipid levels is complex and remains to be elucidated. Clarifying this relationship, however, could have important consequences for our understanding of the interactions between lipid metabolism, apoptosis, and disease.

Tube size control mechanisms in mammals

There are many diverse epithelial tubes in mammalian organ systems, and the size of each tube must be precisely regulated in order to ensure its function. Given studies in mammalian model systems, however, we now know comparatively more about the molecular mechanisms that govern the morphogenesis of various vertebrate tubes.

For example, the mammalian lung is a complex organ in which various cell types work together to coordinate efficient exchange of carbon dioxide and oxygen while also warding off infection. The alveoli themselves are comprised of epithelia, smooth muscle, and surfactant-secreting cells, among others.[12] The morphogenesis of the lung begins very early in embryonic development: the lung bud first forms from the ventral foregut at mouse E9.5; the small tube continues to grow, bud, and bifurcate, eventually forming new tree-like branches: domain branching and bifurcation of bronchi give rise to bronchioles, from which the future alveoli, called “terminal sacs”, sprout. Even after birth, the lung continues to develop as the alveoli expand, developing enlarged surface areas through the process of septation. [13, 14] As with *Drosophila* tracheal morphogenesis, the extended process of lung development involves great amounts of cell shape change and migration, which necessitates significant changes in cell adhesion.

The molecular mechanisms of lung development share some common features with that of tracheal morphogenesis, notably the use of Fgf signaling to facilitate migration and branching. For example, in murine lung development, *Fgf9* is required in the early stages of morphogenesis, where it acts upstream of Wnt factors to regulate cell proliferation, branching, and expansion; *fgf9* loss of function embryos have hypoplasia, smaller lungs caused by reduced branching and proliferation. [15, 16] In *Drosophila*, one of the most important factors in early tracheal development is the FGF homolog Branchless, which acts as a

chemoattractant by binding to its respective RTK, Breathless, in order to mediate the migration of tracheal cells to form the dorsal trunk.[17, 18]

Determination and maintenance of tube size control is so critical that failure to do so can result in severe disease. For example, one disease caused by failure of tube size control is Polycystic Kidney Disease (PKD). In PKD, overproliferated and inflamed nephrons secrete excess fluid, causing cystic tubes and severely impaired kidney function. [19] The autosomal dominant form of PKD alone affects nearly 6 million people in the world, but this figure does not fully encompass the deadly nature of the disease [9].

In the mid-1990s, mutations in the polycystin genes *PKD1/2* were identified as the genetic causes of PKD; the exact mechanisms by which nonfunctional polycystins contribute to PKD are incompletely understood. The mammoth polycystin proteins PC1 and PC2, encoded by the genes *PKD1/2* respectively, have been implicated in regulating calcium signaling in the primary cilia and in the endoplasmic reticulum (ER). [20, 21] The polycystins are transmembrane proteins (PC1, also known as fibrocystin/ polyductin is a massive putative adhesion G-protein coupled receptor, and PC2 is a cation channel) that form a complex within the cilia of renal cells [22]. PC1 and PC2 have been found to associate with, and potentially regulate the function of one another in mediating intracellular calcium release in response to shear stress or stretching, which normally occurs in the process of cilia-mediated flow-sensing. [23, 24] In the absence of functional polycystins, intracellular calcium levels fall, leading to a disruption in cAMP and purinergic signaling, which are also required for shear stress signal transduction. [25] It is unclear how exactly this leads to polycystic kidneys, though a recent model suggests that it is due to hypersensitivity of the distal nephron to the anti-diuretic hormone vasopressin. [26] In the rare case of inheritance of two copies of the autosomal dominant allele of PC1, either termination of pregnancy or neonatal death can result from failure of the fetal kidneys to produce amniotic fluid, which is in turn required for proper alveolar expansion and neonatal respiration. [27, 28] PKD ultimately results in end-stage renal failure that can be abated only by transplant. [29] The autosomal dominant form of PKD (ADPKD) alone accounts for almost 5% of all kidney transplant patients. [9, 10] As patients await transplant, they must receive regular kidney dialysis or, more recently, drugs that slow—but

do not prevent— disease progression.

Additional knowledge about the molecular mechanisms that govern the size of tubes in the body could facilitate the advent of more effective therapeutics for currently incurable diseases like PKD. In fact, last year the FDA approved the very first drug for PKD treatment, Tolvaptan. The drug, from Japanese company Otsuka Pharmaceuticals, acts as a vasopressin receptor antagonist. [29, 30] While Tolvaptan has been successful in slowing the progression of renal disease, it has significant side effects including liver toxicity—indeed, a major roadblock in the search for PKD drugs is off-target effects, as therapeutic targets are often expressed throughout other organs and tissues. [31, 32]

Tube size control mechanisms in *C. elegans*

Whereas mammalian tubes tend to be complex amalgamations of varied cell types and basement membranes, turning to model organisms can provide much-needed clarity. The *C. elegans* excretory cell, for example, falls on the opposite end of the spectrum of complexity, as it involves a single-cell epithelium that forms a long H-shaped tube, with a tapered lumen, that runs the entire length of the worm and mediates the osmolarity of the animal. A number of *Exc* genes have been identified as required for size determination of the excretory cell. In *Exc* mutants, the tip of the cell forms an enlarged bulb of cytoplasm reminiscent of cystic nephrons or tracheae. One of these genes, *Exc-4*, encodes a Chloride Intracellular Channel (CLIC) that is required for the formation of a transient lumenal matrix that restricts the size of the excretory cell lumen. [33] These CLIC proteins are unique in their ability to switch between soluble and integral membrane proteins where they can associate with a number of membrane-bound organelles and structures. [34, 35]

Although it is tempting to speculate that this process is similar to the secretion and maintenance of the transient apical ECM of the *Drosophila* trachea (detailed below), there are key differences between the trachea and the excretory cell that invalidate any such argument. Importantly, the excretory cell is—as its

name suggests— a single, junction-less cell. The formation of lumen in such “seamless” tubes, including mammalian capillary endothelial cells, originates with the establishment and dilation of an intracellular vacuole. [36] This is in contrast to the lumen of the multicellular Drosophila tracheal system, which occurs as a result of maintained intercellular contacts among polarized cells. [3] Berry et al hypothesize that the mechanism by which *Exc-4* regulates lumen formation may occur through the acidification and therefore directed fusion of vesicles to enlarge that initial vacuole or by regulating the osmolarity of the cell and therefore the extent of swelling. [33]

Another mutant that alters the diameter of the excretory cell lumen is *let-653*, which encodes mucin, a protein secreted into the developing lumen in a function seemingly similar to that of chitin—loss of *let-653* in the elegans excretory cell or of chitin synthase *krotzkopf verkehrt* (*kkv)* in the Drosophila trachea each causes cystic lumen overexpansion of its respective tube. [37, 38]

Tube size control mechanisms in *Drosophila melanogaster*

Work on *Drosophila* has helped reveal some information about the molecular mechanisms that may regulate tube size. The fly hindgut, for example, is a multicellular tube whose diameter is partially regulated by the tenectin (*tnc*), a glycoprotein secreted into the lumen that contributes to the formation of a dense striated matrix that ultimately and non-cell-autonomously inflates the hindgut yet is not required in the trachea. [39] Interestingly, the observation that glycoprotein function contributes to lumen formation and diameter has also been observed in *C. elegans* and MDCK cells [37, 40]. Much remains to be discovered about the mechanisms of tube size control in *Drosophila*, and our efforts have focused on the tracheal system as a model, which is expanded upon in the following section.

II. Detailed mechanisms of *Drosophila* tracheal size control

Overview of tracheal morphogenesis

Important information about the molecular mechanisms of epithelial tube size control can be attributed to research performed on the developing tracheal system of *D. melanogaster*, which serves as the animal's combined pulmonary and vascular systems [41]. (Figure 1.1) The tracheal system arises as two sets of ten clusters of ectodermally-derived precursor cells that originate on the surface of the embryo in structures referred to as the tracheal placodes. At stage 11, in response to EGF signaling, these cells divide and invaginate via apical constriction, while retaining their apical-basal polarity, allowing them to form two sets of ten tracheal sacs. Without undergoing further cell division, tracheal cells instead elongate, migrate, and intercalate, in an FGF-mediated fashion, to form a complete tracheal tree by stage 13. The cells of the trachea continue to elongate for the rest of development, and at stage 17 the transient lumenal matrix is cleared and the trachea is filled with air. The final tracheal network consists of two dorsal trunks, each with a set of ten dorsal branches and ten transverse connectives [42].

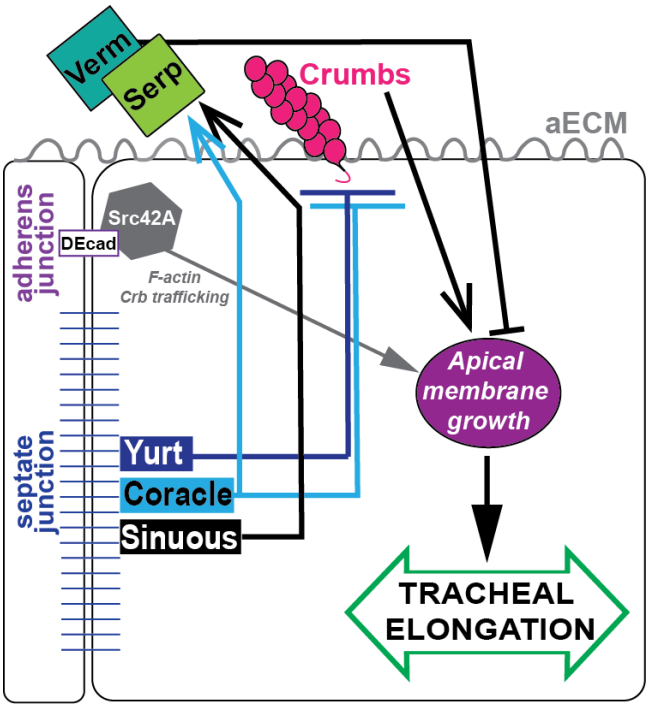

Figure 1.2 Known mechanisms of Drosophila tracheal size control. (a) See text for details.

Previous work on the *Drosophila* trachea has revealed that several processes contribute to tube size *without affecting cell number*: activity of cell polarity proteins, apical extracellular matrix secretion and organization, endocytosis of luminal and apical membrane components, and intracellular signaling pathways. Little is known about the relationships unifying these processes, yet as described below, there is strong evidence to suggest they must somehow work together to form the final size and shape of the trachea.

Signaling molecules at the apical surface regulate tracheal length

One key mechanism of epithelial tube size control is the establishment of cell polarity by the expression and localization of apical signaling proteins. The Crumbs and Par complexes specify apical polarity, while basal identity is regulated by the expression of several proteins including components of the septate junction (SJ), discussed below. Crumbs is an apically-localized transmembrane protein with a massive extracellular domain, which contains EGF-repeats and laminin-A globular domain-like repeats, in addition to a 37-amino acid cytoplasmic domain that has both PDZ- and FERM- binding motifs [43]. In the trachea, overexpression of Crumbs causes over-elongated trachea, and while loss of Crumbs is too destructive to the embryo to allow the measurement of the trachea, expression of only the 37-amino acid cytoplasmic domain, containing PDZ- and FERM-binding motifs, is sufficient to rescue proper development [44]. During development, the Crumbs complex is highly dynamic and has many binding partners (including but not limited to PATJ, Stardust, Lin-7, and certain members of the Par complex), and we have yet to understand

which of the many partners of Crumbs affect tube size. The Par complex itself is required for establishing polarity, but its role in tracheal dorsal trunk size control remains somewhat unclear.[45]

Perhaps best known for its role as an oncogene, the non-receptor tyrosine kinase Src42A is remarkable because it contributes to tracheal length in a unique manner: Src42A modulates tube size by influencing the amount of apical growth and the direction of anisotropic growth [46]. While loss of function mutations in the septate junction, polarity, and endocytic pathways cause over-elongated trachea, loss of Src42A causes shortened tracheae. This is partially because the direction of tracheal cell growth is oriented circumferentially in Src42A mutants, where, in a wild type trachea, the direction of tracheal cell growth is oriented axially, with respect to the tube length.[47] Furthermore, Src42A is particularly noteworthy because it defines one of the few tracheal elongation pathways (the only others being Crumbs and now Yki/DIAP1/DrICE) that is instructive in determining tracheal length—while other components are permissive, their overexpression does not have the opposite effect on tube length compared to their loss of function, as is the case with Src42A and the instructive regulators of tube size. Of note, there is now evidence that part of the mechanism by which Src42A controls tracheal elongation is by controlling the trafficking of the apical polarity protein, Crumbs.[48]

Components of cell-cell junctions regulate tracheal length

The Crumbs complex is also negatively regulated by basal polarity proteins within the Septate Junction (SJ) [49]. The SJ is the basolaterally-located claudin-containing cell-cell junction that performs the barrier function of the vertebrate tight junction. The SJ affects tube size both by negatively regulating the apical polarity protein Crumbs, and by affecting the secretion of the chitin deacetylases Vermiform and Serpentine (see below). Mutations in SJ components lead to increased tube length and apical surface area, but they do so by different mechanisms, depending on the gene. [49] Some SJ components, like Coracle, are required for antagonism of Crumbs and the secretion of apical extracellular matrix (aECM) modifiers Verm and Serp,

while others, like Yurt, have critical polarity functions in antagonism of Crumbs but have not been shown to affect aECM modifiers. [50] (Figure 1.2 and detailed below)

Modifiers of apical extracellular matrix regulate tracheal length

Secretion of the extracellular matrix affects both tube length and diameter; although elongation is a constant process during tracheal morphogenesis, a great deal of tracheal diametric expansion occurs from stages 13-16 of embryonic development. At this point, an apical secretory burst fills the tracheal lumen with both (a) the chitinous material that will make up the apical extracellular matrix, and (b) membrane components that are necessary to support diametric growth. The extracellular matrix is largely comprised of chitin and the chitin modifiers including Vermiform (Verm) and Serpentine (Serp) [51]. In the cuticle, chitin is known to form an organized matrix that provides structural support for the insect body [52]. One might expect, therefore, that loss of the chitin-based matrix in the tracheal lumen would cause a collapsed or shortened trachea, but in fact defects in chitin biosynthesis cause over-elongation in addition to morphological inconsistencies in the trachea including the overinflation of some regions and underinflation of others [38]. Absence of chitin, Verm/Serp, or defects in their secretion (eg, by loss of the SJ components *Sinu*, *Cora*), all cause over-elongated trachea [49, 53]. Because mutations in chitin biosynthesis also result in disorganization of βh-Spectrin, an apical cytoskeletal-membrane tether, it is currently hypothesized that the secretion and organization of the aECM suppress overgrowth by facilitating communication between the cytoskeleton and the lumen. [54]

Intracellular trafficking: known unknowns of tracheal size control

So far, I have described a set of three very broad classes of molecules that regulate tracheal size—it stands to reason that this diverse array would share some crosstalk or molecular commonalities in order to be integrated. Indeed, recently mounting evidence has demonstrated that inter- and intracellular trafficking is required to organize and facilitate this dynamic network of machines in order to rapidly regulate morphogenesis. Perhaps the most obvious demonstration of the importance of endocytic trafficking in embryogenesis is the secretion and maintenance of the aECM and its modifiers during the secretory burst

and its subsequent clearance from the lumen mere hours later, so that the tubes can be filled with air by stage 17[55]. Recently, it has become clear that endocytic trafficking is critical to size control because it mediates the recycling of various junction components and apical membrane components as well as those in the aECM [56]. For example, the dynamic routing of the apical determinant Crumbs (Crb) and the aECM modifier Serpentine (Serp) is significantly altered in the mutant *Shrub*^{4}, which encodes Vps32, a component of the ESCRT machinery that is required for inward budding of the multi-vesicular body (MVB). [57] Indeed, in 2017 Olivares-Castiñeira and Llimargas published further evidence that Crb traffics with Serp, and that their collective sorting can be modified by Epidermal Growth Factor Receptor (EGFR) activity. [58]

Our lab previously demonstrated a non-canonical function for the transcriptional co-activator Yorkie (Yki), the highly conserved *Drosophila* homologue of Yes-Associated Protein (YAP), which is negatively regulated by the Hippo Network. In the trachea, Yki acts by increasing transcription of the E3 ligase Death-related Inhibitor of Apoptosis (DIAP), which in turn decreases activity of the Caspase-3 homologue DrICE, ultimately inhibiting tube elongation (described in detail below). [5] In my project, I have aimed to address questions about the molecular dynamics of this pathway in order to determine exactly how this infamous growth control pathway governs tracheal size.

III. The Hippo Network controls organ & tissue size through evolution

The Hippo Network

Roughly two decades ago, the core components of the Hippo pathway were discovered for their roles as hyperplastic tumor suppressors in *Drosophila melanogaster*. In recent years, however, it has become clear that the Hippo "pathway" is far more complex than originally suspected—together, the kinases Hippo (MST1/2 in mammals) and Warts (LATS1/2 in mammals) and their requisite scaffold and co-activator proteins, Salvador (WW45) and Mats (Mob1A/B), respond to many inter- and intracellular signals, and

regulate multiple processes: tissue growth, apoptosis, suppression of cancer initiation and metastasis, contact inhibition and more. The rapidly growing body of literature on Hippo has thus prompted the

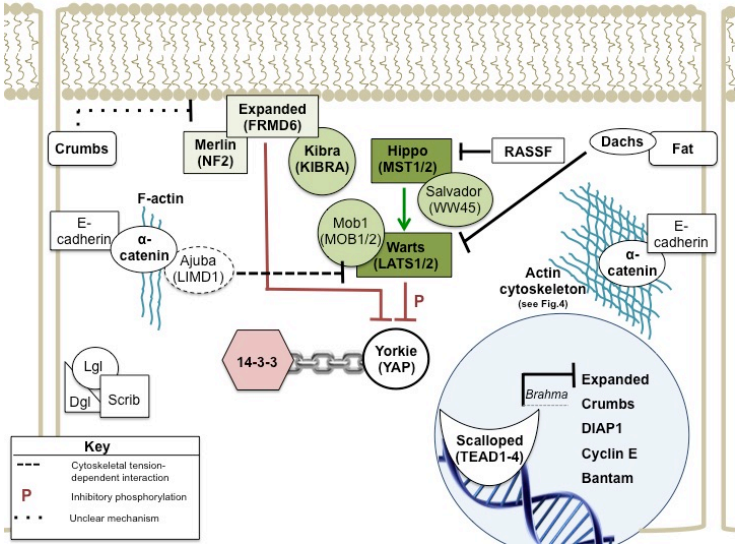

Figure 1.3 The core Hippo kinase cascade (shown here in **green**) consists of the kinases Hippo (MST1/2) and Warts (LATS1/2) as well as their respective scaffold and co-activator proteins, Salvador (WW45) and Mob (Mob1/2).

recognition of the Hippo "pathway" as instead a network with a large number of varied inputs and outputs in many cellular processes, including cell growth, proliferation, and apoptosis—all of which are critical to morphogenesis. It is now necessary, therefore, to critically revisit the many functions of the Hippo network in order to evaluate the nature and mechanisms of its activity during morphogenesis.

A brief history of the Hippo Network

The core pathway of the Hippo network is comprised of two kinases, Hippo (MST1/2) and Warts (LATS1/2). In fruit flies and mammals, with the absence of Hippo kinase cascade activity the unphosphorylated transcriptional co-activator Yorkie (YAP) enters the nucleus where it then binds to one of its DNA-binding co-transcriptional regulators including TEAD-family transcription factor, Scalloped (TEAD1-4).[59, 60] The transcriptional activity of Yorkie (YAP) then upregulates several genes associated with cell survival and proliferation. When the upstream kinases Hippo and Warts (LATS1/2) are activated, however, Yorkie (YAP)

is phosphorylated,[61, 62] consequently inactivating it, and thus preventing the up-regulation of cell survival genes, and potentially shifting the cell's apoptotic potential towards death. [61, 63]

Hippo kinase cascade in yeast

The core components of the Hippo network are highly conserved in the yeast *S. cerevisiae*, where there are two cellular processes that can be activated by the respective homologues—the mitotic exit network (MEN) or the Regulation of Ace2 in Morphogenesis (RAM) network. The matter of which process is modulated by the yeast Hippo pathway is determined by phosphorylation of either the LATS1/2-related kinase Cdc15, or the NDR-related kinase Kic1. When the Hippo homologue Cdc15 associates with Mob1 to activate the NDR kinase, Dbf-2, the mitotic exit network (MEN) becomes activated, driving mitotic exit via phosphatase Cdc14.[64] On the other hand, when the Hippo homologue Kic1 associates with Mob2 to activate the LATS1/2-kinase, Cbk1, this controls the RAM network, which governs the final stages of mother-daughter cell separation (reviewed in [65]).

Discovery of Hippo as a mechanism of organ autonomous size control in D. melanogaster

Thanks mostly to swift advances in biotechnology, but also in part to the epidemic of cancer that seemed to be emerging as a result of the increase in human life span during the later part of the twentieth century, the search for tumor suppressors and oncogenes was in full force during the 1990s. It was during this time that the core components of the Hippo network were identified. In 1995, a number of *D. melanogaster* genetic mosaic screens revealed that loss of the serine/threonine kinase *warts* induced wing and eye imaginal disc overgrowth and hyperproliferation.[63, 66] A short time later, Hippo, Salvador (WW45) and Mats (Mob1) were discovered for their own conserved roles in tissue growth in conjunction with Warts, thus heralding the birth of the Hippo "tumor suppressor" pathway.[67-69]

Around the same time as the genetic screens identified Warts as a tumor suppressor in *D. melanogaster*, the transcriptional co-activator Yes-Associated Protein (YAP) was identified as a putative binding partner of the proto-oncogene Src-family tyrosine kinase, Yes, in murine cells, though the validity of this relationship was never confirmed.[70] The connection to the parallel discoveries in *Drosophila* above, however, remained unknown, and would remain unknown until 2005, when Yorkie (Yki/YAP) was identified as the downstream phosphorylation target of the Hippo/Warts kinase cascade.[70, 71] While at the time, this identification of Yorkie (YAP) as the final destination of the pathway seemed to give a rather complete view of the Hippo "pathway," this core cascade was merely scratching the surface of the complexity within the Hippo network.

The birth of the Hippo Network

Hippo gained a large amount of attention in late 2013, when three separate groups published proteomic studies that identified a large number of interactors in the Hippo Pathway in both *Drosophila* and mammals.[72-76] Together, these studies provided a huge breakthrough in the field because they identified hundreds of Hippo interactions, some of which were completely unexpected cellular functions, such as cytoskeletal components and endocytosis/ vesicle transport proteins. Thanks to these and many other studies, it became clear that there was far more to Hippo than the linear kinase cascade revealed in the mid-1990s and early 2000s. Indeed, the number of confirmed interactions within the Hippo pathway has grown so much in the past decade that the term "pathway" doesn't incorporate the vastness of Hippo and its downstream components. Rather, the term "Network" far better describes the many molecular mechanisms that feed into the three levels of the core "pathway"—regulators of Hippo (MST1/2) function, regulators of Warts (LATS1/2) function, and direct regulators of Yorkie (YAP/TAZ).

Components of the core Hippo kinase cascade and their respective known regulators

Over the last decade, it has become clear that there are a number of cellular and molecular inputs that affect Hippo network activity; many do so in a manner that is independent of the core components: Hippo

(MST1/2), Salvador (WW45), Mats (Mob1), and Warts (LATS1/2). The expanding body of literature on regulators of the Hippo signaling network has provided evidence that the Hippo network is one that is complex and fundamental, with multiple points of input and regulation along its three main stages—the Hippo (MST1/2) kinase, the Warts (LATS1/2) kinase, and the transcription factor Yorkie (YAP). These distinct inputs come from many cellular sources including polarity complexes, cell-cell junctions, cytoskeletal complexes, and more. In order to generate a more accurate view of the Hippo network as such a complex system, this chapter seeks to organize the present body of literature in a more comprehensive manner.

Canonical core kinases Hippo (MST1/2) and Warts (LATS1/2)

The core kinase cascade at the heart of the Hippo network is comprised of the serine/threonine kinases Hippo (MST 1/2) and Warts (LATS1/2). In this section of this document, each of these core kinases and the specific modifiers of their function will be discussed.

Hippo (MST1/2) & Warts (LATS1/2) kinases and modifiers of their function

The founding member of the Hippo network is the Serine/Threonine Ste20-like kinase Hippo (MST1/2). In order to phosphorylate its targets, Hippo must associate with the WW domain-containing scaffold protein Salvador (WW45); when it is associated with Salvador (WW45), Hippo phosphorylates and thereby activates the Dbf-2 related kinase Warts (LATS1/2), which, in the canonical Hippo pathway, ultimately phosphorylates the transcriptional co-activator Yorkie (YAP) at a single key residue, S167 (S128 in mammalian YAP). Whereas activation of Hippo prohibits Yki-mediated cell growth, inactivation of the core kinase cascade triggers the nuclear localization of Yki, which in turn triggers cellular growth.

Neither Hippo nor Warts can phosphorylate their targets in the absence of the scaffolding and co-activation proteins Salvador (WW45) and Mob1 (Mob1).[77] The requirement for such scaffolding and co-activation proteins is thought to be critical to the spatiotemporal regulation of such powerful network nodes as Hippo/Warts. MOB1 is a co-activator of LATS1/2, which serves as a phosphosite-binding protein in yeast

and humans—representing substantial evolutionary conservation.[64] Together, these scaffolds regulate network signaling by (i) providing an additional checkpoint for complex assembly and therefore activation, (ii) potentially creating substrate specificity.

In addition to their role in the activation of Warts (LATS1/2) in this core cascade, Hippo (MST1/2) and its scaffold Mats (Mob1) have retained some of their ancient activity, as they are also responsible for phosphorylation and activation of a different class of kinases, the nuclear-Dbf2- related (NDR) kinases.[78]

Merlin functions by directly activating MST1/2 (Hippo) or by recruiting it to the membrane, where Merlin can activate LATS1/2 (Warts)

Merlin (Neurofibromatosis Type 2 (NF2)) is a FERM-domain containing protein that localizes near adherens junctions (AJs) and tight junctions (TJs) of confluent cells. The FERM (4.1, Ezrin, Radixin, Moesin) domain of these proteins is key because it confers on the protein its membrane-association and actin-binding abilities, which together promote the proteins' association with the cytoskeleton.[79, 80] Additionally, it has been previously shown that the FERM domain has the potential to mitigate Rho GTPase signaling, as the domain can recruit guanine nucleotide dissociation inhibitors.[81] Merlin most likely functions by directly activating Hippo (MST1/2) and/or by recruiting it to the apical membrane, where it activates Warts (LATS1/2).[82] While there are many possibilities that could explain the molecular mechanisms by which Merlin affects the activity of the Hippo network, its exact function remains poorly defined. It is now accepted, however, that Merlin can exist in either an open/ active or closed/ auto-inhibitory conformation, and that its conformation can be regulated by a Ser518 phosphorylation by an unidentified kinase.[83-85] In 2015, Li et al describe that the activity of Merlin can be influenced by the F-actin binding protein Angiomotin (discussed below), which binds to a region containing the phosphorylated residue Ser518, thereby activating Merlin.[82] The remaining question, however, is: are there other factors upstream of Merlin that regulate its autoinhibitory function?

Expanded is localized the apical membrane where its function as an inhibitor of Yki/YAP and promoter of Hippo/Warts localization

Another FERM domain protein, Expanded (FRMD6/ Willin) directly associates with Merlin at the apical membrane, where it is thought to decrease Yorkie (YAP) activity by (a) promoting the interaction between Hippo and Warts, and (b) directly binding to Yorkie (YAP), thereby promoting its cytoplasmic sequestration.[86, 87] Expanded can be regulated by several proteins, including Zyxin, Fat, Crumbs, and even Yorkie (YAP) itself (Fat, Crumbs, and Yorkie are discussed below). Zyxin, suspected to be a force-sensing protein, increases cell growth in part by negatively regulating the function of Expanded.[88] As described by Gaspar et al., this regulation depends on Zyxin's modification of cellular F-actin levels, as it binds the barbed-end actin-regulating protein Enabled (Ena), an interaction that can be inhibited by actin capping proteins.[88] It is also known that the protocadherin Fat is required for apically-localized Expanded.[89]

Intriguingly, Expanded is one of the transcriptional targets upregulated by Yorkie (YAP)—this is not a unique characteristic of Expanded as this is also true of several other upstream regulators of Yorkie, including Crumbs (discussed below). This observation is important because it (i) creates a possibility for a perhaps much-needed mechanism of negative feedback within the Hippo network, and (ii) solidifies its identity as a complex network, rather than simply a linear pathway.

WW-domain protein Kibra promotes the interaction of Merlin and Expanded with Warts

Kibra, named for its abundant accumulation in human kidney and brain tissue, is an apically-localized WW-domain containing protein that physically associates with Expanded (Ex), Merlin (Mer), and Warts (Wts).[90] While the mechanism(s) of Kibra (Kib) activity remain relatively unclear, it has been shown that Kibra can form a complex with the FERM-domain proteins Mer and Ex, thereby promoting their interaction and activity (discussed above). Interestingly, Kibra has also been shown to directly bind the Hippo-Salvador complex.[90, 91] Loss of Kibra leads to a decrease in Mer/Ex activity, loss of Hippo phosphorylation, and consequently, an increase in Yki activity and cell growth. Interestingly, as the case is with Expanded, a potential feedback

loop exists between Kibra and Yki/YAP, as Kibra is a transcriptionally up-regulated target of Yki/YAP. In addition to promoting the interaction between the Mer/Ex complex to the Hippo/ Sav complex, Kibra is also known to promote the interaction of Mer/Ex with the mammalian actin-binding protein Angiomotin, AMOT (discussed below).[90-92]

Crumbs, an apical polarity determinant and growth regulator, influences Hippo signaling in several ways, including via negative regulation of Expanded

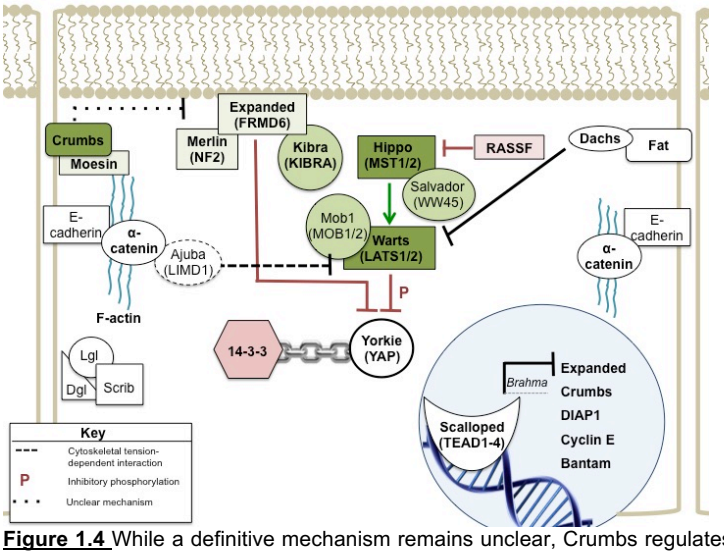

Figure 1.4 While a definitive mechanism remains unclear, Crumbs regulates Hippo output by interacting with the actin-binding protein Moesin, and the FERM domain protein Expanded.

Overexpression of the apical determinant Crumbs leads to an increase in cellular proportion of apical membrane, and also an increase in growth, due to increased Yki activity.[93-95] Crumbs (CRB1) is a conserved single-pass transmembrane protein whose 37-residue intracellular domain is required, and arguably sufficient, for establishing apical-basal polarity in developing epithelia; the intracellular domain confers on Crumbs its ability to associate with a variety of proteins including aPKC, Par6, and Yurt.[50, 96-98] The ability of this 37-residue cytoplasmic tail to bind such a diverse array of proteins is due to its FERM-binding domain, PDZ-binding domain, and aPKC phosphorylation sites. It is currently thought that, for the most part, the ability of these proteins to associate with Crumbs is mutually-exclusive, and can be determined in part by its aPKC-mediated phosphorylation state.[99] These phosphorylation sites are found within the FERM-binding motif of Crumb's intracellular domain, which affects the ability of Crumbs to bind Moesin, which forms a tether between the actin cytoskeleton and, in this case via Crumbs, the apical membrane. It is thought that the association of Moesin with Crumbs generates tension within the apical

membrane, which contributes to the activation of Yorkie (YAP)— in their 2015 study of the structure of Crumbs, Wei et al. proposed that when the sites within the Crumbs' FERM-binding domain are phosphorylated by aPKC, its ability to bind Moesin is reduced, leading to a reduction in cellular tension and consequent downregulation of Yorkie(YAP)-mediated cell growth.[99]

An additional mechanism of Hippo network regulation by Crumbs is thought to occur via its regulation of the levels and localization of the FERM-domain protein Expanded.[100, 101] While the mechanisms whereby the intracellular domain of Crumbs affects Expanded localization are relatively unclear, some data suggest that it occurs via defects in endocytosis. Endocytosis mediated by the ESCRT-II machinery (including Vps25 in *Drosophila*) is well-known to be an important factor in cell growth; Vps25 mutant clones in *Drosophila* imaginal discs, which display defective endocytosis, have been shown to exhibit altered Hippo signaling.[102] In their 2006 study implicating Vps25 in Hippo signaling, Hans-Martin et al. show that a reduction in Vps25 leads to a decrease in apical levels of Expanded protein, which they proposed to occur via the failed endocytosis of a "receptor that controls Hippo activity". Several year later, it was shown that the overexpression of the intracellular domain of Crumbs recapitulates the Vps25 mutant phenotype, both in growth levels and in reduction of apical levels of Expanded.[101]

In 2015, Zhu et al. reported that Yorkie's ability to transcriptionally upregulate levels of Crumbs was dependent on the presence of a conserved subunit of the SWItch/ Sucrose nonfermentable (SWT/SNF) chromatin-remodeling complex, Brahma (Brg1).[103] Brahma was found to physically associate with Yorkie, and ChIP analysis demonstrated Brahma's presence at the Crumbs promoter region. Furthermore, the ability of Yorkie to upregulate Crumbs was lost in the absence of Brahma. Zhu et al. therefore suggest that Brahma exists as a point of Yki regulation and of Crumbs regulation, by forming a complex with Yorkie (YAP) and Scalloped (TEAD 1-4) in order to regulate Hippo pathway feedback by modulating transcription of the upstream Hippo regulator Crumbs.

Polarity determinants Lethal giant larvae and aPKC alter Hippo signaling, but by unknown mechanisms

In the developing *Drosophila* eye imaginal disc, loss of the basolateral polarity determinant Lethal giant larvae (Lgl) leads to increased activity of Yorkie/YAP, and therefore increased proliferation and tissue growth.[104, 105] Lgl performs its polarity-determinant function as a member of the Scribble-Discs large-Lgl complex, in part through the antagonism of the apical kinase atypical Protein Kinase C (aPKC); as may be predicted, loss of aPKC leads to a decrease in Yorkie (YAP)-mediated growth.[93, 106] For a while, it was thought that Lgl accomplishes its regulation of Hippo signaling via ultimately activating the phosphatase Ras-associated factor (RASSF), which in turn dephosphorylates and inactivates Hippo.[106] In 2014, however, Parsons et al showed RASSF's ability to activate Yorkie-mediated growth was independent of Lgl or aPKC.[107] While Lgl may still have some secondary role in controlling RASSF, the upstream mechanisms of RASSF and Lgl/aPKC influence on the Hippo network remain to be determined.

dJub/Ajuba inhibits the function of Warts (LATS1/2), resulting in Yorkie (YAP) activation, cell growth, and a decrease in cytoskeletal tension

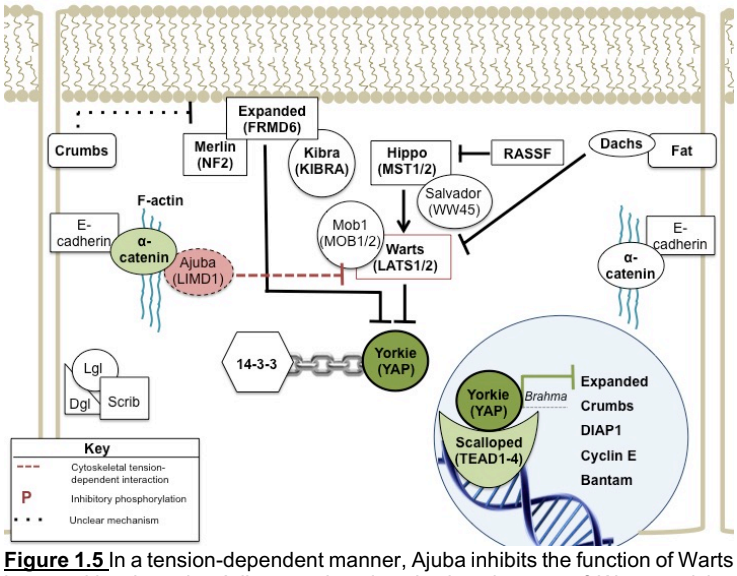

Figure 1.5 In a tension-dependent manner, Ajuba inhibits the function of Warts by recruiting it to the Adherens Junction. In the absence of Warts activity, Yorkie is free to upregulate its transcriptional targets.

dJub (Ajuba) a LIM-domain protein that associates with adherens junctions (AJ), was first described as a regulator of Hippo network signaling in 2010.[108] It has been demonstrated that Warts (LATS1/2)/Ajuba (LIMD1) regulate mitotic spindle orientation in HeLa cells, and that their interactions with each other occur in a cell cycle-dependent manner, with maximum interaction at mitosis [109]. Loss of *Drosophila* dJub causes a failure of centrosomal recruitment of microtubules, and via tissue-specific RNAi, leads to reduction in eye/wing size and cell number, without

disrupting tissue patterning.[108, 109] Several lines of evidence suggest that this function of Ajuba (LIMD1) is evolutionarily conserved: firstly, the undergrowth phenotypes in the fly can be rescued with overexpression of its human homologue, LIMD1.[110] Additionally, *in vitro* data with human and canine epithelial cell lines support that this is a highly conserved function of this family of proteins, with respect to controlling tissue growth in conjunction with the Hippo network.[108] At least one of these functions of Ajuba is conserved across species, as both *in vivo* studies of *Drosophila* and *in vitro* studies of mammalian cells have shown that the c-Jun amino-terminal Kinase (JNK) can promote Yki activation by increasing Ajuba's ability to bind and thereby negatively regulate Warts.[111]

In 2014, Rauskolb et al. found that in the developing *Drosophila* wing disc, Yorkie activity can be up-regulated in response to cytoskeletal tension mediated by ROCK/Myosin-II contractility, which was measured by laser-cutting cell junctions and quantifying recoil velocity.[110] Rauskolb et al propose that, in response to myosin-II contractility, α-catenin undergoes a conformational change to increase its ability to bind, and therefore localize Ajuba (LIMD1) to the AJ; when Ajuba (LIMD1) is recruited to the AJ, it binds and in turn inhibits the function of Warts. The resulting inhibition of Warts leads to the derepression of Yorkie (YAP) activity, and leads to cellular growth, which in turn can reduce the cellular tension that triggered its response. On the other hand, low actomyosin contractility precludes the recruitment of Warts (LATS1/2) to the AJ, thereby decreasing cell growth mediated by Yorkie (YAP).[110] It is also worth noting that, as is the case with many branches of the Hippo network, a feedback loop exists in this cassette, as Warts (LATS1/2) can, in turn, phosphorylate and negatively regulate Ajuba.[109]

The Fat cassette regulates Wts levels: Fat, Dachs, Dachsous, Four-jointed, Approximated, etc

Fat, which localizes at certain points of cell-cell adhesion, is a protocadherin that can influence Hippo network activity upstream of Warts (LATS1/2), in addition to regulating planar cell polarity and appendage patterning.[112] The exact mechanism(s) by which Fat feeds into the Hippo network remains to be determined, but we do know that Fat acts primarily by influencing Wts protein levels via the atypical myosin, Dachs.[113] Dachs is an unconventional myosin that acts downstream of Fat; it physically interacts with and

negatively regulates protein levels of Wts.[113, 114] Dachs's interaction with Fat is negatively regulated by the palmitoyltransferase Approximated (App), which controls the localization of Dachs, but the molecular mechanism by which App regulates Dachs localization is unknown. Normally, Fat sits at the cell cortex where its extracellular domain associates with the extracellular domain of a second atypical cadherin, Dachsous (Ds). The association of Fat with Dachsous can be modulated by their phosphorylation by the Golgi-resident kinase, Four-jointed (Fj), though this is most likely most involved in the role of Fat in PCP.[115, 116]. The phosphorylation of the atypical cadherins by Fj is interesting because the phosphorylation of Fat enhances Fat's ability to bind Dachsous, but phosphorylation of Dachsous represses Dachsous's ability to bind Fat. This enables the resulting gradients of Fat and Dachsous that are observed in the *Drosophila* wing disc, and thereby contribute to PCP. Along the same lines, it has been suggested that it is not absolute levels of Dachsous or Fj that control Hippo activity, but rather differences in expression between neighboring cells [117]—that is, when there is a large difference in cellular levels of Ds and Fj compared to its neighbors, Fat activity is downregulated, leading to a derepression of the unconventional myosin Dachs, which sends Wts for degradation, thereby freeing Yki from Wts-repression, allowing cellular growth. When neighboring cells have similar levels of Ds/Fj, however, Fat activity is upregulated, putting the breaks on cellular growth.[117] Interestingly, there is some evidence in mammalian cells that suggests Fat could act through the mechanically regulated force-sensing protein Zyxin, discussed below.[118-120]

Non-Yorkie (YAP) outputs of Hippo (MST1/2) and/or Warts (LATS1/2)

As mentioned above, in addition to their role in the activation of Warts (LATS1/2) in this core cascade, Hippo (MST1/2) and its scaffold Mats (Mob1) are also responsible for phosphorylation and activation of a different class of kinases, the nuclear-Dbf2- related (NDR) kinases, which, like LATS1/2 kinases, have conserved functions in growth and development, but are poorly understood.[78] In *D. melanogaster*, the NDR kinases have been associated with actin-rich cell projections and sensory neuron maturation.[121, 122] In humans, they are thought to drive cell cycle progression.[123] Interestingly, a 2015 paper provided evidence

that, in murine intestinal epithelia, both *in vitro* and *in vivo*, NDR kinases directly phosphorylate and inactivate YAP; before this study, direct phosphorylation regulators of YAP in the intestine were unknown.[124]

The following are two examples of non-Yorkie (YAP) outputs of Hippo and Warts: the core components of the Hippo network are highly conserved in the budding yeast *S. cerevisiae*, wherein there are two cellular processes that can be activated by the respective homologues—the mitotic exit network (MEN) or the Regulation of Ace2 in Morphogenesis (RAM) network. The matter of which process is modulated by the yeast Hippo pathway is determined by phosphorylation of either the LATS1/2-related kinase Cdc15, or the NDR-related kinase Kic1. When the Hippo homologue Cdc15 associates with Mob1 to activate the NDR kinase, Dbf-2, the mitotic exit network (MEN) becomes activated, driving mitotic exit via phosphatase Cdc14.[64] On the other hand, when the Hippo homologue Kic1 associates with Mob2 to activate the LATS1/2-kinase, Cbk1, this controls the RAM network, which governs the final stages of mother-daughter cell separation (reviewed in [65]). An additional example of non-YAP mediated output of Warts (LATS1/2) in a morphogenetic process has been its recently demonstrated role in promoting restricted F-actin polymerization during *Drosophila* border cell migration—a process critical to germ cell maturation— via phosphorylation and inhibition of the actin polymerizing protein Enabled (Ena).[125]

Regulation of the transcriptional co-activator Yorkie (YAP)

Hippo signaling culminates with changes in transcription mediated by the YAP/ Yorkie

The most well-described regulation of Yorkie (YAP) activity occurs, of course, via phosphorylation by Warts (LATS1/2) kinase. In the absence of Hippo kinase cascade activity in fruit flies and mammals, the unphosphorylated transcriptional co-activator Yorkie (YAP) enters the nucleus where it then binds to one of its DNA-binding co-transcriptional regulators including TEAD-family transcription factor, Scalloped (TEAD1-4).[59, 60] The transcriptional activity of Yorkie (YAP) is known to upregulate genes associated with cell survival and proliferation. When the upstream kinases Hippo and Warts (LATS1/2) are activated,

however, Yorkie (YAP) is phosphorylated.[61, 62] consequently inactivating it, and thus preventing the up-regulation of cell survival genes, and potentially shifting the cell's apoptotic potential towards death.[61, 63]

Because Yorkie (YAP) lacks a DNA-binding domain, it must associate with other transcription factors that can bind DNA. Yorkie (YAP) was found to bind, and be necessary for the activity of the TEAD family of transcription factors including the Drosophila homologue Scalloped.[126] All four mammalian TEAD family transcription factors (TEAD1-4), which lack activation domains, bind the same sequence of DNA, but each TEAD has a non-redundant expression pattern throughout development and/or adulthood. All of the TEAD family transcription factors require the presence of a transcriptional activator to be active.

The phosphorylation of Yorkie reveals a binding site for a cytoplasmic tether 14-3-3, which thereby inhibits its nuclear translocation and transcriptional activity.[63, 68, 127] 14-3-3, a cytosolic scaffolding protein, shuttles YAP out of the nucleus by competing for its binding to TEAD; overexpression of YAP in mouse cells causes accumulation of YAP/14-3-3 complexes in the cytoplasm, suggesting there is a mechanism in place to regulate the amount of YAP/TEAD transcriptional activity.[126]

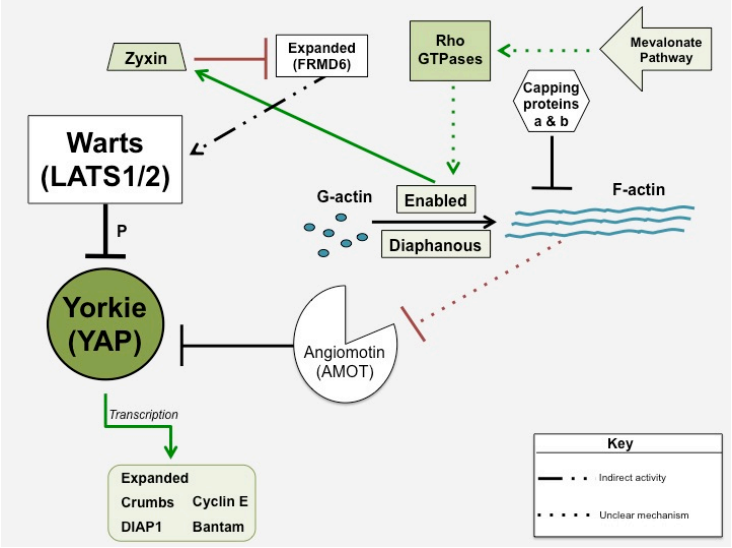

Figure 1.6 Schematic of the regulation of Warts (LATS1/2) and Yorkie (YAP) by the actin cytoskeleton

When Yorkie remains unphosphorylated, however, it is free to travel into the nucleus, where it upregulates genes associated with cell growth and proliferation, including Drosophila Inhibitor of Apoptosis (DIAP), Cyclin E (promotes transition from G1-S phase of cell cycle), and the microRNA Bantam, discussed below.[128-130]

Naturally, Hippo/Warts-mediated phosphorylation of Yki is, in turn, regulated by the upstream regulators of Hippo and Warts (discussed above). While it is unclear what precisely triggers the activation or inactivation of Hippo and Warts, it is well-known that high levels of cell tension, including that caused by cell-cell contact, is sufficient to increase cellular levels of Warts-phosphorylated (inactive) Yki (discussed below). In *Drosophila*, Yki upregulates transcription of the upstream genes Ex, Kib, Crb and Fj, all negative regulators of Yki signaling, suggesting yet another negative feedback loop.

Cytoskeletal dynamics and cellular tension regulate Yki activity

Within recent years, the role of mechanotransduction in biological processes has been mostly overshadowed by the "oncogenic revolution",[131] yet evidence to support the idea that mechanical forces influence cell and organ growth has existed, largely unaddressed, for decades, with only a recent resurgence of interest in the topic.[132-134] It has now been shown in multiple ways and in many cell types, that Yki/YAP activity is induced by cytoskeletal dynamics and/ or by cellular tension—negative regulation of Yorkie/ YAP has been shown to occur, for example, by an decreasing cellular F-actin concentration (via upregulation of capping proteins), or by loss of myosin II-mediated contractility (mediated by Ajuba).[108, 135, 136] The resulting model, where increasing cell growth in response to cellular tension is a very logical one—there is a point at which cell growth becomes unsustainable (due to, for example, a lack of support provided by F-actin), and at that point, continued growth might cause an increase in cellular tension that could damage a cell. On the other hand, it would benefit a cell to grow in response to increased actomyosin contractility. By that logic, (i) tissue growth or proliferation mediated by Yki (YAP) and (ii) the tension sensing mechanisms that may regulate YAP activity, provides a mechanism for cells to sense and generate a respective growth response to cellular tension. As one might imagine, such a response to cellular tension would have to be conserved across many species, by providing a finely tuned mechanism for the tuning of cell growth in response to tension that may be generated by various events— extracellular forces exerted by the ECM, tension generated by cells pushing up against each other when cell-confluence is achieved, or information about a neighboring cell's levels of tension transmitted through cell-cell junctions. While the

mechanisms that govern a cell's response to each of these sources of tension maybe inherently distinct, it seems likely that they each ultimately input to the same growth response pathway, potentially the Hippo Network. Some of these mechanisms are independent of Hippo's upstream kinase cascade, but others are not (details below).

F-actin levels affect Yorkie (YAP) activity by mechanisms that can be either Hippo-dependent or Hippo–independent

Affecting F-actin dynamics can alter Hippo-mediated tissue growth—in 2011, Sansores-Garcia et al. found that increasing cellular F-actin levels by (i) eliminating actin capping proteins or (ii) overexpressing a constitutively active version of the formin Diaphanous, causes Yorkie-mediated overgrowth in developing *D. melanogaster* wing and eye discs, without affecting polarity or localization of the upstream FERM-domain proteins Expanded or Merlin.[137] These data were corroborated by a similar study in 2011.[138] Interestingly, both groups found that overexpression of Expanded was sufficient to rescue the overgrowth phenotypes caused by loss of actin capping proteins or by overexpression of constitutively active Diaphanous, suggesting that whatever role is played by F-actin in regulating Yorkie/YAP activity occurs upstream of Yorkie/YAP. These results, which were obtained in *D. melanogaster*, have been supported and elaborated on by work done in mammalian systems. In their experiments using non-tumorigenic mammary epithelial-derived MCF10A cells, the Dupont and Piccolo groups showed that the increased F-actin stress fiber accumulation resulting from growing populations of cells on a stiff extracellular matrix (ECM) or on a stretched ECM, induces the activity of YAP in a manner that is *independent* of its phosphorylation by LATS1/2 (Warts)—YAP primarily localizes to the nucleus of cells grown on a stiff extracellular matrix (ECM) or on a stretching, curved surface.[136, 139]

Two questions remain, however: (i) what is the mechanism by which F-actin accumulation affects Hippo output? and (i) Do these different processes of directly affecting actin polymerization and affecting a cell's ECM use the same mechanisms to affect Yorkie/YAP activity? One possible explanation that is that

changes in F-actin dynamics alter the recycling of Hippo network components at the apical surface, since F-actin is required to regulate the formation of endocytic vesicles for recycling and degradation of proteins at the apical surface.[140] Another possible mechanism for F-actin influence on Hippo signaling in mammalian cells is that of YAP binding to Angiomotin. F-actin levels, however, have also been shown to contribute to Hippo signaling in a Warts-dependent manner. In a 2013 paper from Doujia Pan's group, F-actin levels were shown to contribute to Hippo signaling by negatively influencing the interaction between Merlin and Warts at the apical membrane.[141]

Cellular tension mediated by actomyosin contractility, β-Spectrin, and Zyxin regulate Hippo activity

Cytoskeletal dynamics may affect Hippo signaling by relaying information about mechanotransduction. For example, a 2014 study of the *D. melanogaster* wing disc involving the LIM domain protein Ajuba, found that the relationship between Yorkie-mediated growth output and cellular tension to be dependent on the phosphorylation state of Yorkie as determined by Warts.[110] *For further details, see below.*

In 2015, Deng et al. showed that the Spectrin Based Membrane Skeleton (SBMS) regulates Hippo signaling by inhibiting the phosphorylation, and therefore activity, of non-muscle myosin II in *Drosophila* eye and wing imaginal discs, as well as in mammalian MCF10A cells.[142] Although it had not been clearly shown whether this occurs in a Wts-dependent or Wts-independent manner, the data suggested, perhaps surprisingly, that this mechanism of Yki regulation occurs independently of the LIM-domain protein Ajuba (*see below*). That means that SBMS regulation of Yorkie (YAP)-mediated growth provides an additional mechanism by which cellular tension can be transmitted into molecular signaling inputs into Yorkie (YAP).

Also in 2015, Gaspar et al. published a crucial study of the putative force-sensing protein Zyxin, wherein they demonstrated that Zyxin has the ability to bind and negatively regulate Expanded, but this negative interaction requires the presence of its Enabled-binding domain—which is relevant to the cytoskeleton because Enabled is a critical part of the actin polymerization machinery.[88] Zyxin is suspected to be a mechanical force-transducing protein because Zyxin-null mammalian cells fail to build up thickened actin

bundles in response to cell stretching,[143] and because, in migrating D. melanogaster border cells, laser ablation of actin filaments, which served to decrease actin fiber tension, caused a decrease in Zyxin localization to these cables.[144] Because of Zyxin's abilities to (i) transduce information about force to influence the actin cytoskeleton, as well as (ii) negatively regulate Expanded, Zyxin is an excellent candidate for a molecular mediator of cell tension and Hippo-mediated growth.

Cell Polarity determinants and Yki activity

As mentioned above, several polarity proteins can influence the output of the Hippo network, as measured by Yorkie (YAP) activity. For example, loss of the basolateral polarity gene Scribble (Scrib) in the *Drosophila* eye imaginal disc causes increased cell proliferation and upregulated levels of Yorkie (YAP) target genes CyE, DIAP1, etc, which can be rescued by heterozygous Yorkie (YAP).[93] This result is corroborated by data from experiments in mammalian cancer cells, wherein Scrib has been shown to directly bind the mammalian Yorkie homologue TAZ via its interactions with MATS and LATS, thereby promoting its phosphorylation and inactivation.[145]

Non-Hippo mediated regulation of Yorkie (YAP)

There are several non-Warts phosphorylation-mediated mechanisms of Yorkie (YAP) regulation in addition to those mentioned above, such as the NDR kinase regulation of YAP within the murine intestinal epithelium mentioned.[124] For example, it was shown that phosphorylation of YAP/ Yki by Akt inhibits its function. As with Warts (LATS1/2), Akt-mediated phosphorylation of YAP's serine 127 residue sequesters it in the cytoplasm by revealing its 14-3-3 binding site.[146] Additionally, vesicle trafficking and endocytic signaling have also been shown to regulate the ubiquitination and degradation of Yki/YAP, which can be promoted by the α-arrestin protein, Leash.[73]

Angiomotin

Angiomotins are a class of actin-binding proteins exclusive to mammals, that were named for their ability to regulate endothelial cell migration (reviewed in [147]), but seem also to be capable of regulating YAP activity, as evidence from recent publications suggests that Angiomotin (Amot) has the unique ability to regulate YAP activity in both a LATS1/2-independent/ phosphorylation-independent manner as well as in a LATS1/2-dependent manner.[148, 149] Angiomotin normally binds to F-actin, but it can also bind directly to YAP.[150] As discussed below (*Metabolic control of YAP/TAZ*), it has been hypothesized that this causes a potential inhibition of Yorkie by Angiomotin in a manner that is dependent on F-actin levels.[135] Furthermore, in their 2015 study of the structure of Crumbs, Wei et al. proposed that when the sites within the Crumbs' FERM-binding domain are phosphorylated by aPKC, its ability to bind Moesin is reduced, leading to a reduction in cellular tension and consequent downregulation of Yorkie(YAP)-mediated cell growth.[99] Interestingly, it was also shown that LATS1/2 can phosphorylate Angiomotin, thereby inhibiting its function—which may decrease YAP activity— by disrupting its ability to bind F-actin.[151]

Metabolic control of YAP/TAZ: Phospholipid-activated GPCRs & cholesterol synthesis genes control YAP/TAZ function, potentially by regulating Rho GTPase and angiomotin activity

In 2012, two groups showed that serum-starving cells of either sphingosine phosphosate-1 (S1P) or lysophosphatidic acid (LPA) was sufficient to reversibly inactivate YAP activity.[152, 153] This effect, they found, was mediated by their respective G-protein coupled receptors (GPCRs), Gα13 and Gα12. In response to the presence of their substrates, these GPCRs trigger a signaling cascade that activates Rho GTPases and additional F- actin. The activation of YAP by Rho GTPase-mediated F-actin accumulation, as facilitated by G-protein coupled receptors (GPCRs), was also demonstrated in 2014, when Feng et al showed that uveal melanoma cells, many of which possess mutations in Gαq/11—these mutations render the GPCRs constitutively active—possess abnormally high levels of active YAP, due to the resulting increase in activation of Rho GTPases by the guanine exchange factor, Trio.[135] It was suggested by Feng et al. that this modulation of YAP activity occurs by influencing Angiomotin—in their proposed mechanism,

increased cellular levels of F-actin via Trio outcompete YAP for Angiomotin binding, resulting in an increase in activated YAP.

In 2014, Sorrentino et al. showed that treating flies with the HMG-CoA Reductase inhibitor Cerivistatin was sufficient to (i) sequester YAP to the cytoplasm of human breast cancer-derived MDA-MB-231 cells, and (ii) reduce the eye-overgrowth phenotype of Yki-overexpression mutants.[154] HMG-CoA Reductase is the rate-limiting step of the metabolic pathway that controls fatty acid synthesis in both *D. melanogaster* and humans, and additionally controls cholesterol synthesis in human; these data, therefore, suggest that metabolic pathways could control YAP/TAZ activity.[154] Sorrentino et al. hypothesize that this effect could be due to the loss of the protein prenylation that occurs downstream of the mevalonate pathway, which is critical for the membrane-recruitment of many proteins, including Rho family GTPases.

Is there a regulatory function of the YAP mRNA?

Based on data published by the Zhang group in 2015, a highly-conserved 20-nt segment of the YAP 3'UTR (YAP-sh-3p20) can downregulate NF2 (Merlin) protein levels, and is sufficient to reduce proliferation in HepG2 cells.[155] This has yet to be replicated in an *in vivo* context, but if this is true, it provides an additional point of regulation between YAP and its upstream regulators.

The Hippo network in morphogenesis

Control of tissue size and shape

During development, it is critical that an embryo adopts a proper (i) size and (ii) three-dimensional shape—that is, proper morphogenesis must occur—both of which have been shown to be regulated by the Hippo network. Of course, the Hippo network is perhaps best known for its role(s) in controlling organ size; in *Drosophila*, loss of Yorkie, or anything that positively regulates Yorkie activity leads to a decrease in organ size; loss of Hippo, Warts, or anything that negatively regulates Yorkie activity leads to an increase in organ

size. The Hippo network, however, is also important for maintaining organ shape, as shown, for example, in the development of the medaka fish, where Hippo regulates 3D organ shape via interactions with the cytoskeleton.[156] This, in combination with other evidence outlined above, suggests that the Hippo network also interacts with the known, but perhaps far underappreciated and potentially critical regulator of organ size and shape during development, cellular tension—that is, the forces exerted on cells by their environment and/or neighboring cells. Studies in cultured cells have shown that presence or absence of external physical forces can influence cell proliferation and cell fate.[157-159] In the context of a developing embryo in particular, several questions remain, including: (a) what is/are the molecular mechanism(s) that relay information about external force, and (b) how is this information transferred into signals that regulate growth? These questions are particularly compelling because recent evidence points to the Hippo network as a key node wherein signals regarding mechanotransduction are relayed to cell size control.[136, 139] Thus, many of the emerging molecular details regarding the Hippo network paint a picture of a pathway that is increasingly likely to be critical for organismal development and morphogenesis.

Tube size control in D. melanogaster

One known exception to Hippo's negative regulation of size during morphogenesis is the developing *D. melanogaster* tracheal system. The Hpo/Yki/DIAP pathway has an unexpected instructive effect on *D. melanogaster* tracheal development—with no changes occurring either in cell number or cell volume, loss of Yki causes an unexpected increase in tracheal length, while its overexpression reduces tracheal length.[5] This indicates (i) not only a novel, but also an *instructive* role for Yki in restricting biological tube size. Furthermore, since the effect is mediated by the highly conserved caspase drIce—upon activation, Yki upregulates the transcription of DIAP, which in turn decreases the activity of the caspase DrICE, a positive regulator of tracheal elongation—(ii) this is the first and only known example of the Hippo network regulating non-apoptotic caspase function. Many questions about the function of the Yki/DIAP/DrICE pathway in tracheal development remain unanswered, mainly: what is its relationship between other known tracheal size control pathways, and what are the downstream mechanisms of drIce-mediated size control? For

example, while Zyxin, an upstream member of the Hippo pathway, has been shown to be important in tracheal filling,[160] it remains to be determined whether it also plays some role in embryonic tracheal size control. The role of Yorkie and the seemingly myriad upstream components of the network in tracheal morphogenesis remain obscure. Furthermore, while individual components of this tracheal size control pathway, including Yorkie and DrICE, are highly evolutionarily conserved, it is unclear whether this pathway as a whole is conserved in mammalian species as a mechanism of tube size control.

Loss of YAP/ TAZ in development: Angiogenesis, cortical stiffness, kidney development, and more to be discovered

In 2007, the role of Yki in organ size control was demonstrated to be functionally conserved in its mouse homologue, YAP65.[61] Murine embryos lacking YAP65 die at E8.5, exhibiting, among other phenotypes, a loss of yolk sac vasculogenesis and a shortened body axis, despite the fact that gene expression patterns seemed to remain unchanged.[161]

The YAP null defect in yolk sac vasculogenesis suggests that YAP also plays a role as a regulator of angiogenesis, and this claim is supported by recent data describing the critical role of YAP in influencing endothelial cell (EC) junctional stability and angiogenic activation, wherein Choi et al. find that expression of constitutively active YAP in ECs leads to angiogenic sprouting in an Angiopoietin-2- dependent manner.[162] VE-cadherin, a component of mammalian EC junctions, and putative mechanical stress transducer, has the capacity to mediate cells' response to angiogenic signals (haemodynamic flow-induced mechanical forces, inflammatory cytokines, and growth factors) by associating with and regulating the activity of growth factor receptors like VEGFR and TGFβR, interacting with GTPase signaling to influence actomyosin contractility, and by up-regulating transcriptional activity of certain transcription factors including FoxO and β-catenin[146, 162]; VE-cadherin is therefore a master regulator of angiogenesis. In June 2015, Choi et al. presented a novel finding: upon angiogenesis, VE-cadherin triggers the PI3K-Akt-mediated phosphorylation (and subsequent inactivation) of YAP,[146, 162] thereby preventing YAP upregulation of the

transcription factor Angiopoietin-2, which has a key role in angiogenesis and vascular remodeling. Therefore, as Choi et al. describe, the localization of YAP to the nucleus, leading (via an unknown mechanism) to the transcriptional upregulation of Angiopoietin-2, is diminished by VE-cadherin clustering, providing a potential mechanism of halting angiogenesis via EC contact inhibition. Another interesting find is that the microRNA miRNA-302-367, has been demonstrated to target the murine kinases MST1/2 and LATS1/2 to promote cardiac regeneration and cardiomyocyte proliferation.[163] Together, these findings suggest that the Hippo network is important for the formation of blood vessels and the maintenance of the cardiomyocyte population within the mammalian heart.

Although there were no apparent gastrulation defects in YAP-null animals, the shortened body axis of YAP-depleted murine embryos, on the other hand, remain unexplored, but could have several causes, including failed cell proliferation, migration, or perhaps differentiation.[161] This finding is particularly interesting given another 2015 paper showing that YAP is required for maintaining the 3D body plan of the medaka fish, a cousin of zebrafish, whose development is, upon YAP knockdown, subject to gravitational pull. In 2015, Porazinski and Wang et al. report that body flattening due to loss of YAP is due to the fact that YAP is required for cortical actomyosin network formation, which is in turn required for body shape and tissue alignment.[156]

A severely complicating factor for assessing the role of YAP and Hippo in morphogenesis is that mammals have a second Yorkie homologue, Transcriptional co-Activator with PDZ-binding motif (TAZ). TAZ is structurally similar to YAP, and (i) its phosphorylation by LATS1/2 is required for 14-3-3 binding and subsequent inactivation, and (ii) its overexpression leads to a number of YAP-common defects including increased organ size and cell proliferation.[164] In murine development, however, TAZ is expressed later than YAP, and cannot compensate for its loss; while YAP-null mice cease development at E8.5, TAZ null mice are viable, but exhibit Polycystic Kidney Disease, which causes enlarged and largely non-functional nephrons.[161, 165] YAP and TAZ are somewhat functionally redundant, however, as murine embryos lacking both YAP and TAZ die extremely early in development—before the morula stage— suggesting that both

YAP and TAZ are required even before lineage specification; indeed the authors' further investigation using a dominant negative YAP revealed that early in development, YAP and TAZ work in combination with TEAD4 to upregulate expression of Cdx2, which is required for specifying the outside and inside cells of the developing blastocyst.[166] In other words, although more information is needed to determine the exact mechanism, this provides evidence that YAP and TAZ are required to integrate information about cell positioning in the very early mouse embryo.

Providing further evidence that Hippo belongs to a morphogenetic network, there are several critical morphogenetic signaling pathways that have been demonstrated to be affected by the Hippo network, including Wnt, BMP, Notch, Hedgehog, and TGFβ.[167, 168] For example, the polycystic kidneys of TAZ-null mice mentioned above contain increased levels of the Wnt effector β-catenin, which likely occurs via TAZ's ability to bind to Dishevelled (DVL).[168] Dishevelled binds and inhibits β-catenin unless phosphorylated by Casein Kinase (CK1δ/ε), but because TAZ binds DVL, β-catenin becomes upregulated. Fascinatingly, the relationship between YAP and Wnt were shown to be important in restricting stem cell proliferation in the development of the mouse intestine, where YAP has the same growth-restrictive effects as in the development of the *D. melanogaster* tracheal system.[169]

Concluding remarks on the Hippo Network

Many specific questions regarding the molecular mechanisms of the Hippo network remain unanswered: what are the exact mechanisms by which F-actin controls Yorkie (YAP) activity? How do Lethal giant larvae and atypical Protein Kinase C modulate Hippo? But there are also more broadly intriguing questions that remain, for example: In what way is the cellular context of the developing *D. melanogaster* tracheal system and mouse intestine unique, such that loss of Yorkie (YAP) leads to the opposite of the canonically expected phenotype? Tissue-specific phenotypic differences such as these indicate that cell context—such as presence or absence of (unknown) regulators, post-translational modifications that alter phosphosite

recognition, tissue environment, differences in cell-cell communication, and so on—play an important role in the phenotypic output of the Hippo network. These tissue-specific differences provide an opportunity to explain contradicting data—for example, some groups have found that increasing cell tension increases Yorkie activity in a Warts-dependent manner, while other find it does so in a Warts-independent manner.[110, 139] This apparent complexity suggests again that the nature of Hippo signaling is indeed that of a vast network whose output is highly context-dependent. It is therefore critical to appreciate that there is no one linear "Hippo pathway"—there are in fact a greater number of inputs and feedback mechanisms at play than original "pathway" studies could have ever expected. Rather, the kinase cascade that defines the canonical linear "pathway" has instead been integrated into an extensive network in eukaryotic cells with many outputs.

Consistent with this notion, the Hippo network is centered around an ancient core kinase cascade that has been conserved by evolution since before the animal radiation.[170] In the budding yeast, Hippo dictates the function of the MEN and the RAM network, making it indispensable for cellular survival and fitness. Over the course of evolution and the advent of the multicellular organism, however, this core cascade has extended its reach to a broad range of morphogenetic processes within the multicellular organism, whereby Hippo has interfaced with new proteins such as Yorkie (YAP) and Angiomotin, allowing the Hippo network to gain new functions.

The study of the Hippo network is rapidly evolving, creating a picture of an elastic and nuanced network that has many alternate mechanisms and interactions that can diverge from tissue to tissue. Viewing Hippo as a network presents many opportunities for the reconciliation of these data into a more complete snapshot of the many faces of Hippo as a critical network within morphogenesis, and one that can be traced through various morphogenetic "themes" such as growth in response to cellular tension, metabolic input, and cell-cell signaling, which are all imperative for morphogenesis.

IV. Rationale, goals, and approach

Rationale

Work from the Beitel lab published in 2014 established that the Hippo Network is required for proper tracheal size control.[5] The evolutionarily conserved Hippo Network is a complex signaling network centered around a core kinase cascade that regulates cell growth and death in response to a wide array of intra- and extracellular cues (reviewed in detail above). Hippo Network kinases promote the inactivation of the transcriptional co-activator Yorkie (YAP/TAZ). Phosphorylated Yorkie is sequestered in the cytoplasm and is therefore unable to facilitate transcription of its target genes, which are required for growth and resistance to apoptosis. Consequently, the vast majority of previous studies in a variety of organisms show that loss of Yorkie causes reduced tissue size due to decreased cell proliferation and/or increased cell death.

Although the Hippo Network's extensive evolutionary conservation may have led us to expect that this infamous growth control pathway would be involved in tracheal size determination, its *output* was anything but expected: *yorkie* loss-of-function mutants have an overgrowth phenotype in the *Drosophila* trachea. This is striking because it implies that de-repression of cell death machinery *elongates* the trachea; in other words, cell death machinery is required for the normal developmental process of elongation. Robbins's observations led to a counterintuitive hypothesis that cell death machinery is necessary for tracheal growth. The model derived from this hypothesis has especially critical implications in the fields of cell and developmental biology as well as cancer research, as it adds evidence to support the growing implication in the field that cell death machinery can be required for cellular processes beyond apoptosis.

Goals

The overarching goal of this project was to uncover the molecular mechanisms by which the executioner caspase DrICE governs *Drosophila* trachea morphogenesis. I sought to determine the molecular mechanism(s) of DrICE-mediated growth and tease apart its potentially differing roles in tracheal apoptosis and morphogenesis. **Specifically, I wanted to define the epistatic relationships between DrICE and known size control pathways, resolve the spatiotemporal activity of DrICE *in vivo*, and identify the proteolytic substrate of DrICE that elongates the trachea.**

Approach

Epistasis experiments

One step I took toward uncovering the mechanism by which DrICE controls tracheal size was to conduct epistasis experiments between a loss-of-function allele of *DrICE* and one gene from each category of known tracheal size control genes. This classical genetic approach allowed us to determine whether DrICE could be placed “upstream of” or “in parallel to” apical tracheal size determinants, cell-cell junction components, or modifiers of the apical extracellular matrix. This approach was also used to determine the nature of the epistatic relationships between DrICE and the known regulators of tracheal length, as well as between DrICE and canonically upstream members of the Hippo Network.

Candidate approach for substrate identification

We initially sought to understand the molecular mechanism by which DrICE affects tracheal length by identifying a proteolytic substrate of DrICE that was responsible for tracheal elongation. A review of known caspase substrates revealed two putative substrates, a-catenin and Sterol Regulatory Element Binding Protein (SREBP). The review of the literature, however, also revealed that caspase substrate recognition sequences are not as well-defined as previously thought.

Microscopy

In addition to using microscopy to assay tracheal lengths for my aforementioned genetic approach, I used microscopy to visualize alterations in abundance and/ or localization of tracheal size determinants in mutant backgrounds that represented either DrICE loss of function (*DrICE*^{17}, *DrICE*$^{\Delta 1}$) or overexpression (*btl>DrICE*)/ de-repression (*yorkie*^{B5}).

Perhaps one of the most informative experimental approaches was visualizing the localization of DrICE in wild type embryos—the punctate and apical localization of the caspase gave us insight into its putative endocytic role. Once it became clear that DrICE affects intracellular trafficking, I used microscopy to confirm that (a) DrICE could be observed in close physical proximity to early endocytic machinery and (b) that the abundance/ localization of various molecules associated with tracheal size control were improperly distorted during tracheal morphogenesis in backgrounds corresponding to altered DrICE abundance.

Transgenics and CRISPR mutants

In order to further confirm and characterize the role of DrICE in endocytosis, we searched the protein sequence of DrICE for any indication that it could be targeted to the endocytic pathway. We were stunned to find a dileucine motif in the small subunit of DrICE; this motif, DXXXLL, has been previously described as a binding site for Clathrin adaptor complexes. Even more striking, this sequence was strongly conserved in all *Drosophila* and mammalian executioner caspases, three out of four *Drosophila* initiator caspases, the human initiator caspases-8 and -9, and in both *Drosophila* and human caspase activators (Dark and APAF-1, respectively). This motif is even found in *C. elegans* caspases CED-3 and CED-4. The conservation of the Clathrin adaptor recognition motif in apoptotic machinery over 500 million years of evolution strongly implied a functional significance. In order to test the functional significance of DrICE's conserved dileucine motif, I generated an overexpression transgenic and examined its effects on tracheal length compared to overexpression of the wild type DrICE sequence.

Please note that details of all methods are described in each respective chapter.

CHAPTER 2: DrICE acts downstream of the Hippo Network in apoptosis and tracheal size control

Nothing can be said to be certain, except death and taxes.

– Benjamin Franklin, 1789

I. Overview of cell death and apoptotic machinery

Cell death is, counterintuitively, an essential part of life— from sponges to humans, almost all animals experience some form of "programmed" death executed by genetically encoded proteins; even single-celled organisms contain programmed death machinery.[171] What is the evolutionary advantage conferred by the genetic ability of a cell to die? In this chapter, I will begin with a description of cell death.

In multicellular organisms, requirement for cell death persists through embryonic development, adult homeostasis, and stress response as a mechanism of removing sick, injured, or otherwise unwanted cells. In development, programmed death is crucial for shaping developing tissues *in utero*: in humans, apoptosis patterns the hindbrain during mammalian neural tube closure, removes the webbing between embryonic fingers and toes, and more. In human adult homeostasis, immature T- and B-cells in the human immune system undergo abundant recombination in order to generate a seemingly infinite series of receptors and antibodies that recognize sequences on diverse pathogens. Although this is eminently useful for variability to ensure lymphocyte-mediated protection against a wide variety of pathogens, self-recognition of host tissue can lead to debilitating autoimmune disorders. For this reason, nascent T- and B-cells are first screened in the thymus and bone marrow such that unwanted ones with self-recognizing receptors or

antibodies can be safely eliminated by apoptosis. The requirement of a death program seems at first glance to place cells in a risky situation— the ready accessibility of killer proteins puts a cell on the razor's edge of death.

Indeed, either excessive or ineffective cell death can lead to a variety of severe pathologies in humans.[172] Excessive cell death can cause pathologies like neurodegeneration, auto-immune disorders, and cirrhosis. For example, hepatocytes found in the liver are particularly susceptible to apoptosis because they have a large concentration of FAS receptors, which can trigger extrinsic death pathways. Under healthy conditions, the ability of hepatocytes to die can prevent the systemic spread of infection. Due to the vulnerability of hepatocytes to apoptotic signals, however, excessive stimulation of their death can lead to liver cirrhosis, which is caused by fibrosis and massive inflammation.[173, 174] In the recent past, cirrhosis had been treatable only through targeting any known cause of the cirrhosis (ie, alcohol dependence, Hepatitis C, etc), but within the last year, Conatus Pharmaceuticals published promising results in a pre-clinical study of Emricasan, a pan-caspase inhibitor, for a direct treatment of cirrhosis in mice. Emriscasan is among the first of its kind, however, because development of caspase inhibition drugs has not yet been fully explored for a prevailing—and not unwarranted— fear that blocking cell death would lead to cancer.

Indeed, cancer is a major clinical issue that can arise from failed execution of cell death. Cancer cells can accumulate numerous genetic mutations that allow them to resist apoptotic cues, which is a key hallmark of cancer. Their resistance to apoptosis makes cancer cells especially dangerous as they gain the ability to spread throughout the body and interfere with homeostatic processes, as these unwanted cells cannot be eliminated by apoptosis. Many chemotherapeutic drugs, therefore, seek to deactivate cell cycle progression and reactivate cell death machinery. It's disconcerting, therefore, that recent evidence has shown that activation of caspases, the executioners of cell death, can actually increase tumor cell invasion and metastasis, and that activation of caspases may be counterintuitively necessary for resistance to treatment and even for angiogenesis and vascular mimicry.[175-179]

Exploration into the therapeutic potential of caspase inhibitors or other molecules that interfere with cell death machinery, therefore, urgently requires a more complete understanding of the complex nature of cell death machinery in various cell contexts, and the mechanisms by which cells die.

Just as there are many forms of taxation, there are many mechanisms by which a cell can die: necrosis, ferroptosis, pyroptosis, apoptosis, and many more. Each form of death occurs under different and specific cellular contexts, utilizes different cellular machinery, and results in varying extents of regulation of cell disassembly, ranging from careful packaging up of cellular contents into discrete packets to full-blown explosion of cellular material. Apoptosis falls on the “neat packaging” end of this spectrum.

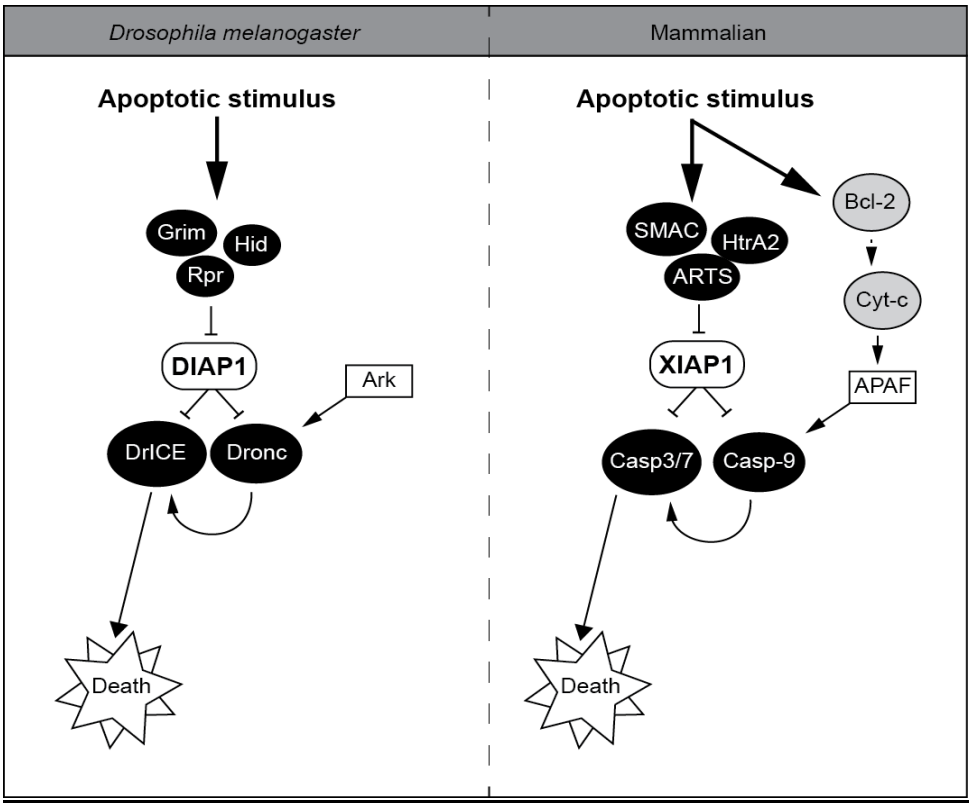

Figure 2.1 Schematic of apoptotic machinery in Drosophila and mammals. See text for details.

The organized execution of the apoptotic death program relies on a signaling cascade that ultimately regulates the cysteine aspartate-specific family of proteases known as caspases. Caspase activity

catalyzes cleavage of apoptotic substrates, which together cause the cell to adopt the progressive characteristics of apoptosis as described below, including: ROCK-mediated membrane blebbing, cytoplasmic condensation, nuclear breakdown, cell rounding, and the loss of cell polarity & cell junctions.[180, 181] Two benefits of programming such a regulated process of cell death via apoptosis are that (i) dead cells can be safely removed from a tissue without damaging neighboring tissue and (ii) its relative energetic favorability, as discrete packets of the dead cell's contents are recycled upon their engulfment by phagocytes or nearby cells.

Characterization of apoptotic machinery

Forms of cell death machinery are found throughout evolutionary history from single-celled fungi to man; in multicellular eukaryotes, apoptosis is carried out by a signaling cascade of caspases[182]. Upon induction of cell death, executioner caspases cleave key substrates that initiate the breakdown of cellular material. The full complement of apoptotic machinery consists of initiator and executioner caspases, inhibitors of apoptosis, the apoptosome, and pro-apoptotic proteins that contain IAP-Binding motifs (IBMs). While several molecular events leading up to the activation of the executioner caspases during apoptosis have been characterized, the precise mechanisms of their spatiotemporal regulation, and the factors that determine their proteolytic target(s) remain largely unknown.

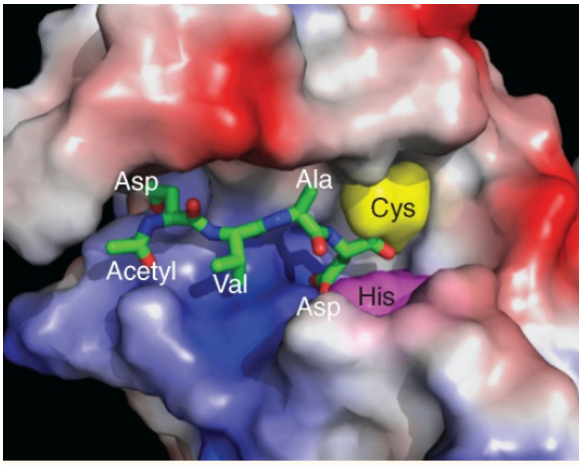

Figure 2.2 Active site of the executioner caspase. The active site of the protease, comprised of a cystine and a histidine, facilitates the cleavage of a peptide bond at a negatively charged Asp residue. From Poreba et al, 2013[4]

Caspases

Caspases were first recognized for their roles in cell death in the mid-1990s, when Horvitz and colleagues performed screens in *C. elegans* that identified a handful of genes required for cell death.[183] Among these was the Caspase-3/ DrICE homologue, *ced-3*, the absence of which prevented fated cell death in a cell-autonomous manner.[184-187] The mammalian

homologue of this protein, Caspase-3, was subsequently identified for its role in inflammation through cleavage and activation of Interleukin-1β.[188, 189]

We now know that caspases are initially produced as zymogens in the cell, meaning they initially lack proteolytic activity; their activation occurs as a result of cleavage and processing. This cleavage, which can be carried out by an initiator caspase or by auto-cleavage, frees the large N-terminal domain of the caspase (p20), which contains the catalytic cysteine and histidine residues, from the smaller C-terminal domain (p10). The resulting p20 and p10 subunits then assemble together with each other and then with a second set of p20 and p10 subunits, together forming an active tetramer with two catalytic sites. Caspases cleave their substrates using an active site "dyad" comprised of a cysteine and histidine, as seen in the crystal structure (Figure 2.2).

Traditionally, caspases have been known to preferentially target substrates at aspartate residues, specifically at a DEVD motif.[190] Although caspases are known for this specificity, recent evidence shows that they can also cleave at other residues, including a glutamate or phosphoserine.[191] Further discussion of caspase substrates can be found in Chapter 4.

As first described by Kerr and colleagues in 1972 and then expanded upon in *C. elegans* by the Horvitz lab, apoptotic cell death occurs in an ordered, stereotypical fashion indicative of the programmed nature of the process: the cell shrinks as cellular contents are condensed and bundled into discrete membrane-bound packets, which are then engulfed by phagocytes or neighboring cells.[192-195] Indeed, one of the main differences between apoptosis and other forms of death such as necrosis, is the nature of this organized and relatively energetically-favorable breakdown of cellular components, which can provide the engulfing cell with energy and can also avoid a systemic immune response.

There are several distinct morphological features of apoptosis that each are a direct result of executioner caspase activity. Apoptotic cells undergo ROCK-mediated membrane blebbing as cytoplasmic contents are

packaged into vesicle-like apoptotic bodies that are released into the cellular milieu in a myosin-dependent fashion; this process is activated when ROCK-1 is cleaved by caspases at Asp1113, thereby removing the inhibitory C-terminal domain of ROCK.[180] Eventually, apoptotic cells will undergo nuclear envelope breakdown via caspase-mediated Lamin cleavage.[196] Interestingly, an uncleavable Lamin mutant delays, but does not prevent, apoptosis, suggesting other nuclear envelope components are also cleaved.[197] Upon breakdown of the nuclear envelope, DNA is fragmented into progressively smaller units in a process that requires caspase cleavage and activation of DNA Fragmentation Factor (DFF), a DNAse enzyme.[198-200] Finally, caspases cleave the proteasome leading to decreased proteasome activity during apoptosis, presumably because the proteasome normally degrades apoptotic machinery.[201-204]

In flies, the executioner caspases that carry out such cleavage events include DrICE and DCP-1, which share sequence homology with the three human executioner caspases—caspase-3, -6, and -9. [205] In non-apoptotic cells, DrICE is inhibited by the E3 ubiquitin ligase Death-related Inhibitor of Apoptosis (DIAP1); this inhibitory function is, in fact, universally essential for preventing ubiquitous caspase activation and apoptosis. Although originally thought to inhibit DrICE by directing its proteasomal degradation, some evidence now suggests that the ubiquitination of DrICE by DIAP1 inactivates it in a proteasome-*independent* manner.[1] In apoptotic cells, on the other hand, Grim, Reaper, and Hid family proteins bind to and antagonize IAPs, thereby promoting the activity of DrICE. Interestingly, some studies have shown that Grim, Reaper, and Hid cause degradation of DIAP1, and may decrease protein translation. [206-209]

Inhibitors of apoptosis (IAPs)

The Inhibitors of Apoptosis (IAP) proteins encode E3 Ubiquitin Ligases that directly inhibit caspases. The *Drosophila* IAP, DIAP1, can directly bind DrICE and other executioner and initiator caspases, which is thought to inhibit the catalytic activity of the caspases by physical occlusion from catalytic substrates and its ubiquitylation of the caspases is required for their inactivation.[210, 211]

There is contradicting data in the field, however, about the consequences of IAP-mediated caspase ubiquitination; some groups have found that ubiquitination leads to degradation of these killer proteins, while others find that the mechanism does not. In 2008, Ditzel et al showed that DIAP1-mediated ubiquitination of DrICE does not result in DrICE degradation, but some other Ub-dependent mechanism of inhibition.[1] Mutation of 9 lysine residues to arginine in the p20 subunit was sufficient to prevent DIAP's inhibition of catalytic activity (measured by cleavage of PARP), and did so, interestingly, without interrupting its physical interaction with DrICE. Ditzel et al speculate that the mechanism by which the Ub chains inhibit DrICE is by blocking substrate contact with the proteolytic site of the caspase and potentially altering the structure of the proteolytic site itself. (Figure 7 in Ditzel et al)

One question that has not been experimentally addressed is whether ubiquitination can change the binding affinity of the caspase. It could be, for example, that ubiquitylated DrICE has a preference for non-apoptotic substrates but its non-ubiquitylated form prefers canonical apoptotic substrates (PARP, etc). It should be noted that the DrICE K→A experiments in Ditzel et al were carried out in an *in vitro* assay, and it would be interesting to see whether they hold up *in vivo* using CRISPR mutations. Additionally, Ditzel et al had to mutate a whopping 9 lysine residues on the surface of the p20 subunit of DrICE (K110, K72, K178, K76, K91, K137, K142, K183, K127) to get failure of DIAP1 to inhibit DrICE, yet a crystallographic study of a "minimalist" fraction of DrICE-BIR1 failed to identify a structural reason that those lysine residues would affect substrate binding to DrICE, and it appears that none of these lysine residues are evolutionarily conserved.

Initiator caspases and the apoptosome

A cell's commitment to death via apoptosis is under strict regulation. One of the failsafe mechanisms that ensures a commitment to cell death only occurs when necessary involves the activation of the executioner caspases, which, in the traditional model of apoptosis, strictly occurs as a result of their cleavage by initiator caspases. Biochemical studies on this complex system suggest that these many failsafe mechanisms are determined by abundant competition among proteins for DIAP1 binding—diap1 inhibits itself, N-terminal

regions of RHG outcompete Dronc/ DrICE for DIAP1 binding (at BIR1/2 domains respectively). The released Dronc is activated at the apoptosome, at which point it can then cleave and activate DrICE.[212]

Caspase activation by extrinsic mechanisms

Extracellular ligands bind to death receptors (Fas) at the plasma membrane to cause their activation. The receptors oligomerize, recruiting proteins to their intracellular domain (FADD), which in turn recruits the initiator caspases-6 and -8, resulting in their proximity-induced dimerization [213]. Together this complex is known as the Death Induced Signaling Complex (DISC) [214], and allows caspase-6 mediated cleavage and consequent activation of the executioner caspases including Caspase-3.

Caspase activation via intrinsic (mitochondrial dependent) mechanisms

Upon an intrinsic signal like membrane permeability, the mitochondrial proteins Bak and Bax mediate the release of cytochrome c from the intermembrane space of the mitochondria. This induces activation of the apoptosome complex through its interaction with the adaptor protein Apoptotic Protease Activating Factor 1 (Apaf1), to induce dimerization and autocatalytic activation of Caspase-9, which can also cleave and activate the executioner caspases including Caspase-3.

Non-apoptotic caspase function

Consistent with our findings that DrICE is essential to tracheal elongation in the developing embryo, it is clear that caspase activity is not restricted to cell death. Our system does not seem to be an exception to the rule—there is now a growing number of caspase-dependent processes that are known to promote cell proliferation, differentiation, and morphological changes in non-apoptotic cells. For example, non-apoptotic caspase functions have been implicated in the following processes: (a) *D. melanogaster* sperm individualization and (b) border cell migration, and (c) human terminal differentiation.[215-218]

Drosophila spermatid individualization

In *Drosophila*, DrICE is required for male gamete maturation, specifically for a process called spermatid individualization. After meiosis, clusters of precursor *Drosophila* sperm cells are attached together as cysts of round cells that must be separated from each other, elongated, and dramatically lose mass before they are mature. This process requires DrICE, the *Drosophila* Cytochrome c gene, cyt-c-d, and requires the Ubiquitin-conjugating enzyme dBruce.[215, 219] The phenotypic changes associated with spermatid individualization, which also require endocytic machinery such as Clathrin and Rab11, appear very similar to apoptosis, but whether these processes also overlap in mechanism is unclear.[220, 221]

Drosophila border cell migration

During the development of *Drosophila* germ cells, a group of somatic epithelial border cells normally undergoes a migration toward the oocyte. In 2004, Geisbrecht and Montell demonstrated that the process of border cell migration is dependent on the presence of DIAP1 (though independent of its function as an E3 ubiquitin ligase).[222] Their experiments demonstrate that DIAP1 is **downstream** of the GTPase Rac, which is known to affect border cell migration via actin rearrangement: overexpression of DIAP1 suppresses the migration defect caused by a dominant negative allele of Rac. Because Caspase-3 had previously been shown to directly cleave and inactivate Rac, the authors speculated that overexpressing DIAP is sufficient to rescue the migration defect by suppressing caspase-mediated inactivation of Rac.[223] This speculation, however, would place DIAP1 **upstream** of Rac, a fact that is inconsistent with their data, including the clear result that overexpression of Rac^{WT} resulted in increased DIAP1 staining. This inconsistency could be explained by two hypotheses: (b) a non-linear pathway in which caspase activity could serve as a negative feedback loop to inactivate Rac does not seem likely, as, they do not observe an increase in abundance of Rac-GTP in S2 cells overexpressing DIAP1, which suggests that derepression of caspase activity is not sufficient to derepress Rac. The second, more likely, hypothesis is that DIAP1 transcription is increased due to inactivation of upstream components of the Hippo Network, which has previously been shown to occur as a result of F-actin rearrangements.[137] They were able to pull down both Rac-GTP and Rac-GDP with GST-DIAP1, suggesting that there is a physical interaction between DIAP1 and Rac, a finding

replicated in human cells in 2012.[224] Altogether, Geisbrecht and Montell show that DIAP1 is required for border cell migration, and that overexpression of the DrICE inhibitor p35 fails to rescue the Rac migration defect, suggesting that the effects of DIAP1 is not DrICE-dependent. The mechanism of caspase-mediated inhibition of border cell migration remains to be determined, but was recently corroborated by experiments in *Drosophila* imaginal discs, where loss of DrICE resulted in the acquisition of migratory capacity in irradiated cells, which was lost with concomitant loss of Rac. [225]

Terminal stem cell differentiation in humans

The terminal differentiation steps of many tissues require drastic cytological changes. For example, during terminal mammalian erythropoiesis, red blood cells lose all of their organelles, in part involving exosomes.[226] The enucleation of red blood cells is specifically aided by caspase cleavage of Lamin in the nuclear envelope.[227] This is similar to the process of terminal differentiation of human skin cells, keratinocytes, in which the nucleus must be lost.[228] Unlike tracheal morphogenesis, these morphological changes are reminiscent of those of in apoptotic cell—loss of nuclear material, ejection of cytoplasm, etc—with each of these processes requiring Caspase-3.[229]

Caspases inhibit autophagy

Cellular contents can often be degraded for energy in autophagy, the process of "self-eating." In autophagy, various contents of the cell are sequestered into self-contained double-membrane vesicles called the autophagosome, which then fuses with the lysosome where constituent proteins can be broken down for energy. The precise mechanisms by which caspases contribute to apoptosis remain unknown, but in general, caspases tend to push a cell away from autophagy, in favor of apoptosis. Some data has shown that caspases can directly cleave autophagic proteins (ATGs), in order to inhibit their function. In addition, caspases have been shown to cleave Beclin-1, which sits at the nexus between death and autophagy. However, data from human endothelial cells has shown that caspases promote autophagy by facilitating exocytosis of autophagic vacuoles. [230]

Caspase activity in apoptosis & cell survival: two sides of the same coin

Apoptosis-independent caspase activation and substrate cleavage has now been demonstrated in many systems, including proper neuronal development, *Drosophila* spermatid individualization, and many others. [215, 231] The fact that caspases contribute to essential cellular processes in addition to cell death is consistent with the observation that DrICE is maternally deposited in the *Drosophila* embryo. [232]

Such apoptotic machinery must be tightly regulated, since excessive death can be catastrophic to tissues and organisms. In humans, alterations in apoptotic function are found across varied forms of cancer, neurological disorders, cardiovascular disorders, and autoimmune diseases [233-243]. Despite the potential for disaster mediated by unfettered caspase activity, however, there are several essential cellular processes that are, in fact, known to require executioner caspase activity. Perhaps the biggest question in the study of non-apoptotic caspase function is how cells utilize deadly apoptotic machinery—including caspases—without inducing cell death. We do not clearly understand the molecular mechanisms that determine a cell's apoptotic potential. One model from Florentin and Arama proposes the existence of "major and minor" caspases to regulate a course and fine focus of death. In this model, for example, while DrICE and Dcp1 are both executioner caspases related to the mammalian Caspase-3, their different abilities to execute apoptosis would be attributable to "intrinsic properties" that make DrICE a much more efficient killer (a major caspase) than Dcp1 (a minor caspase).[244] Although this is possible in some contexts, we favor several hypotheses to explain our observations in the trachea: (a) distinct subcellular localization of activated executioner caspases protects apoptotic substrates,[245] (b) caspases have an increased binding affinity for non-apoptotic substrates, (c) post-translational modifications such as ubiquitination can affect caspases' substrate specificity, and others that are discussed in Chapter 4.

Fifteen years ago, it was thought that the non-apoptotic targets of caspases were "not relevant substrates but simply 'innocent bystanders'." [246] The revelation that caspases can be critical for non-apoptotic processes, is critical for many reasons, and has broad implications in the fields of developmental biology,

cell biology, cell death and medicine, which are also discussed at length in Chapter 4.

II. Introduction

The majority of the following text was published in Nature Communications in March of 2019.[247]

Although well known for its role in apoptosis, the executioner caspase DrICE has a non-apoptotic function that is required for elongation of the epithelial tubes of the *Drosophila* tracheal system. Here, we show that DrICE acts downstream of the Hippo Network to regulate endocytic trafficking of at least four cell polarity, cell junction and apical extracellular matrix proteins involved in tracheal tube size control: Crumbs, Uninflatable, Kune-Kune and Serpentine. We further show that tracheal cells are competent to undergo apoptosis, even though developmentally-regulated DrICE function rarely kills tracheal cells. Our results reveal a developmental role for caspases, a pool of DrICE that colocalizes with Clathrin, and a mechanism by which the Hippo Network controls endocytic trafficking. Given reports of *in vitro* regulation of endocytosis by mammalian caspases during apoptosis, we propose that caspase-mediated regulation of endocytic trafficking is an evolutionarily conserved function of caspases that can be deployed during morphogenesis.

Epithelial tubes of precise sizes are essential for gas exchange and nutrient delivery in animal tissues. Failure of correct tube sizing can lead to fatal disease[7, 8], yet the cellular and molecular mechanisms that regulate tube size remain poorly understood. To uncover these mechanisms, we study the tracheal system of the *Drosophila* embryo, a ramifying tubular network that serves as the fly's combined pulmonary and vascular systems[248].

The diameter of the largest tube in the tracheal system, the dorsal trunk (DT), increases two-fold as length increases ~15% over a 2.5 h period during mid-embryogenesis, and it does so with no accompanying changes in cell number[249]. Instead, DT dimensions are regulated by a complex set of interacting pathways that all rely on the endocytic system. An apical/lumenal extracellular matrix (aECM) that restricts elongation

depends on regulated secretion and endocytosis of matrix-modifying proteins such as Serpentine (Serp)[56]. Basolateral cell-junctional complexes called Septate Junctions (SJs) also restrict DT dimensions. SJs contain a diverse range of proteins including the claudin-family member Kune-Kune (Kune), the FERM-domain protein Yurt (Yrt)[250, 251] and the MAGUK Discs Large (Dlg)[252]. As with the aECM, formation and maintenance of SJs require endocytic trafficking[253]. Apically-localized regulators of DT dimensions also interact with the endocytic pathway, including the polarity protein Crumbs (Crb)[57, 58, 254, 255] and the transmembrane protein Uninflatable (Uif)[256]. The endocytic system therefore plays a central role in regulating diverse tracheal size determinants, but how the endocytic pathway is itself regulated in this context is poorly understood.

One candidate pathway that could regulate intracellular trafficking is the highly conserved Hippo Network (HN), which controls growth in diverse organisms and tissues[257]. Organ growth is promoted upon nuclear translocation of the HN effector Yorkie (Yki) in *Drosophila*, or its mammalian homolog Yes-Associated Protein (YAP). Yki and YAP are transcription factors that activate genes required for growth and resistance to apoptosis, including the Inhibitors of Apoptosis (IAPs), which inactivate caspases[258]. When Yki/YAP activity is low, organ size is typically reduced due to apoptosis resulting from derepressed caspase activity[259]. However, we previously observed that loss of Yki or Death-associated inhibitor of Apoptosis (Diap1*)* causes overelongated trachea despite a normal number of cells. Thus, Yki and Diap1 regulate tube size independently of apoptosis[5].

Here, we show that the caspase-3 homolog DrICE acts downstream of Yki and Diap1 to regulate tracheal elongation. Instead of causing cell death, DrICE regulates endocytic trafficking of tracheal size determinants. This work reveals an intersection of the HN, caspases and the endocytic system that has critical functions during normal development. Consistent with previous evidence that mammalian caspases can control endocytic trafficking during apoptosis[260], we propose a model in which regulation of endocytic trafficking is an evolutionarily conserved function of caspases that can be activated with or without triggering cell death, to contribute to morphogenesis or apoptosis, depending on cellular context.

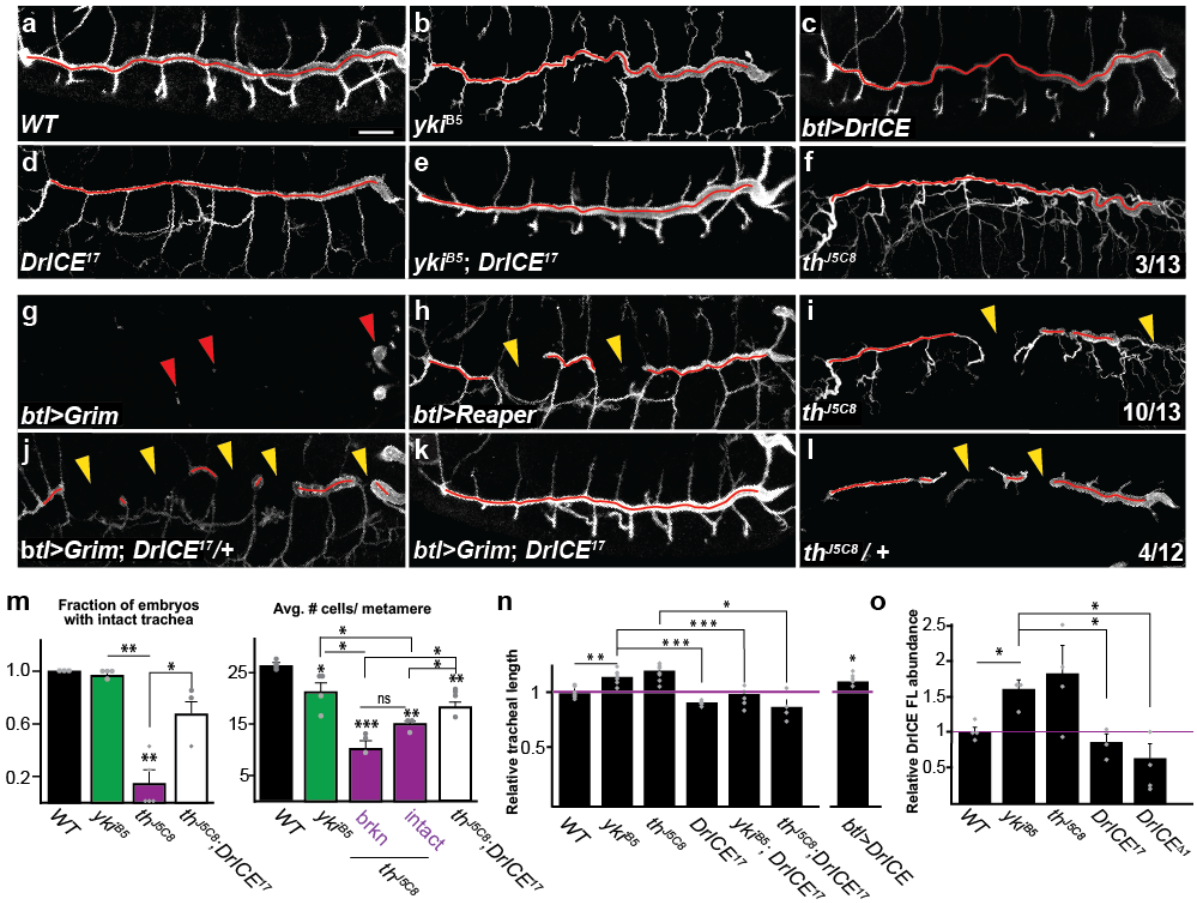

Figure 2.3 DrICE governs tracheal size downstream of Yorkie without triggering apoptosis.
(a-l) Compared to WT (w^{1118}) (a), the dorsal trunks (DTs) of yki^{B5} mutant embryos (b) and those overexpressing DrICE in the tracheal system (*btl>DrICE*) (c) are elongated, while DTs in $DrICE^{17}$ are too short (d). $DrICE^{17}$ is epistatic to yki^{B5} since yki^{B5}; $DrICE^{17}$ double mutants do not have long trachea (e). Loss of the DrICE inhibitor Diap1/*th* can cause tracheal over-elongation (f) or missing DT segments when homozygous (i) or heterozygous (l). Expression of the pro-apoptotic genes *btl>Grim* (g) or *btl>Reaper* (h) causes segment loss dependent on $DrICE^{17}$ dosage (j, k). Red arrows in g mark remnants of the tracheal system, while yellow arrowheads in h-l mark missing dorsal trunk segments. Scale bar for a-l in a, 25 μm. **(m)** Loss of Diap1 (th^{J5C8}) decreases the number of embryos with intact dorsal trunks (N=17 embryos over 5 experiments) and the number of tracheal cells (N=6 embryos total: 3 broken, 3 intact), indicating apoptosis. The loss of intact trachea and overall cell numbers can be suppressed by $DrICE^{17}$ (N=20 over 3 experiments and N=4 respectively). Neither cell death nor dorsal trunk breaks are present in yki^{B5} embryos (N=4). **(n)** DT length in single and double mutant combinations of HN and DrICE mutants. DT length normalized to WT (w^{1118}) (N=10) for HN and DrICE mutants, and to *btl-Gal4, UAS-GFP/+* for overexpressed DrICE (*btl-Gal4 UAS-GFP/+; UAS-DrICE/+*) ($N \geq 5$ for all except N=4 for th^{J5C8};$DrICE^{17}$). **(o)** Western blot of stage 16 embryos using the α-$DrICE^{CST13085}$ antibody, which recognizes full-length DrICE. The 47kDa DrICE full-length band was quantified relative to total protein from at least three experiments. DrICE protein levels in $DrICE^{17}$ homozygotes are not different than WT, consistent with $DrICE^{17}$ being a dominant negative allele that causes more severe tracheal phenotypes than $DrICE^{\Delta 1 5}$ (n,o). (N=4 blots). For all graphs, each data point is indicated as a point. Error bars, S.E.M. *p<0.05; **, p<0.005; ***, p<0.0005 Student's t-test.

III. Results

DrICE governs tracheal size downstream of the Hippo Network

We previously showed that DrICE is required for tracheal dorsal trunk elongation, potentially downstream of the HN[5]. Tracheae fail to elongate normally in embryos homozygous for the *DrICE$^{\Delta 1}$* allele, which deletes the DrICE coding sequence[219], but embryos mutant for Yki and Diap1, both of which negatively regulate DrICE, have overly elongated tracheae at stage 16. These results were consistent with, but did not show, that DrICE acts downstream of Yki and Diap1 in tracheal elongation.

We tested whether reduction of DrICE could suppress the long tracheal phenotypes caused by the *yorkie^{B5}* mutation[261], or that of its transcriptional target Diap1, which is encoded by the *thread (th)* locus[5, 71, 262]. Single loss-of-function mutants *yki^{B5}* and *th^{J5C8}* each have elongated trachea that follow irregular sinusoidal paths (Fig. 2.3b,f,n), but double mutant trachea of the genotypes *yki^{B5}*; *DrICE^{17}* or *th^{J5C8}*, *DrICE^{17}* are straight and have either WT lengths or have reduced lengths of *DrICE^{17}* mutants (Fig. 2.3d,e,n). These results indicate that DrICE acts downstream of, or in parallel to, Yki, Diap1 and the HN.

For the above experiments, and most of the subsequent experiments in this report, we used the *DrICE^{17}* allele, which has a point mutation[263] in a region near the substrate binding site of DrICE. However, in contrast to a previous report that *DrICE^{17}* is a protein-null allele[263], using different antibodies we find that *DrICE^{17}* generates a stable protein (Fig. 2.3o and Fig. 2e-f), and causes a stronger tracheal phenotype than *DrICE$^{\Delta 1}$*, the null allele[5]. Thus, *DrICE^{17}* behaves as a dominant negative allele that competes with maternally contributed DrICE.

To distinguish between downstream or parallel action of DrICE with respect to the HN, we used western blotting on stage 16 embryos to show that wild-type (WT) DrICE protein levels are elevated by approximately 50% in both *yki^{B5}* and *th^{J5C8}* mutant embryos (Fig. 2.3o). Together, these results confirm that DrICE is necessary for dorsal trunk elongation and that DrICE acts downstream of the HN.

DrICE is sufficient to elongate trachea

We then asked if DrICE expression is sufficient to drive tracheal elongation without increased upstream HN activity by expressing UAS-DrICE in the tracheal system using the UAS-Gal4 system[264], specifically with the *breathless (btl)-Gal4* driver[264, 265]. This overexpression results in elongated tracheae, similar to *yki*^{B5} mutants (Fig. 2.3c,n). DrICE is therefore necessary and sufficient to drive tracheal elongation.

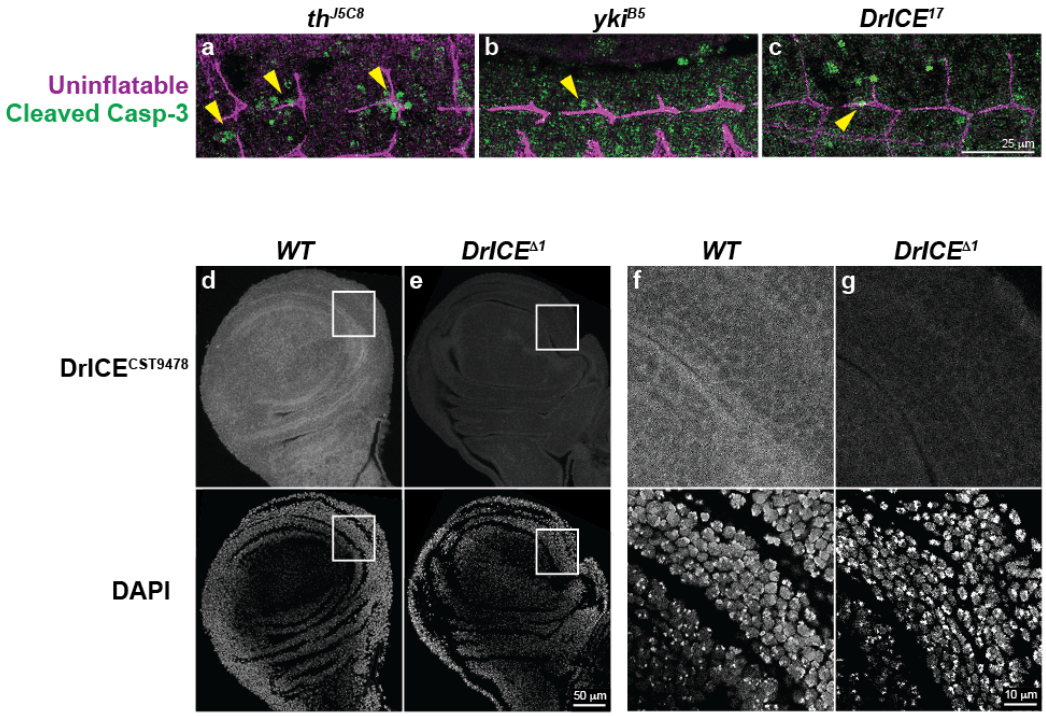

Figure 2.4 Cleaved caspase staining in Diap1/*th embryos* and *DrICE*$^{\Delta 1}$ imaginal discs.
(a-c) Maximum projections of anti-cleaved caspase-3 staining, considered a marker of apoptotic cells,[2] shows that trachea of stage 13 *th*^{J5C8} embryos have noticeably more cleaved Caspase-3 staining than either (b) *yki*^{B5} or (c) *DrICE*^{17} embryos. As *th*^{J5C8} embryos also have a decreased total number of tracheal cells (Fig. 2.3m), these data support the conclusion that missing in the dorsal trunk segments in *th*^{J5C8} embryos (Fig. 2.3i) result from increased tracheal cell apoptosis. Scale bar for a-c in c, 25 µm.
(d-g) Staining WT (*w*^{1118}) late larval wing imaginal discs with DrICE^{CST9478} (low magnification view in e; magnification of the boxed region is shown in f) reveals a pattern of subcellular localization similar to embryonic tracheal cells. (e, g) DrICE^{CST9478} staining is absent in *DrICE*$^{\Delta 1}$ mutant wing discs, supporting the conclusion that the DrICE^{CST9478} signal present in *DrICE*$^{\Delta 1}$ mutant embryos (Fig. 2.5h) results from maternal contribution of DrICE. Bottom row shows DAPI staining of tissue. Scale bar for d-e in bottom of e, 50 µm; for f-g in bottom of g, 10 µm.

Tracheal cells are not refractory to apoptosis

Although the executioner caspase DrICE is necessary for tracheal elongation, few (<3%) tracheal cells undergo apoptosis during wild-type morphogenesis.[2] This raises the question of how a caspase can act in a developmental process without triggering apoptosis. We investigated the possibility that apoptosis maybe disabled in the developing trachea by analyzing loss-of-function mutants for the caspase inhibitor Diap1 (*th*^{J5C8}). We previously showed that *th*^{J5C8} mutant embryos with contiguous dorsal trunks have elongated trachea despite a WT number of cells[5], but a more comprehensive analysis of *th*^{J5C8} mutants here revealed that the majority of *th*^{J5C8} embryos, are in fact missing dorsal trunk segments (Fig. 2.3i). Strikingly, 25% of heterozygous[266] *th*^{J5C8} embryos displayed missing tracheal segments (Fig. 2.3l), suggesting that tracheal cells are capable of undergoing caspase-mediated apoptosis.

We confirmed the existence of apoptosis in *th* mutant trachea by counting the number of tracheal nuclei. In stage 16 *th*^{J5C8} DT segments, tracheal cell number is reduced by an average of 55% compared to WT ($p<0.0001$ Student's t-test for DT segments 5-6, Fig. 2.3m). Notably, average DT cell number drops from 26 in WT to 15 in *th* DT segments that are intact, and to only 10 in broken DTs, suggesting that there is a minimal number of cells that are required to assemble or maintain DT segments (Fig. 2.3m). Further evidence that the missing tracheal cells in *th* mutants underwent caspase-mediated apoptosis is provided by the presence of cells with strong cleaved caspase staining in *th* mutants (Fig. 2.4a), and by the 150% suppression of DT breaks and 140% increase in the number of tracheal cells in *th*^{J5C8} *DrICE*^{17} mutants (Fig. 2.3m). Thus, the apoptotic roles of Diap1 and DrICE are maintained in tracheal cells during normal morphogenesis.

Interestingly, in contrast to *th*^{J5C8} mutants, loss of Yki, which is a key transcriptional co-activator of Diap1[68, 267], does not induce DT breaks and only reduces tracheal cell number from 26 to 21 (Fig. 2.3m). This observation suggests that a basal level of Diap1 expression may protect tracheal cells from DrICE-mediated apoptosis in *yki*^{B5} mutants, yet still allow elevated DrICE activity to elongate tracheal cells.

To further test the apoptotic potential of tracheal cells, we expressed the pro-apoptotic genes Grim and Reaper [268] in the developing trachea using the *btl*:*Gal4* tracheal driver. Overexpression of Grim largely eliminates the tracheal system (Fig. 2.3g). Reaper overexpression results in the loss of one or two tracheal dorsal trunk segments in most embryos, similar to the homozygous th^{J5C8} mutant phenotype (Fig. 2.3h,i). Critically, the lethal effects of Grim overexpression are dominantly suppressed by one copy of the $DrICE^{17}$ allele (Fig. 2.3j), and homozygous $DrICE^{17}$ blocks the ability of Grim to destroy the tracheal system (Fig. 2.3k). Taken together, these results demonstrate that tracheal cells are not refractory to apoptosis— they have a functional caspase-dependent apoptotic system that does not kill cells during normal development, despite the requirement for DrICE in tracheal elongation.

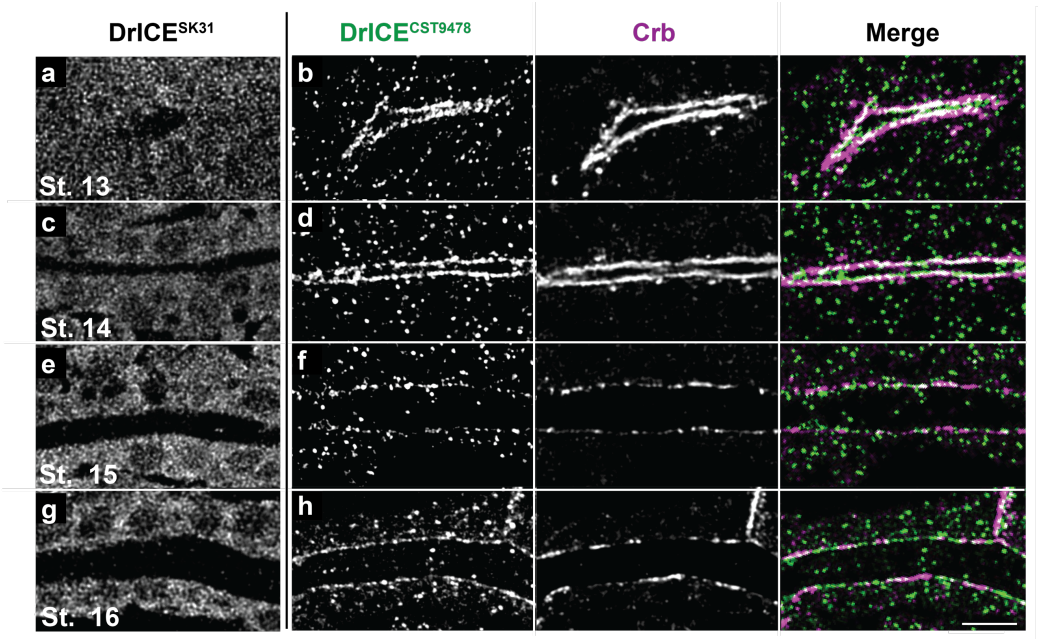

Figure 2.5 Developmental profile of DrICE with Crumbs (a-h) The α-$DrICE^{SK31}$ antibody against full-length $DrICE^{1}$ (a,c,e,g) reveals broad cytoplasmic staining during stages 13-16 (St.13-St. 16). Staining with the α-$DrICE^{CST9478}$ antibody that was raised against a peptide that is cleaved during DrICE activation (Cell Signaling Technologies #9478) reveals a more restricted punctate pattern that is enriched at the tracheal apical surface (b, d, f, h; green) where it overlaps with staining for the apical marker Crumbs (Crb, b, d, f, h; magenta), particularly during tube expansion at stages 13 and 14 (b,d). Scale bar for a-h 5 μm.

Punctate DrICE is enriched at the tracheal apical surface

To explore the mechanism by which DrICE mediates tracheal elongation, we considered whether DrICE might be spatially compartmentalized in non-apoptotic cells. Previous studies in both mammalian and non-mammalian tissues have revealed intriguing patterns of caspase localization (Table 2.2). For example, Amcheslavsky *et al.* showed that the initiator caspase Dronc is localized basally for non-apoptotic roles in larval imaginal discs[269]. In our case, staining with the α-DrICE^{SK31} antibody, raised against full-length DrICE protein[1, 270], produces a diffuse cytoplasmic signal in WT trachea that is greatly reduced in the nucleus (Fig. 2.4a). A different pattern of staining is observed with the α-DrICE^{CST9478} antibody, which is raised against a peptide N-terminal to the Asp230 cleavage site of DrICE and is reported to preferentially recognize the cleaved form of DrICE (Cell Signaling Technologies, #9478). α-DrICE^{CST9478} signal is localized to numerous cytosolic punctae that are enriched at the apical surface of tracheal cells, particularly during stages 13 and 14 (Fig. 2.6b, Fig. 2.5b,e,h,k). Thus, there is a pool of DrICE that is localized separately from the inhibitor Diap1 which could potentially allow DrICE to elongate the trachea without triggering apoptosis.

Cellular localization of caspase-3	Tissue	Method	Reference
	Mammalian:		
Cytosol (uniform)	HeLa cell line	GFP-tagged casp-3 transfected	[271]
Shifting localization from inside surface of cell membrane to cytoplasm and finally nuclear region, upon induction of apoptosis with x-ray radiation	MOLT-4 cell line	?	[272]
Cytosol / nucleus (uniform; apoptotic cells)	Lymph nodes of patients with oral squamous cell carcinoma	Immunohistochemistry	*See note*
Cytosol / nucleus: (slightly punctate, mostly uniform)	Human liver carcinoma cell line	Poly- and monoclonal antibodies against peptide near proteolytic Cysteine	[273]
Cytosolic (uniform)	Human liver carcinoma cell line	GFP-tagged casp-3 transfected	[273]

Cytosolic (uniform; apoptotic cells)	Small intestine and colon	Immunohistochemistry	[274]
Cytosolic? varied parts of dental epithelium over time	Developing mouse molars	Immunohistochemistry	[275]
Largely cytosolic	Neuroblastoma cell lines	Cytosolic / nuclear isolation + western	[276]
	Non-mammalian:		
Plasma membrane	Non-apoptotic *Drosophila* imaginal discs	Immunohistochemistry for Dronc	[269]
Punctate Cytosol	Dissected *Drosophila* salivary gland	Immunohistochemistry for DrICE	[277]
Perinuclear	*C. elegans* germ cells	GFP-tagged Ced-3	[278]
Colocalizes with F-actin at cell boundaries	*Drosophila* salivary gland (larvae)	Dronc IF (Fig 3)	[279]

Table 2.1 Previously observed caspase localization. See text for details.

DrICE partially co-localizes with Clathrin

The punctate pattern of α-DrICE^{CST9478} signal resembles that of intracellular trafficking machinery, suggesting that this pool of DrICE may associate with trafficking compartments. We tested for colocalization of α-DrICE^{CST9478} signal with markers of endocytic vesicle formation (Clathrin), and for early (Rab5), recycling (Rab11), or late (Rab7) endosomes. Punctate DrICE^{CST9478} signal partially overlaps with Clathrin both at the apical surface and in cytosolic regions (yellow arrowheads, yellow box and inset in Fig. 2.6l, respectively; 23% overlap; Pearson R= 0.25). However, there is only sporadic co-localization with Rab5 (Fig. 2.6m; 3.8% overlap, R=0.06), Rab11 (Fig. 2.6n; 6% overlap, R=0.1) or Rab7 (Fig. 2.6o; 2% overlap, R=0.12,) early, late and recycling endosomes respectively. The pool of DrICE defined by α-DrICE^{CST9478} is therefore positioned to regulate tracheal size by influencing Clathrin-mediated endocytosis and subsequent trafficking of proteins that determine tracheal size. In addition, the incomplete co-localization of DrICE^{CST9478} signal with Clathrin suggests that multiple pools of DrICE exist, which supports the idea that DrICE acts in multiple independent functions, including apoptosis.

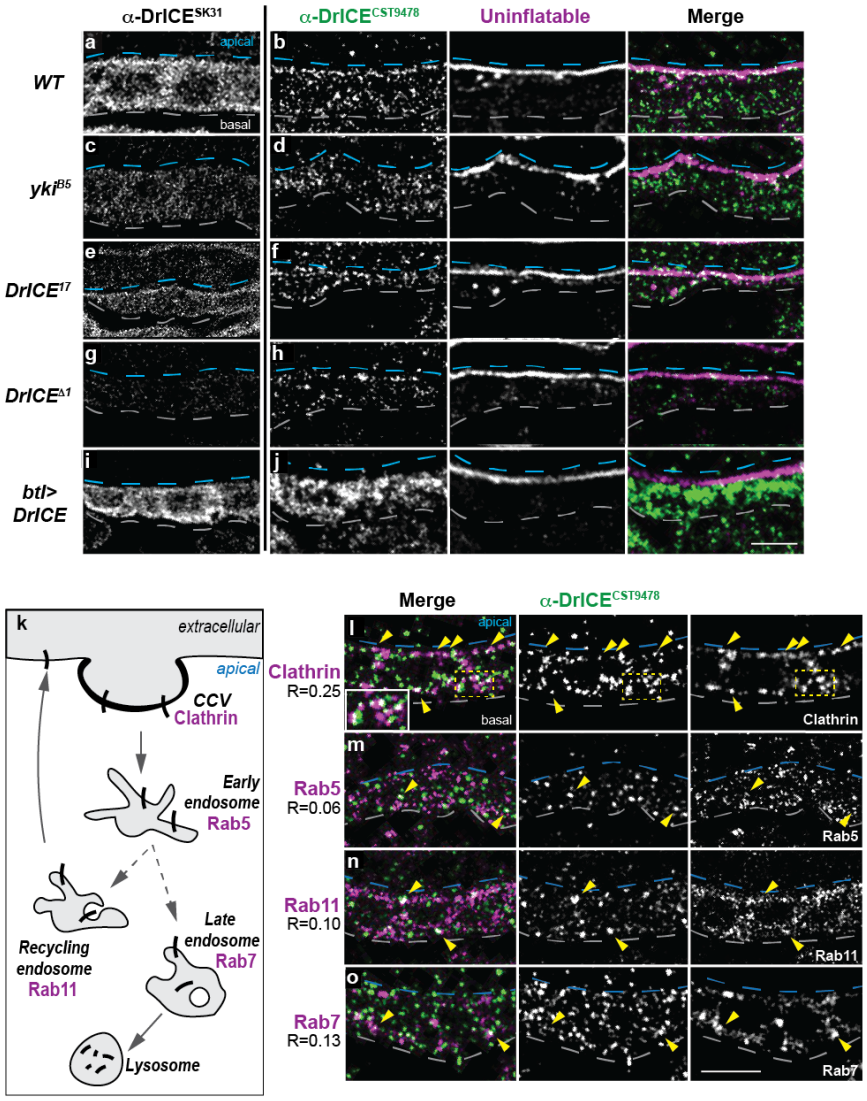

Figure 2.6 A pool of DrICE partially co-localizes with Clathrin. (a-j) Staining with the α-DrICE^{SK31} antibody against full-length DrICE (a,c,e,g,i) reveals broad cytoplasmic signal in WT trachea (a) that is reduced in trachea zygotically homozygous for the null allele *DrICE^{Δ1}* (g) and elevated in trachea overexpressing DrICE (i). Staining with α-DrICE^{CST9478} (b,d,f,h,j), which was raised against a peptide containing the DrICE sequence that is cleaved during activation, reveals a more restricted punctate pattern that is enriched at the tracheal apical surface in WT trachea (dashed blue lines), and particularly at earlier developmental stages (Fig. 2.5b,e). α-DrICE^{CST9478} signal is reduced in *DrICE^{Δ1}* trachea (h), elevated in trachea overexpressing DrICE (j). DrICE^{CST9478} signal in h results from the maternal contribution of DrICE that is also observed by western blot in Fig. 2.3o and is absent in late larval tissue (Fig. 2.4d-g). **(k)** Partial schematic of the endocytic system showing the roles of endocytic markers. **(l-o)** Localization of DrICE^{CST9478} signal with markers of the endocytic system in WT (*w^{1118}*) trachea. α -DrICE^{CST9478} signal shows partial colocalization with Clathrin (l) but not and Rab5 (m), with Rab11 (n) or Rab7 (o). Colocalization was quantified in 2 ROIs in each of *N*≥3 z-slices for *N*≥4 embryos. Source data are provided as a source data file. Blues dashed lines mark the apical cell surface, white dashed lines mark the basal cell surface. Scale bar for a-j in j, 5 μm; for l-o in o, 5 μm.

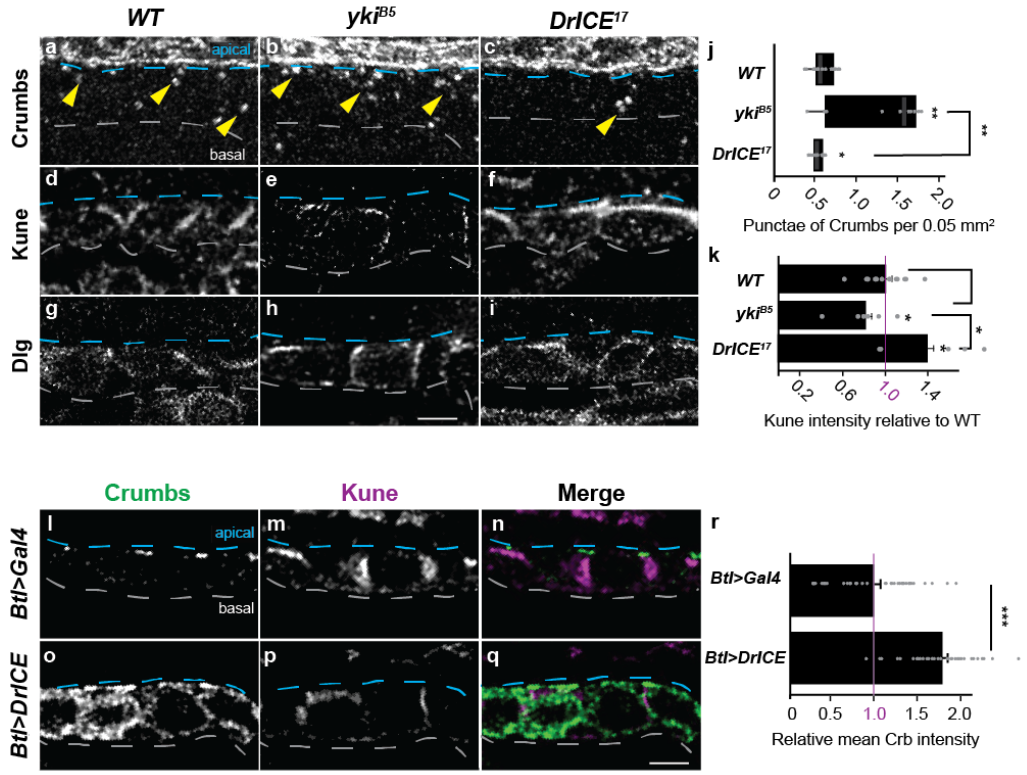

Figure 2.7 DrICE regulates abundance and localization of the size determinants Crb and Kune
(a-c) Number of Crb cytosolic punctae (yellow arrowheads) is increased in *yki*^{B5} mutants (b) but decreased in *DrICE*^{17} mutants (c) compared to WT (*w*^{1118}) (a) at stage 14.
(d-f) Cytoplasmic Kune abundance is decreased in *yki*^{B5} and increased in *DrICE*^{17} relative to *w*^{1118}. Quantification in k. **(g-i)** Levels of the basolateral septate junction protein Dlg appear minimally affected in *yki*^{B5} and *DrICE*^{17} mutants, indicating that the ability of DrICE to regulate trafficking is selective.
(j) The number of cytoplasmic punctae of Crumbs at embryonic stage 14 is reduced in *DrICE*^{17} tracheal cells compared to *w*^{1118} and increased in *yki*^{B5} relative to *w*^{1118}. Punctae were counted in 2 ROIs in each of 2 *z*-slices for *N*≥5 embryos and normalized to ROI area. Center line represents the median, box limits are the upper and lower quartiles, whiskers are 1.5X interquartile range. **(k)** Mean intensity of Kune in a maximum projection of the fifth tracheal metamere was measured in N≥5 embryos of each genotype then normalized to the WT (*w*^{1118}) control. **(l-q)** Overexpression of DrICE in the trachea increases Crb levels relative to the control at stage 16 (l vs. o), consistent with the decrease of Crb punctae in stage 14 *DrICE*^{17} mutants. Quantified in **r**. Conversely, Kune levels are decreased when DrICE is overexpressed (m vs. p). **(r)** Cytoplasmic Crb abundance is dramatically increased in *btl>DrICE* relative to *btl>Gal4/+*. Mean Kune intensity was measured in 2 ROIs in each of 5 *z*-slices for *N*=4 embryos of each genotype and quantified relative to the *btl>Gal4/+* control.
For all graphs, error bars represent S.E.M and each data point is represented as a point. Source data are provided as a source data file. Blues dashed lines mark the apical cell surface, white dashed lines mark the basal cell surface. Scale bar for a-i in i, 2.5 μm; for l-m in m, 2.5 μm. *p<0.05; **, p<0.005; ***, p<0.0005 Student's t-test.

In addition to its role in early endocytosis, Clathrin also mediates protein trafficking from the transgolgi network (TGN). Because the overlap of Clathrin with DrICE appears to be both apical and cytosolic (Fig.

2.6l, arrowheads), the intracellular co-localization of α-DrICE^{CST9478} signal and Clathrin suggests that DrICE could also influence Clathrin-mediated TGN trafficking.

DrICE alters the trafficking of apical Crbs and Uif

Because transmembrane determinants of tracheal tube size including Crb and Uif are known to be trafficked through endocytic compartments[57, 58], we asked if DrICE associates with compartments containing these proteins. In WT stage 16 tracheae, DrICE^{CST9478} signal partially overlaps with Uif (Fig. 2.6b, 12% colocalization, Pearson correlation R=0.21) and Crb (Fig. 2.5h, magenta; 17% colocalization, R=0.27), but shows stronger overlap with Crb at the apical surface during tube expansion at stages 13-14 (Fig. 2.5b,d). An apical pool of DrICE is therefore positioned to directly regulate trafficking of apical markers.

We tested if there were functional interactions between DrICE and transmembrane apical markers by examining Crb and Uif in *DrICE^{17}* mutants. Overall apical/basal polarity as assessed by Crb staining is largely unaffected in *DrICE^{17}* mutations. Levels of apical and cytosolic Crb are not significantly altered in *DrICE^{17}* mutants at stage 16, but in stage 14 embryos, fewer Crb-positive cytosolic punctae were visible in *DrICE^{17}* mutants than in WT ($p<0.05$ Student's t-test, Fig. 2.7a, c, j) and conversely more punctae were present in *yki^{B5}* mutant trachea than in WT ($p<0.005$ Student's t-test, Fig. 2.7a-b, j). Similarly, over-expression of DrICE in the tracheal system increases Crb levels at stage 16 ($p<0.0005$ Student's t-test, Fig. 2.7l-r). No significant changes in Uif abundance or distribution were observed in *DrICE* mutant tracheae (Fig. 2.6f,h), but *DrICE^{17}* suppresses the increased abundance of Uif positive punctae in the tracheae of embryos mutant for the basolateral polarity protein Yurt ($p<0.005$ Student's t-test; Fig. 2.8a-d, i). Moreover, *DrICE^{17}* also suppresses the increased tracheal length of the *yrt^{65A}* mutants ($p<0.005$ Student's t-test, Fig. 2.8j).

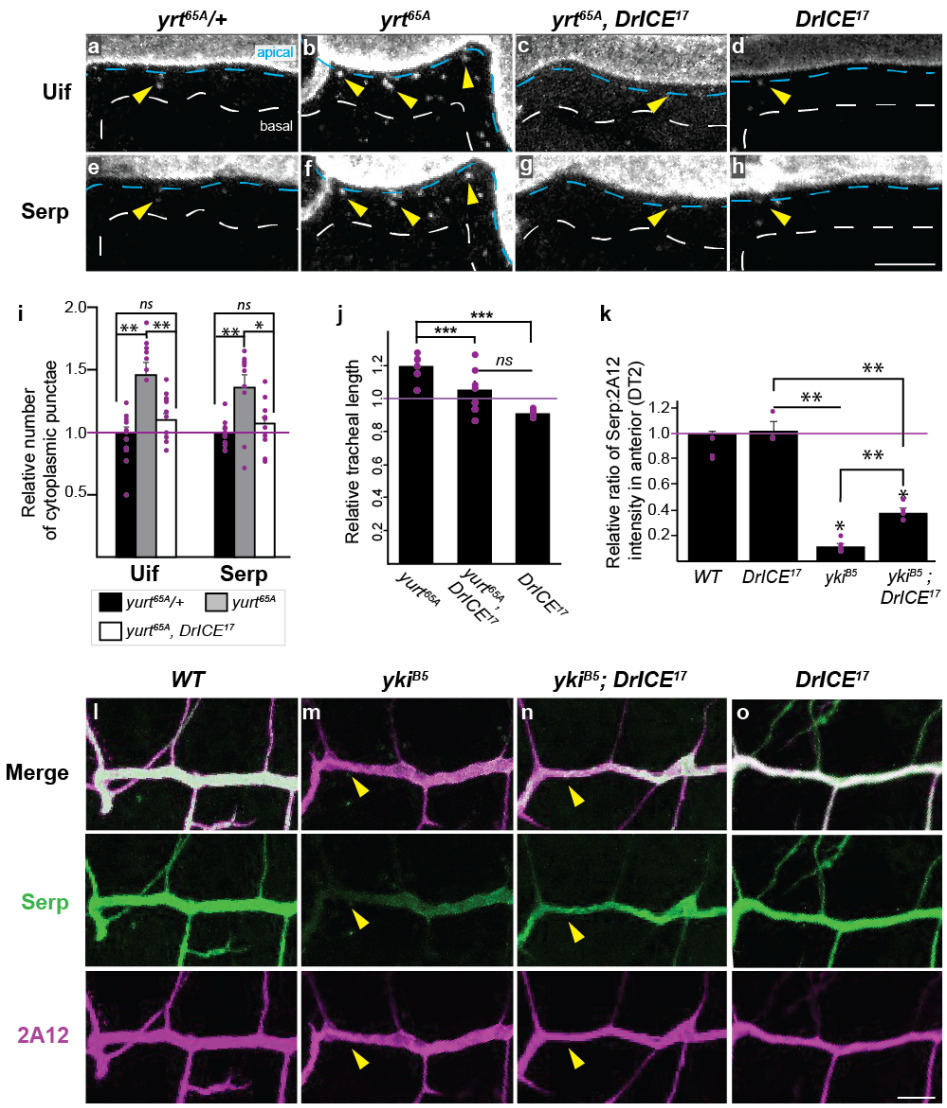

Figure 2.8 DrICE is required for trafficking of tracheal size determinants Serpentine and Uif
(a-h) Mutation of the basolateral polarity protein Yurt (*yrt*^{65A}) causes abnormal intracellular accumulation of the tracheal size determinants Uif (b, arrowhead) and Serp (f, arrowhead), an effect that is suppressed by *DrICE*^{17} (c, g). White dashed lines outline basal cell surface; blue dashed lines outline apical surface. Scale bar a-h in h, 5 μm. Relative number of cytoplasmic puncta quantified in (i), where the number of punctae in each of two ROIs in a maximum projection of *yrt*^{65A} (*N*=5 embryos), *yrt*^{65A}/+ (*N*=5 embryos), and *yrt*^{65A}, *DrICE*^{17} (*N*=6 embryos) was counted, then divided by the area of the given ROI. Resulting number of puncta per area is reported relative to *yrt*^{65A}/+. **(j)** The *DrICE*^{17} mutation suppresses tracheal overelongation caused by a mutation in the basolateral polarity gene *yrt*. Quantification of tracheal DT length at stage 16 for *yurt*^{65A} (*N*=6) and *yurt*^{65A}, *DrICE*^{17} (*N*=7) and *DrICE*^{17} (*N*=5) mutants reveals that *yurt*^{65A}, *DrICE*^{17} double mutants are shorter than *yurt*^{65A} mutants. Tracheal lengths normalized to body length and reported relative to WT (*w*^{1118}). For all graphs, each data point is represented as a point. **(k-o)** Mutation of the Hippo Network component Yki (*yki*^{B5}) reduces the levels of Serp (green) in the tracheal anterior relative to the lumenal chitin binding protein Gasp, marked by staining with the monoclonal antibody 2A12 (arrowhead, m). This reduction is suppressed by *DrICE*^{17} (n). (k) Quantification of the mean intensity of Serp divided by the mean intensity of 2A12 in a maximum projection of *N*=4 embryos for WT (*w*^{1118}), *N*=4 embryos for *yki*^{B5} ; *DrICE*^{17}, *N*=7 embryos for *yki*^{B5}, *N*= 3 embryos for *DrICE*^{17} Numbers reported as relative to *w*^{1118}. Scale bar l-o in o, 12.5 μm. For all graphs, error bars represent S.E.M and each data point is represented as a point. Source data are provided as a source data file. p<0.05; **, p<0.005; ***, p<0.0005 Student's t-test.

DrICE alters the trafficking of the claudin Kune-kune

We tested whether DrICE mutants exhibited alterations in trafficking of basolateral junctional components, which are known to be constitutively recycled through the endocytic system through tracheal development [280, 281]. Immunostaining for the claudin Kune-Kune (Kune) revealed that junctional and overall levels of Kune are reduced in *yki*^{B5} trachea ($p<0.05$ Student's t-test; Fig. 2.7e, k), and in trachea overexpressing DrICE (Fig. 2.7p), both conditions in which DrICE is elevated. Conversely, in *DrICE*^{17} mutants, strong ectopic staining for Kune is apparent at the apical (lumenal) surface and overall levels of Kune are increased (Fig. 2.7f, k). However, not all SJ components are negatively regulated by *DrICE*. For example, levels of the MAGUK Discs Large (Dlg) were only modestly affected in *yki*^{B5} and *DrICE*^{17} mutants (Fig. 2.7g-i), and we previously reported that the FERM-domain protein Coracle was unaffected by Yki and DrICE mutations. Thus, DrICE does not globally regulate endocytic trafficking, but rather is required for trafficking of a subset of tracheal markers.

DrICE alters the trafficking of Serpentine

We investigated whether DrICE is required for trafficking of lumenal determinants required for tracheal size control, including the putative chitin deacetylase Serpentine (Serp). As with the apical determinant Uif, we found that *DrICE*^{17} suppresses the overabundance of Serp-containing punctae in *yrt*^{65A} ($p<0.05$ Student's t-test; Fig. 2.6e-i). Furthermore, overactivation of DrICE resulting from loss of *yki* decreases the amount of t-test; Fig. 2.8e-i). Furthermore, overactivation of DrICE resulting from loss of *yki* decreases the amount of lumenal Serp in tracheal anterior, a phenotype that is partially suppressed by *DrICE*^{17} ($p<0.005$ Student's t-test; Fig. 2.8k and green in Fig. 2.8l-o). DrICE therefore affects trafficking of lumenal tracheal size determinants and mediates the effects of the HN on their trafficking.

Together, these results reveal that DrICE activity selectively modulates the trafficking of cargo originating from both the apical and basolateral membranes, and at minimum affects the trafficking of at least four different proteins required for tracheal size control.

DrICE may affect trafficking through interaction with the Clathrin adaptor Adaptin (AP47)

We hypothesized that one mechanism by which an executioner caspase like DrICE could affect intracellular trafficking and could explain its differential effects on different cargos is through an interaction with a Clathrin adaptor protein Adaptin (AP-1). We searched for the Adaptin substrate recognition motif (E/D-X-X-X-I/L-L) in apoptotic machinery, and confirmed that it is present in DrICE, but also in other initiator caspases, and in the apoptosome component Dark, but it is absent from the caspase inhibitor DIAP1. (Fig. 2.9a) Strikingly, this Adaptin recognition motif is evolutionarily conserved among all these pro-apoptotic components: in the large subunit among executioner and activator caspases as well as upstream apoptotic machinery including APAF. This observation has massive implications for a functional role of an interaction between apoptotic machinery and the Clathrin adaptor.

We next sought evidence of a functional consequence of the AP-1 (AP47) recognition sequence on DrICE. Indeed, the pattern of AP-1 subcellular colocalization with DrICE is strikingly similar to that of Clathrin. (Fig. 2.9c). Additionally, we generated a transgenic allele of DrICE with mutated dileucine motif, *DrICE*$^{\Delta LL}$ whose tracheal overexpression had limited effects when compared to overexpression of wild-type DrICE. For example, while tracheal overexpression of wild-type DrICE is sufficient to cause overelongation of the trachea, overexpression of *DrICE*$^{\Delta LL}$ ablates its ability to overelongate the trachea. (Fig. 2.9b) Furthermore,

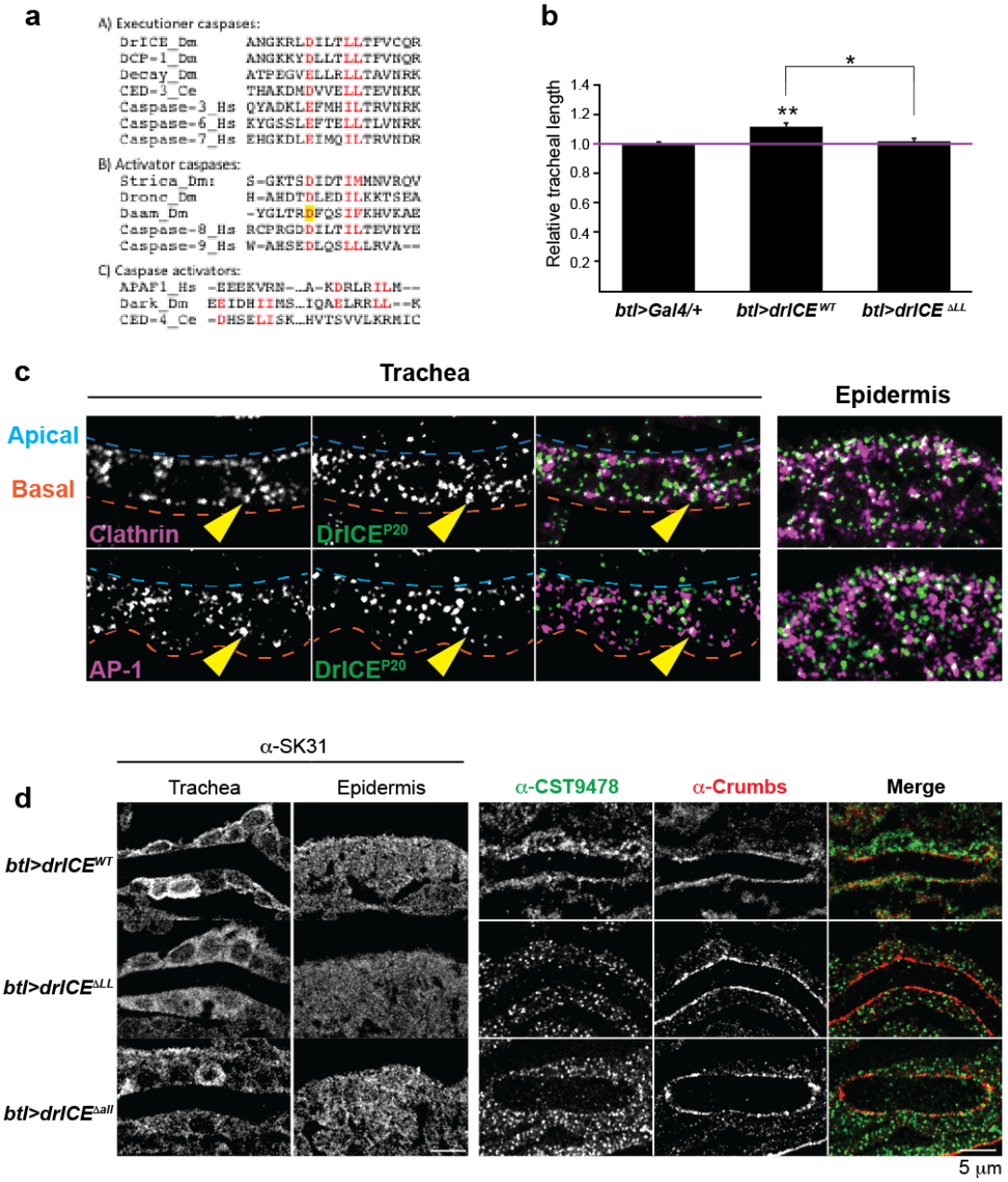

Figure 2.9 Dileucine motif for Adaptin recognition in DrICE and other caspases. (a) The dileucine motif (E/D-X-X-X-I/L-L) is evolutionarily conserved in the large subunit among executioner and initiator caspases as well as upstream apoptotic machinery including APAF, which suggests a putative interaction between apoptotic machinery and the Clathrin adaptor. (b) While tracheal overexpression of wild-type DrICE is sufficient to cause overelongation of the trachea, overexpression of DrICE with mutated dileucine motif ablates its ability to overelongate the trachea. (c) In WT trachea, DrICE colocalization with Clathrin is comparable to its colocalization with Adaptin (AP-1). (d) Overexpression of the mutated forms of DrICE is sufficient to produce an excess protein product in the trachea relative to epidermis, the effects on α-DrICE CST 9478 and on Crumbs do not appear to be equivalent, suggesting the dileucine motif maybe required for activation of DrICE.

overexpression of the dileucine-mutated DrICE is sufficient to produce an excess DrICE in the trachea

relative to epidermis, yet the Crumbs trafficking defects are not equivalent to those in *btl>DrICE^{WT}* (Fig. 2.9d), suggesting that the dileucine motif is required for its role in trafficking that is perhaps due to a failure of DrICE$^{\Delta LL}$ activation, as evidenced by the altered pattern of α-DrICE^{CST9478} staining (Fig. 2.9d).

These preliminary data imply that the Clathrin adaptor protein Adaptin (AP47) is necessary for the effects of DrICE on intracellular trafficking. As further discussed in Chapter 4, we hypothesize that AP47 recruits DrICE and its activators to sites of Clathrin-mediated intracellular trafficking in order to control the spatiotemporal activation of DrICE, which may consequently help determine its substrates.

IV. Discussion

Our work shows caspase-mediated regulation of endocytic trafficking during normal morphogenesis. Moreover, the caspase activity responsible for the endocytic function does not trigger apoptosis, even though the cells are competent to undergo caspase-mediated apoptosis. We also demonstrate a link between the Hippo Network (HN) and the endocytic system. While previous studies focused on the effects of the endocytic system on the *output* of the Hippo Network[73-75, 282], we report the converse: the Hippo Network acts as *input* to the endocytic system that alters endocytic trafficking.

A notable aspect of the role of DrICE in trafficking is that DrICE is required for trafficking of select—not all—trafficked cargo. For example, the abundance and localization of the SJ protein Kune is affected by alterations in DrICE, but Coracle and Dlg are not strongly affected (Fig. 2.7i,j and [5]). We also observe defects in the trafficking of the lumenal protein Serp, but no defects have been observed in the trafficking of the similar chitin deacetylase Vermiform (Verm)[5]. The differential trafficking of Serp and Verm in DrICE mutants is commensurate with observations by Dong et. al[57], who observed that a mutation in *shrub/VPS32* that disrupts multivesicular body formation also altered the localization of Serp, but not Verm. This similar differential effect on Verm and Serp trafficking provides further evidence of the involvement of DrICE in

endocytosis. It is also notable that not only does DrICE regulate specific cargos, the effect on each cargo is also cargo specific. For example, DrICE activity *promotes* Crb accumulation, but *suppresses* Kune accumulation. These results are consistent with DrICE acting directly on individual cargos, cargo-adaptors such as sorting adapters, or on both cargo and adaptors.

The counterintuitive requirement of an executioner caspase to promote growth in an epithelium has not previously been reported in mammals. However, there is *in vitro* evidence that mammalian caspases regulate endocytic trafficking[260]. For example, Duclos et al. showed that activation of activator and effector caspases in HeLa and HEK293 cells resulted in cleavage of Sorting Nexins 1 and 2 (SNX1 and SNX2), which control intracellular trafficking of specific cargos[260, 283]. Cleaved SNX increased activation of the hepatocyte growth factor receptor (HGFR) and ERK1/2 signaling. Additionally, Han et al. showed that Caspase-3 cleavage of junctional component Gap43 was required for endocytosis of the AMPA receptor A in non-apoptotic cells in vitro[284]. Together, the previously published *in vitro* mammalian results and these *in vivo Drosophila* results suggest a developmental role for caspase-mediated regulation of endocytic trafficking that is evolutionarily conserved and may also function in mammalian development.

The conserved involvement of caspases in endocytic trafficking raises the possibility that there is a deeper mechanistic connection between apoptosis and trafficking of junctional components. In the current model of apoptosis, caspase-mediated proteolysis of cell junctions results in decreased cell adhesion, which allows an apoptotic cell to be cleanly extruded from an epithelium (Fig. 5, middle; reviewed by [285]). However, in mammals and flies, junctional components are constitutively cycled through the endocytic system even in non-apoptotic epithelia[280, 281, 286]. This presents an opportunity for caspases to alter trafficking of junctional components. Perhaps the ability of caspases to regulate endocytic trafficking arose as an ancient apoptotic function that allowed dying epithelial cells to more efficiently downregulate junctions by using both endocytosis and caspase-mediated proteolysis rather than caspase-mediated proteolysis alone (Fig. 5, bottom). We hypothesize that caspase-mediated alterations in cell junction trafficking has been co-opted in morphogenesis, when growing epithelia require rapid remodeling of junctional components (Fig. 5, top).

Experimental evidence from mammalian cerebral ischemic injury supports the proposed model that limited activation of caspases alters junctional endocytosis. During cerebral ischemic injury, blood flow in the brain is blocked, which leads to extensive caspase activation, downregulation of claudin-based tight junctions,

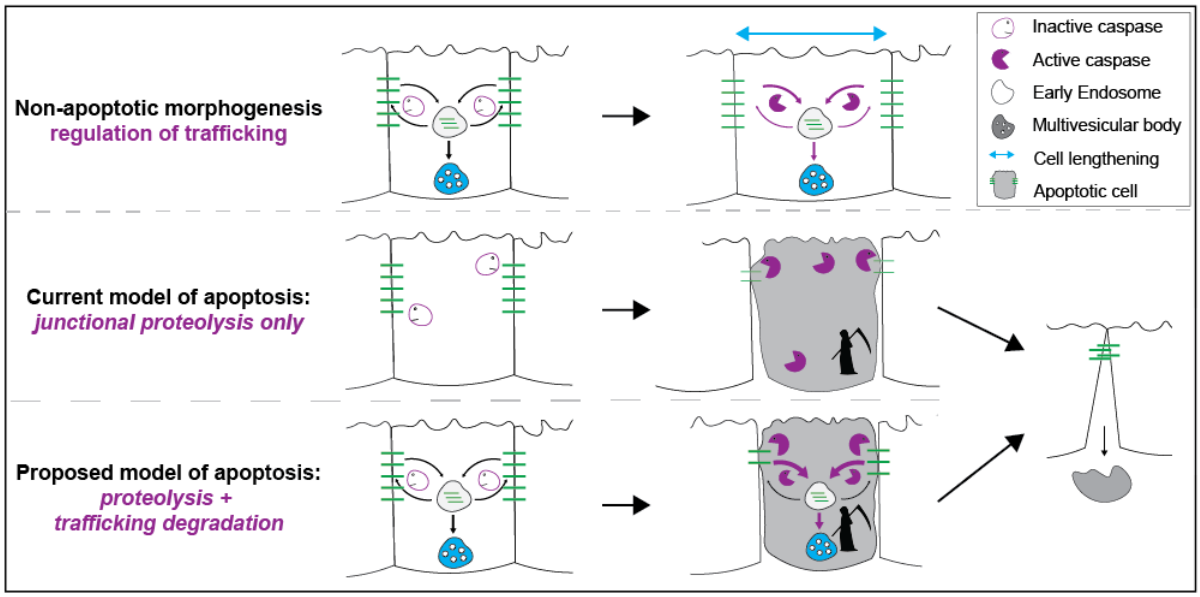

Figure 2. 10 Model for caspase-regulated endocytic trafficking in apoptosis See text for details.

and a large and damaging increase in vascular permeability[287]. Pretreatment of tissue with caspase inhibitors increases junctional continuity and integrity including junction components claudin-5 and the tight junction marker ZO-1, and ultimately reduces tissue damage. Strikingly, more endothelial cells show caspase activation than undergo apoptosis, suggesting that caspase activation is sufficient to induce junctional downregulation and vascular permeability.

The ability of caspases to regulate endocytic trafficking has significant implications for cancer treatments, which frequently result in caspase activation. Sub-apoptotic activation of effector caspases in surviving tumor cells after anti-cancer treatment could potentially result in reduced junctional integrity, which could further promote epithelial-to-mesenchymal transformation (EMT) and metastasis. Additionally, caspase-driven changes in the trafficking of polarity proteins such as Crb and of growth factor receptors could also contribute to EMT and disease progression. Consistent with this possibility, previous evidence has indicated

that human Caspase-3 is required for migration, invasion and metastasis HCT116 colon cancer cells[288], and for tumor cell repopulation upon irradiation[176].

In summary, this work reveals a function of the effector caspase DrICE during development: modulating endocytic trafficking of cell junctional components and signaling molecules. Given that mammalian effector caspases can also modulate endocytic trafficking, we propose that regulation of the trafficking of junctional components is a conserved caspase function that can be brought into play during normal morphogenesis or in pathologic conditions by localized, sub-apoptotic caspase activation.

V. Acknowledgements

For reagents we thank Rob Ward (α -Uif), Pascal Meier (α - DrICE^{SK31}), Christos Samakovlis (α-MTf), Matthias Behr (α-Clathrin). We also thank Benjamin Kraft for assistance in epistasis experiments; Andreas Bergmann for helpful discussions; J. Hornick and the Northwestern University Biological Imaging Facility for technical and imaging support; and Laura Lackner, Heike Fölsch, and I. Tanelli Helenius for comments on the manuscript. Stocks obtained from the Bloomington Drosophila Stock Center (NIH P40OD018537) were used in this study, and FlyBase was a critical resource [289]. This work was supported by NIH RO1GM108964 to GJB. S. McSharry was supported by the National Institute of General Medical Sciences training grant T32GM008061.

VI. Materials & methods

Fly Stocks

The following mutant alleles were used in this paper: *th^{J5C8}*, *yorkie^{B5}*, *DrICE^{17}*, *DrICE^{Δ1}*, and *yurt^{65A}*. DrICE overexpression in the trachea was achieved using the UAS/Gal4 system: the *btl>Gal4* driver was used to express Gal4 in all tracheal cells; *btl>Gal4* flies were crossed to *UAS-DrICE* flies, which had a transgenic

DrICE cDNA downstream of UAS (see *Transgenic Constructs* below). The double mutant *yurt*^{65A}*, DrICE*^{17} was generated using standard recombination crosses. Each single male resulting from the recombination crosses was screened for *yurt*^{65A} via failure to a complement *yurt*^{65A} single mutant and screened for the presence of the *DrICE*^{17} mutation by sequencing to identify the point mutation N116Y.

Transgenic constructs

To create the UAS-DrICE transgenic line, full length DrICE cDNA sequence was cloned into the MCS of pUAST vector using Gibson cloning and subsequently inserted into the attP2 site into flies with the phiC31 integrase system.

Embryo staining

Parental flies were placed in empty food bottles capped with a molasses-agar plate spread with wet yeast. After 24 hours, plates were removed and embryos were fixed and stained as follows: embryos were dechorionated with 50% bleach for 4 minutes and fixed in equal parts heptane and 4% formaldehyde on a shaker for 25 minutes. Embryos were then devitellenized for 1 minute with 100% methanol/heptane, rehydrated to PBS-T (0.1% Triton-X100) (100%, 100%, 100%, 50%, each for 5 min), washed in PBST for 5x5' and then 3x30'. PBS-BT (3% BSA in PBS-T) was used to block for 30 minutes at RT before addition of primary antibody, in which embryos were incubated for 48 hours at 4 °C on a rotator. See the attached chart below for appropriate antibody dilutions. PBS-T and PBS-BT steps were repeated on the third day before addition of fluorescent secondary antibodies, in which embryos were incubated O/N at 4 °C. The use of the Alexa+ secondary antibodies (see chart for details) was essential to visualize DrICE α-DrICE^{CST9478} staining as regular Alexa secondary antibodies did not produce adequate signal-to-noise. On the final day, PBS-T washes were repeated, embryos were dehydrated using an ethanol series (50%, 70%, 90%, 100%, 100% EtOH, each for 5 min), incubated in methyl salicylate for 15 min at RT, and then mounted

with methyl salicylate and Permount mounting media (Fisher Scientific, SP15-500). More information about reagents can be found in Table 2.3.

Image acquisition

Confocal z-stacks were obtained with the 63X NA 1.24 oil objective on the Leica SP8 image format greater than or equal to 2048x2048, pinhole size 0.7AU, and system optimized z-step sizes of approximately 0.2 um. Images were subsequently deconvolved using Leica HyVolution software with a Huygens Essential Automatic setting. All quantification was performed on the resulting images.

Image quantification and general statistics

Quantification of junctional components was performed using ImageJ, in which a region of interest in the fifth dorsal trunk metamere of tracheal cells was used to calculate the mean pixel intensity of each junctional component. The number of punctae for Crumbs, Uif, or Serp was calculated by acquiring the number of spots with the ImageJ SpotCounter plugin (Gaussian pre-filtering, box size=8, and noise tolerance=20) and then dividing that number by the total area of that region of interest. Each individual embryo's ratio of spots per unit area was then divided by the WT average, and a Student's 2-tailed t-test was used to calculate the p-value.

Tracheal lengths were determined by tracing the length of the dorsal trunk through 3D in Volocity Demo 5.5.1.

Western blot

Parental flies (heterozygotes with the CyO GMR-dfd YFP or TM6B GMR-dfd YFP balancers were placed in empty food bottles capped with a molasses-agar plate spread with wet yeast. After 1 hour, plates were removed and stored in a humid chamber at 25 °C for 18 hours. Embryos were then washed with water and treated with 50% bleach for 4 minutes. The bleached embryos were sorted to collect only homozygous

embryos, which lacked the fluorescent marker denoting the presence of the balancer chromosome. Approximately 30 embryos of each genotype were lysed in RIPA buffer using a micropestle, and then incubated on ice for 30 minutes before 15-minute centrifugation at 4°C. Protein concentration of the resulting supernatant was measured by Nanodrop 2000 Spectrophotometer (ThermoFisher Scientific), and all samples were diluted with RIPA buffer to the same protein concentration before Laemmeli Buffer was added. Samples were denatured using in a boiling water bath for 5 minutes, loaded in a gradient gel and run for 90 minutes at 100V. Transfer of proteins to the nitrocellulose membrane was carried out at 60V for 20 minutes at 4 °C in order to retain low molecular weight caspases. After total protein levels were detected and imaged using the LiCor REVERT total protein stain and Odyssey CLx imaging system (Li-Cor), blots were incubated in blocking solution (5% BSA in TBS with 0.1% Tween20) for one hour, and then in rabbit anti-*Drosophila* DrICE^{CST13085} (1:1000) overnight at 4°C. Fluorescent Li-Cor goat anti-Rabbit IRDye CW800 secondary antibody was then used to detect the resulting bands, and the mean signal for the 47kd band of each genotype was then normalized to the corresponding lane's total protein signal. More information about reagents can be found in Table 2.3.

REAGENT or RESOURCE	SOURCE	IDENTIFIER
Antibodies		
Guinea pig anti-uninflatable (1:800)	Rob Ward	
α-DrICE^{CST9478} Rabbit anti-cleaved Drosophila ICE Asp230 (1:100)	Cell Signaling Technology (CST)	9478S
α-DrICE^{CST13085S} Rabbit anti- Drosophila ICE (1:100)	Cell Signaling Technology (CST)	13085S
Mouse anti-Crumbs extracellular domain (1:25)	Developmental Studies Hybridoma Bank (DSHB) at the University of Iowa	
Mouse anti-2A12 (1:1)		
Rabbit anti-Serp (1:400)		
IRDye 800CW goat anti-Rabbit 0.5mg	Li-Cor	926-32211
Guinea-pig anti-DrICE (SK31)	Pascal Meier	SK31
Rat anti-Clathrin (Chc) (1:40)	Matthias Behr	n/a
Mouse anti-Rab5 (1:100)	BD Biosciences	610281

Mouse anti-Rab7 (1:50)	Developmental Studies Hybridoma Bank (DSHB) at the University of Iowa	Rab7
Mouse anti-Rab11 (1:100)	Fisher Scientific	BDB610656
Guinea pig anti-Melanotransferrin	Christos Samakovilis	n/a
Rabbit anti-Kune-Kune	[250]	
Rabbit anti-Dlg		
Goat anti-mouse IgG (H+L) highly cross-adsorbed secondary antibody Alexa Fluor 488 Plus	Life Technologies	A32723
Goat anti-mouse IgM (H+L) highly cross-adsorbed secondary antibody Alexa Fluor 488	Life Technologies	A10680
Goat anti-rabbit IgG (H+L) highly cross-adsorbed secondary antibody Alexa Fluor Plus 647	Life Technologies	A32733
Goat anti-guinea pig IgG (H+L) highly cross-adsorbed secondary antibody Alexa Fluor 568	Life Technologies	A11075
IRDye 800CW Goat anti-Rabbit 0.5 mg	Li-Cor	926-32211
Critical Commercial Assays		
REVERT Total protein stain kit		
Pre-cast gel 4-15%, 15 well		
Software and Algorithms		
Fiji (ImageJ) SpotCounter plugin		
Volocity Demo 5.5.1		
Leica Application Suite X (LAS X) HyVolution and colocalization calculation		
Li-Cor Image Studio Software		

Table 2.3 Additional information on reagents. See Methods section for details.

VII. Contributions

SM and GJB conceived and designed the experiments. SM performed the experiments. SM and GJB analyzed the data. SM and GJB wrote the manuscript.

CHAPTER 3: Sterol Regulatory Element Binding Protein (SREBP) as a putative substrate of DrICE

Fat gives things flavor.

–Julia Child

I. Introduction

We have recently shown that during morphogenesis of the *Drosophila* tracheal system, the executioner caspase DrICE plays a non-apoptotic role in size control by modulating trafficking of diverse cargoes such as the apical polarity determinant Crumbs and the ECM component Serpentine.[247] Through the novel discoveries of this and other non-apoptotic caspase functions, a critical question becomes: what are the substrates of caspases that contribute to non-apoptotic processes? Previous *in vivo* and *in vitro* work in *Drosophila* and in mammals has shown that one substrate that can be cleaved by the executioner caspase DrICE/ Caspase-3, is the Sterol Regulatory Element Binding Protein (SREBP), which is best known for its role in upregulating lipid and cholesterol production.[290-292]

Found in both flies and mammals, SREBP is a transcription factor that resides in the membrane of the Endoplasmic Reticulum (ER), where it associates with its membrane-bound partner SREBP Cleavage Activating Protein (SCAP). (Figure 3.1a) When lipid levels of the ER membrane are low, SCAP undergoes a conformational change that reveals COPII binding sites. This allows the SREBP-SCAP complex to be transported from the ER to the Golgi, where SREBP is cleaved by the proteins Site 1 Protease (S1P) and Site 2 Protease (S2P), thereby freeing the N-terminus of the protein, containing a DNA-binding bHLH-Zip domain, from its transmembrane domains.[293, 294] As a consequence of its proteolytic processing, SREBP can translocate to the nucleus and upregulate lipid synthesis through transcription of genes encoding rate-limiting enzymes of the mevalonate pathway, including Acetyl CoA Carboxylase (*ACC*).[295]

Interestingly, mammalian diseases can be induced by dysregulation of Sterol Regulatory Element Binding Protein (SREBP).[296, 297] In fact, several studies have now connected the severity of end stage chronic kidney

disease—such as that caused by Polycystin mutation in PKD— to alterations in lipid metabolism. For example, glomerular sclerosis, which is kidney scarring characterized by excessive apoptosis and extracellular matrix (ECM) accumulation, is associated with hypercholesterolemia and increased lipoprotein production. Encouragingly, trials with lipid-lowering therapies have been successful in reducing inflammation and ameliorating renal scarring.[298] Development of more universally effective treatments for this pathology, may therefore involve targeting lipid synthesis pathways. Consequently, elucidating the molecular interplay between lipid metabolism by SREBP and apoptotic machinery could be important for better understanding of human pathologies like chronic kidney disease (CKD).[299]

Here, we have taken advantage of our model, the *Drosophila* tracheal system, to explore the relationship between dSREBP and DrICE as mediators of lipid synthesis and apoptosis, which are abnormal in glomerular sclerosis. In this initial characterization, we demonstrate the complexity of the relationship between DrICE and dSREBP in the tracheal system and suggest some experiments for future exploration.

II. Results

Caspase cleavage of dSREBP is conserved

Human SREBP-1a and *Drosophila* dSREBP, which share 48% overall conservation, and 82% conservation of the DNA-binding bHLH-Zip domain, are each critical for lipid production. Additionally, they have both been shown to be cleaved by Caspase-3 in apoptotic mammalian cells, and by the Caspase-3 homologue DrICE in

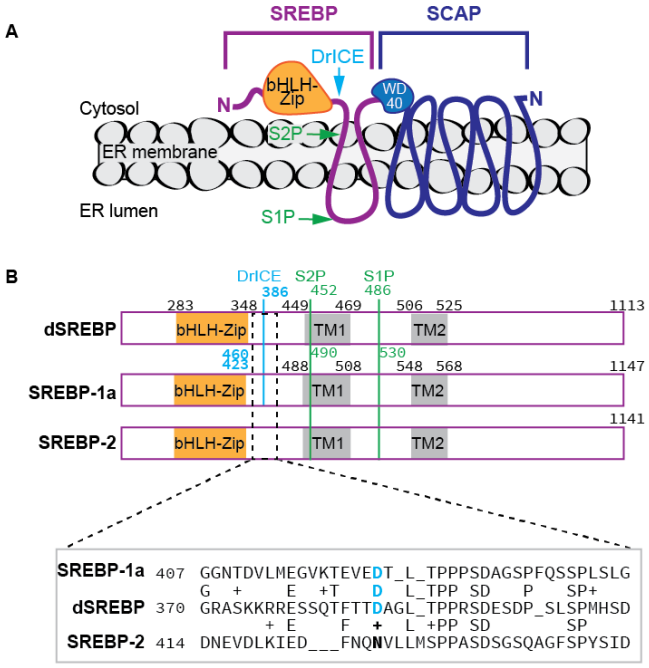

Figure 3.1 Drosophila Asp386 is conserved in human SREBP-1a, but not SREBP-2. (A) Schematic of SREBP and SCAP as they interact in the membrane region of the ER. DrICE cleavage site is shown in blue arrows, while S1/S2P sites are shown in green. (B) DrICE/ Caspase-3 cleavage site is conserved from Drosophila dSREBP to mammalian SREBP-1a, but it is absent in SREBP-2.

Drosophila.[11, 290-292] Interestingly, the site of *Drosophila* caspase cleavage of dSREBP, Asp386, is also conserved to human SREBP-1a, which is required for both lipid and cholesterol synthesis, but not in SREBP-2, which is specific to cholesterol synthesis.[300] (Figure 3.1)

SREBP affects tracheal elongation

Like the mammalian kidney, the *Drosophila* tracheal system is comprised of a network of ramifying tubes. The trachea, which serves as the fly's combined pulmonary and vascular system, begins to develop soon after fertilization. We recently showed that DrICE is necessary and sufficient for tracheal elongation; we hypothesized that if dSREBP were a tracheal size-regulating substrate of DrICE, dSREBP mutant alleles would affect tracheal morphogenesis comparably to *DrICE* alleles.[247] In order to determine whether dSREBP plays a role in tracheal elongation downstream of DrICE, we examined the tracheal length of several diverse dSREBP alleles, including two previously available alleles of dSREBP: $dSREBP^{1}$ and $dSREBP^{189}$. (Figure 3.2a) The first allele, $dSREBP^{1}$, which lacks the C-terminal region by which SCAP regulates dSREBP, does not have any length defects. (Figure 3.2b) The other allele, $dSREBP^{189}$, which is a deletion the spans the preceding gene (*Gyc76C*) and regulatory regions of dSREBP, does not have a significant length defect compared to w^{1118}. $dSREBP^{189}$ is, however, overelongated compared to its heterozygous counterpart, which suggests that dSREBP may have a role in suppressing the elongation of the trachea, though this result was confounded by the concomitant loss of the neighboring gene. Because it is not possible to rule out that the phenotype of $dSREBP^{189}$ is not due to the deletion of the neighboring gene, *Gyc76C*, we generated $dSREBP^{\Delta ORF}$, a deletion of the open reading frame of dSREBP using CRISPR, which did not have a significant impact on tracheal length. (Figure 3.2a)

Seeking further clarification, we examined a loss-of-function allele in a transcriptional target of dSREBP, *Acetyl CoA Carboxylase* (ACC^{B131}), and found that it caused overelongation of the trachea. (Figure 3.2c) Together, these data suggest that alterations in lipid metabolism by SREBP and/or its target genes can restrict the elongation of the tracheal system, although the precise relationship between the DrICE and dSREBP remains ambiguous. This result also suggests—because DrICE and dSREBP loss of function

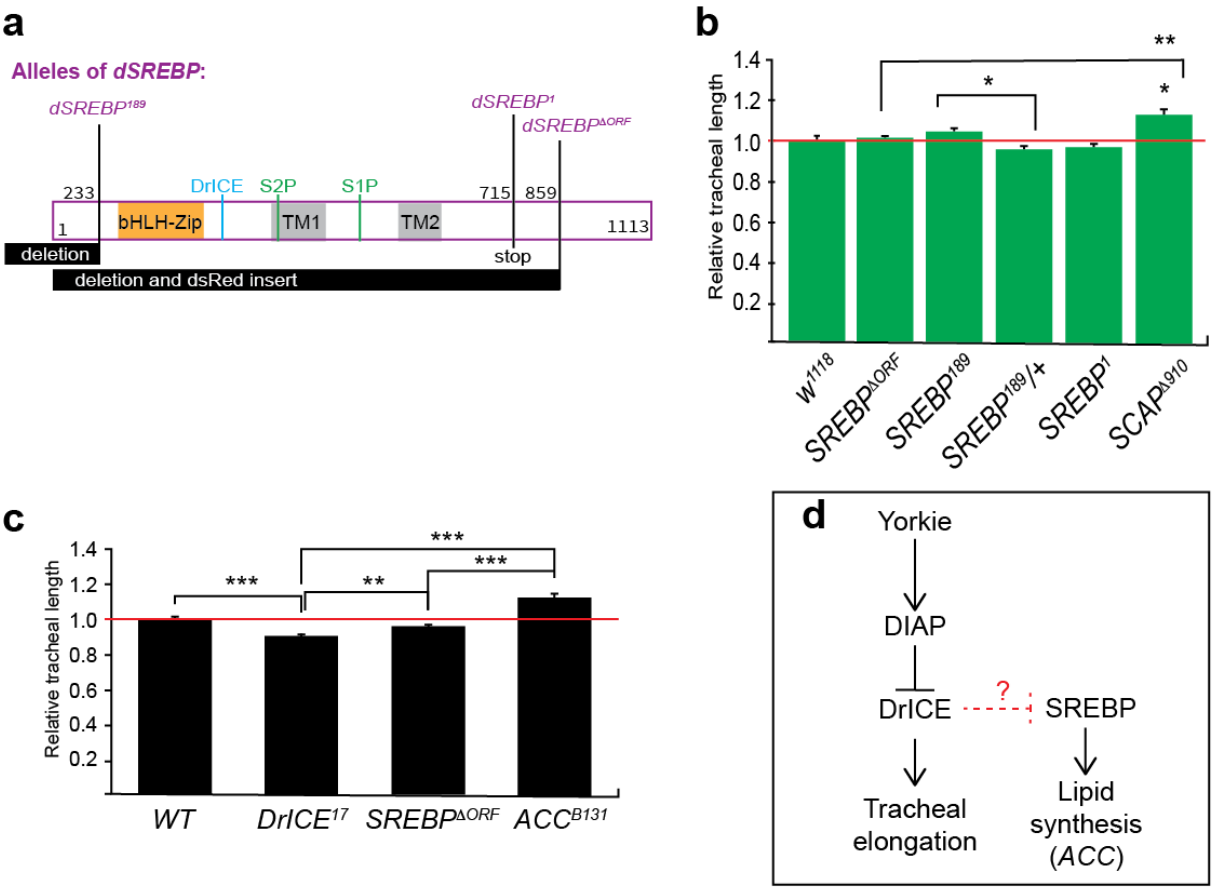

Figure 3.2 dSREBP plays a role in tracheal size control. (a) Schematic depicting the nature of each dSREBP allele. 189 is a deletion that spans the preceding gene, *Gyc76C*, through amino acid 233 of dSREBP. 1, an EMS-mediated point mutant, changes Q715 to a stop codon, resulting in a truncated protein product that lacks the regualtory region affected by SCAP. ΔORF is a CRISPR allele in which the open reading frame of dSREBP up to amino acid 859 has been deleted and replaced with 3XP3-driven dsRed. **(b)** Each allele of dSREBP and its effects on tracheal length. The 189 allele results in an elongated tracheal phenotype only when compared to its heterozygous counterpart, and the Δ910 allele of the SREBP regulatory protein, SCAP, a P-element mediated deletion that also deletes the upstream gene *dream*, which encodes the caspase Strica, has overelongated trachea. The other alleles show no statistical significance compared to WT or to their heterozygous conterparts. **(c)** Summary of the comparison of the effects of DrICE, dSREBP, and its transcriptional target ACC on tracheal elongation. **(d)** Diagram of our hypothesis about the relationships between the Hippo Network and dSREBP. See text for details.

mutants have opposite outputs in tracheal length—that DrICE cleavage of dSREBP is an inactivating, rather than an activating event, a finding contrary to the previous study that DrICE can cleave and activate dSREBP in the absence of its normal processing by S2P.[11]

SREBP acts downstream of or in parallel to the HN and DrICE

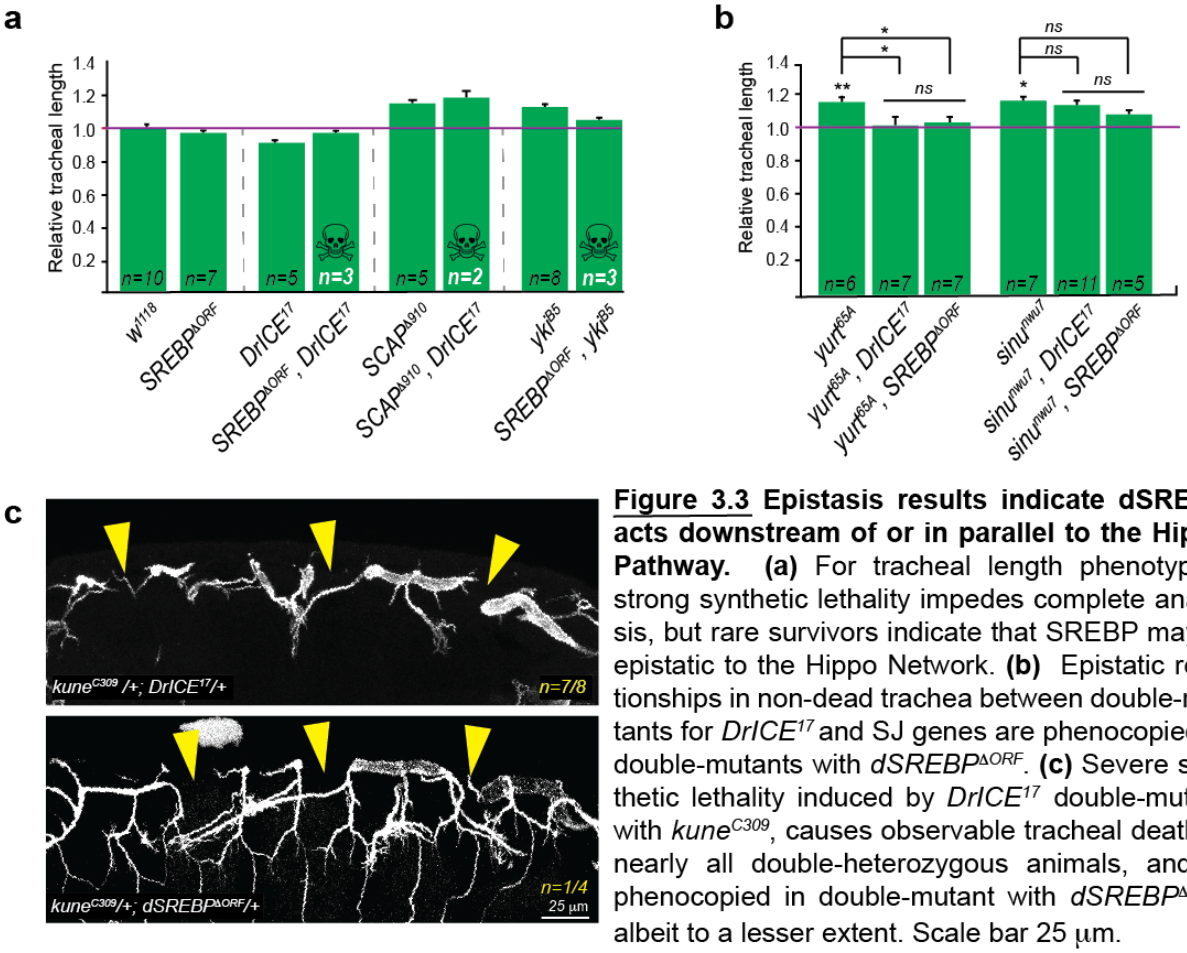

Figure 3.3 Epistasis results indicate dSREBP acts downstream of or in parallel to the Hippo Pathway. **(a)** For tracheal length phenotypes, strong synthetic lethality impedes complete analysis, but rare survivors indicate that SREBP maybe epistatic to the Hippo Network. **(b)** Epistatic relationships in non-dead trachea between double-mutants for *DrICE*^{17} and SJ genes are phenocopied in double-mutants with *dSREBP*$^{\Delta ORF}$. **(c)** Severe synthetic lethality induced by *DrICE*^{17} double-mutant with *kune*^{C309}, causes observable tracheal death in nearly all double-heterozygous animals, and is phenocopied in double-mutant with *dSREBP*$^{\Delta ORF}$, albeit to a lesser extent. Scale bar 25 μm.

In order to determine whether dSREBP can affect tracheal length downstream of DrICE, we created double-mutants between the *SREBP*$^{\Delta ORF}$ allele and loss-of-function alleles of *DrICE* and of the Hippo Network gene that regulates DrICE, *yorkie*. Somewhat surprisingly, we found that the combination of *SREBP*$^{\Delta ORF}$ with *yorkie* or *DrICE* caused a severe synthetic lethality in the tracheal system that is not observed in either single mutant alone. (Figure 3.3a) This synthetic lethality, which is recapitulated in the double-mutant combination of *SCAP*$^{\Delta 910}$ and *DrICE*^{17}, could imply that dSREBP and the Hippo Network do not directly interact, but rather act in parallel pathways such that when both pathways are missing such critical components, tracheal cells perish. Of note, however, is the fact that in the rare embryos we found with intact trachea, *SREBP*$^{\Delta ORF}$ and *SCAP*$^{\Delta 910}$ appear epistatic to components of the Hippo Network. (Figure 3.3a)

In order to assay whether *SREBP$^{\Delta ORF}$* was capable of suppressing length defects downstream of DrICE, we tested the epistatic relationships between *SREBP$^{\Delta ORF}$* and other genes that impact tracheal length in a DrICE-dependent or -independent manner. Indeed, *dSREBP$^{\Delta ORF}$* phenocopies epistatic relationships that are observed between *DrICE^{17}* and other tracheal size control regulators; for example, both *DrICE^{17}* and *dSREBP$^{\Delta ORF}$* are able to suppress the length defect of the Septate Junction component *yurt^{65A}*, but neither is able to suppress the elongated defect of *sinu^{nwu7}*. (Figure 3.3b) Furthermore, the severe synthetic lethality created by a double-heterozygote for the genes encoding the claudin Kune-kune, *kune^{C309}* and *DrICE^{17}* was also observed in the *kune^{C309}* ; *dSREBP$^{\Delta ORF}$* double-mutant, though it was less penetrant. (Figure 3.3c) Together, the commonalities between the epistatic relationships among *DrICE^{17}* and *dSREBP$^{\Delta ORF}$* with other tracheal size control genes are consistent with our hypothesis that DrICE cleaves dSREBP downstream of the Hippo Network in tracheal cells.

The state of DrICE-mediated cleavage of dSREBP affects phenotypic output

Because DrICE has been shown to cleave dSREBP both in vitro and in vivo, we next wanted to verify the effect(s) of DrICE cleavage of dSREBP.[11] In order to determine whether the DrICE cleavage state of dSREBP could contribute to any tracheal elongation or lethality, we compared the effects of transgenic tracheal overexpression of S2P-cleaved SREBP (*btl>SREBP$^{1-452}$*) with DrICE-cleaved SREBP (*btl>SREBP$^{1-386}$*). In agreement with the mammalian data that overexpression of dSREBP causes cell death, overexpression of this activated form of dSREBP was 100% lethal (data not shown) and caused a stark embryonic phenotype in which 93% of embryos had missing segments in the trachea, indicating substantial apoptosis comparable to overexpression of pro-apoptotic genes or loss of the anti-apoptotic factor DIAP1. (compare Figure 3.4d to Figure 2.3i,l-m) On the other hand, however, overexpression of the DrICE-cleaved form of dSREBP (*btl>SREBP$^{1-386}$*) led to no observable defects in tracheal length or morphology in 70% of embryos. (Figure 3.4c-d) Excess accumulation of fatty acids has previously been

shown to induce cell death in diverse cell types, so from these experiments, we hypothesized that the state of DrICE-mediated dSREBP cleavage reduces any lethality that would be caused by lipid-mediated toxicity through increased abundance of dSREBP transcriptional activity.[301-304]

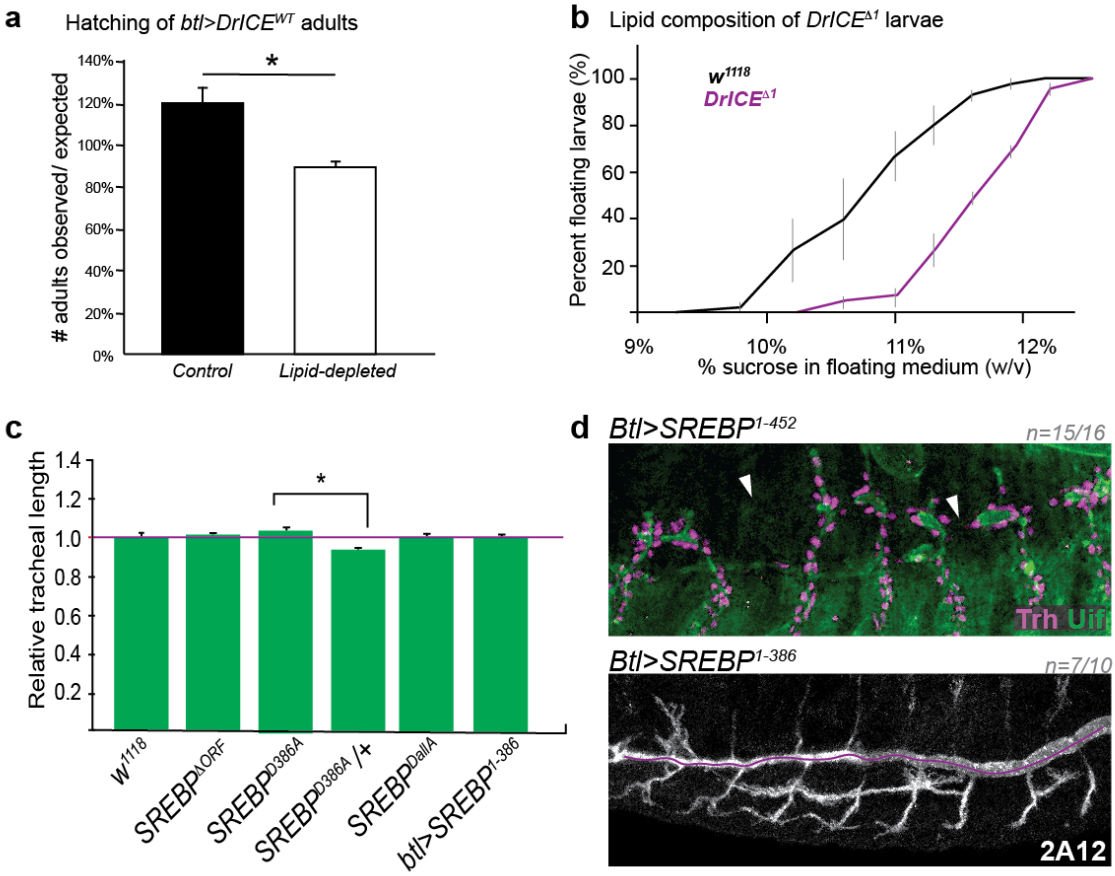

Figure 3.4 DrICE cleavage state of dSREBP alters phenotypic output. **(a)** DrICE overexpression results in altered survival based on hatching rates of adults. On a control diet containing lipids, *btl>DrICE* adults survive at more than the expected Mendelian rates, suggesting a slight competitive advantage. On a lipid-depleted diet, however, the expected number of adults falls significantly. **(b)** When fed a lipid-depleted diet, the lipid composition of DrICE loss-of-function third instar larvae is reduced compared to w^{1118} controls, suggeting that DrICE is required for lipid production in the absence of dietary lipids. **(c)** Caspase-incleavable CRISPR mutant $dSREBP^{D386A}$ has an elongated tracheal phenotype compared to its heterozygous counterpart, which supports a model in which DrICE is required for dSREBP's tracheal function. There is no observable length defect in the mutant $dSREBP\text{-}^{DallA}$, in which all 5 Asp residues between its first transmembrane domain and the S2P cleavage site are mutated to Ala, or in the overexpression of dSREBP up to its caspase-cleavage site, D386. **(d)** Tracheal overexpression of S2P-cleaved dSREBP causes large missing portions of the trachea suggestive of tracheal cell death, but overexpression of the caspase-cleaved dSREBP results in normal tracheal morphology.

We next sought to determine whether DrICE cleavage of dSREBP abrogates dSREBP-mediated lipid toxicity by testing the effects of mutating the caspase cleavage site in dSREBP, Asp386, using CRISPR. We generated two alleles of *dSREBP* that produce a version of dSREBP protein that cannot be cleaved by DrICE: $SREBP^{DallA}$ (mutated all 5 Asp residues in the region between the bHLH domain and the S2P cleavage site to alanine) *and* $SREBP^{D386A}$ (mutates only Asp386, which was previously shown to be required for DrICE-mediated cleavage of dSREBP[11]). Tracheae in embryos homozygous for $SREBP^{\Delta ORF}$ or in $SREBP^{DallA}$ did not display any elongation phenotypes, but those homozygous for the single Asp mutant, D386A, were over-elongated compared to heterozygotes. These data imply that Asp386—and therefore DrICE cleavage of dSREBP— is required for dSREBP-mediated restriction of tracheal elongation. This observation appears to contradict our previous hypothesis that DrICE-mediated cleavage of dSREBP is inactivating: as with loss of DrICE, we might predict that loss of the DrICE-mediated processing of dSREBP caused by D386A would cause decreased tracheal length if the cleavage event is inactivating. Because the loss of DrICE-mediated processing of dSREBP leads to elongated trachea similar to the ACC phenotype, however, DrICE-mediated cleavage of dSREBP, is more likely to be an activating event. Alternative hypotheses, however, are that (a) DrICE operates in a parallel pathway to dSREBP or (b) that DrICE cleavage of dSREBP is required for SREBP transcription of a gene product that is not produced by S2P-cleaved SREBP alone, and (c) D386A is detrimental only when heterozygous, or (d) these phenotypes are very sensitive to genetic background.

It's worth noting that the short tracheal phenotype of DrICE alleles are robust, but subtle, such that the loss-of-function mutant length is nearly 90% of the wild type tracheal length. Because dSREBP also appears to affect tracheal length in a subtle and, additionally, in a background-sensitive manner, it will be necessary to (a) backcross the *dSREBP* CRISPR alleles into the w^{1118} background to eliminate genetic differences, and (b) assay trans-heterozygotes for tracheal phenotypes, as was rigorously tested for *DrICE*. [5]

In order to further support the hypothesis that DrICE activates dSREBP transcriptional function in supporting lipid synthesis, we sought to quantify lipid levels of third instar larvae raised on control or lipid-depleted

food. We predicted that in a *DrICE*$^{\Delta 1}$ deletion mutant, transcriptional activation of SREBP would be decreased, causing a depletion of larval lipid levels. A buoyancy-based method for determining larval lipid content revealed that *DrICE*$^{\Delta 1}$ larvae fed a lipid-depleted diet have lower lipid levels than controls.[305] These preliminary data may support the hypothesis that DrICE is required for dSREBP-mediated lipid production.

In an effort to distinguish between whether DrICE acts in a parallel pathway to dSREBP or acts directly upstream of dSREBP-mediated lipid metabolism, we examined the larval lethality of overexpressed DrICE in the trachea when fed control and lipid-depleted diets. We hypothesized that if DrICE were acting in a truly parallel pathway to dSREBP, overexpression of DrICE would not affect viability on a lipid-depleted diet, as it does not affect viability on a normal diet. If it were required for the activation SREBP's transcriptional role, however, overexpression of DrICE may cause hyperactivation of SREBP, causing decreased viability. Consistent with DrICE activating dSREBP, we observed that the viability of *btl>DrICE*^{WT} was significantly reduced when raised on lipid-depleted food, which favors the hypothesis that DrICE can activate dSREBP. (Figure 3.3c)

III. Discussion and future directions

In 2009, Asp386 of *Drosophila* dSREBP was identified as a necessary residue for the processing of dSREBP by DrICE in the absence of the canonical protease S2P.[11] In their report, Amarneh et al presented evidence that DrICE cleavage of dSREBP at Asp386 is sufficient to activate SREBP in the absence of S2P; they demonstrate that larvae lacking both DrICE and S2P do not survive to the same extent as either single mutant alone when fed a lipid-depleted diet. Furthermore, they demonstrate that DrICE and Dronc are necessary for development of S2P-null flies that are raised on food lacking fatty acids.[11]

In our investigation of the nature of DrICE-mediated dSREBP cleavage, we noted that the caspase-cleaved form of dSREBP has 66 fewer amino acids than the form produced by lipid-sensitive cleavage by the canonical proteases S1P/ S2P. (Figure 3.1a) The evolutionary conservation of the truncated region is 38%,

suggesting it could be important for canonical S2P-mediated transcriptional function of dSREBP. We first used a genetic approach to show that, although with *SREBP$^{\Delta ORF}$* does not have an obvious tracheal elongation phenotype, loss of its transcriptional target *ACC* causes tracheal overelongation; because DrICE and ACC affect tracheal elongation with opposite outcomes, we reasoned that if these proteins do act in the same pathway, DrICE might inactivate dSREBP, a curious observation that would be contradictory to the previously published study from Amarneh et al.[11] We next used CRISPR and transgenic alleles of dSREBP to test whether DrICE inactivates dSREBP. Based on the epistatic relationships among *SREBP$^{\Delta ORF}$*, *DrICE^{17}*, and *yorkie^{B5}*, we hypothesized that dSREBP may act downstream of DrICE and the Hippo Network. Furthermore, we show that *SREBP$^{\Delta ORF}$* recapitulates other epistatic relationships between DrICE the septate junction proteins Sinuous and Yurt. We demonstrate that tracheal overexpression of the S1/S2P-cleaved form of SREBP causes a dramatic phenotype of gross morphological defects that resembles excessive cell death, while tracheal overexpression of caspase-cleaved DrICE, like dSREBP$^{\Delta ORF}$, causes no obvious defects. Finally, we show that overexpression of the caspase DrICE is more lethal in larvae that are fed a lipid-depleted diet—when dSREBP is activated to produce compensatory lipids—presumably due to over-activation of dSREBP and consequent overproduction of lipids.

We also show preliminary evidence—with a buoyancy-based assay— that larvae with defects in DrICE-mediated dSREBP processing have a *lower* lipid content than when they are fed a lipid-rich diet. These data appear to contradict the genetic evidence for DrICE-mediated inhibition of dSREBP because they suggest lower dSREBP function in the absence of DrICE; altogether, these data paint a quite complex portrait of the interplay between DrICE and metabolism.

In addition to the genetic backcrossing and transheterozygous approaches summarized in Part II (above), several key experiments will need to be performed in order to confirm whether DrICE and dSREBP act within the same pathway or if they act in parallel. Because we previously demonstrated that DrICE affects intracellular trafficking, one approach would be to assay whether *dSREBP^{D386A}* is able to suppress the trafficking defects that DrICE does. Here, for example, we show that *dSREBP$^{\Delta ORF}$* suppresses the length

defect of *yurt*^{65A}, but it's unclear whether that's due to a trafficking function of dSREBP related to DrICE or if is due to a role in a parallel pathway. For example, because we know that *DrICE*^{17} suppresses the length and trafficking defects in *yurt*^{65A}, we would predict that *dSREBP*^{D386A} might also suppress the length and trafficking defects in *yurt*^{65A} but only if they act within the same pathway. Similarly, if dSREBP cleavage is required for DrICE to affect tracheal elongation, we would predict that overexpression of btl>*dSREBP*$^{1\text{-}386}$ would be sufficient to suppress the tracheal elongation defects of *DrICE*^{17} and *DrICE*$^{\Delta 1}$.

An alternative approach to assaying whether DrICE affects dSREBP is to compare and contrast the transcriptional outputs of dSREBP in varied genetic backgrounds. Because bHLH proteins like SREBP typically control transcription of target genes in either homo- or heterodimers, we hypothesize that if DrICE cleaves S2P-processed SREBP in the same pathway, the result may alter its ability to bind to transcriptional co-factors by removing the 66 amino acid tail C-terminal to its bHLH-Zip domains. If this is the case, the transcriptional targets of dSREBP would be altered based on DrICE-mediated cleavage. One notable experimental approach will be required to test this hypothesis: a transcriptional profile of dSREBP target gene output in *wildtype, dSREBP*$^{\Delta ORF}$, and *dSREBP*^{D386A} larvae with and without the presence of dietary lipids. This could be accomplished using a variety of experimental approaches: (i) qPCR could be used to test representative candidate genes such as *ACC* or *HMGCR*, (ii) ChIP-seq could reveal patterns in SREBP^{wt} vs *SREBP*^{D386A} backgrounds, or (iii) RNA-seq could provide a non-biased readout of differential gene expression in SREBP^{wt} vs *SREBP*^{D386A}. These experiments would reveal whether DrICE is required for a differential dSREBP-mediated transcriptional output, and if so, how the transcriptional targets vary.

Cellular energy production and consumption are key processes that have recently been recognized for their contributions to diverse phenotypes— for example, immunometabolism is a new field that seeks to understand how metabolic states can both drive and respond to signaling networks that regulate critical organismal homeostatic as well as pathological processes like T cell differentiation and cancer. [306-308] Indeed, recent studies have explored the use of lipid synthesis enzymes as a therapeutic route for various diseases.[309, 310] Although the metabolic changes associated with some disease states are not currently

well understood, clarifying the relationships between them could allow us to create novel therapeutic agents that may be able to target currently incurable diseases like chronic kidney disease and glomerular sclerosis.

IV. Materials and Methods

Fly Stocks

The following mutant alleles were used: *yorkie*^{B5}, *DrICE*^{17}, and *yurt*^{65A}, *SREBP*$^{\Delta ORF}$, *SREBP*^{D386A}. Overexpression of dSREBP in the trachea was achieved using the UAS/Gal4 system: the *btl>Gal4* driver was used to express Gal4 in all tracheal cells; *btl>Gal4* flies were crossed to UAS-dSREBP1-452 or UAS-dSREBP1-386 flies, which include a transgenic SREBP cDNA truncated at the corresponding amino acids downstream of UAS (see *Transgenic Constructs* below). The double mutant *yurt*^{65A}, *SREBP*$^{\Delta ORF}$ was generated using standard recombination crosses. Each single male resulting from the recombination crosses was screened for *yurt*^{65A} via failure to a complement *yurt*^{65A} single mutant and screened for the presence of the *SREBP*$^{\Delta ORF}$ mutation by looking for the fluorescent marker dsRed, which was inserted in place of the SREBP ORF via CRISPR by James Kwon. In the case of the control diet, flies were cultured on food according to the Bloomington media recipe. Food for a lipid-depleted diet followed the same protocol, but yeast powder was omitted and replaced with yeast autolysate (Sigma Aldrich 73145-500G), which includes only the soluble portion of yeast extract.

Transgenic constructs

UAS-SREBP 1-452 was obtained from the Bloomington stock center, where it was deposited by the Rawson lab. In order to create the UAS-SREBP 1-386 transgenic line, the SREBP cDNA sequence corresponding to the N-terminal 386 amino acids was cloned into the MCS of pUAST vector using Gibson cloning and subsequently inserted into the attP2 site into flies with the phiC31 integrase system.

Embryo staining

Parental flies were placed in empty food bottles capped with a molasses-agar plate spread with wet yeast. After 24 hours, plates were removed and embryos were fixed and stained as follows: embryos were dechorionated with 50% bleach for 4 minutes, and fixed in equal parts heptane and 4% formaldehyde on a

shaker for 25 minutes. Embryos were then devitellenized for 1 minute with 100% methanol/heptane, rehydrated to PBS-T (0.1% Triton-X100) (100%, 100%, 100%, 50%, each for 5 min), washed in PBST for 5x5' and then 3x30'. PBS-BT (3% BSA in PBS-T) was used to block for 30 minutes at RT before addition of primary antibody, in which embryos were incubated for 48 hours at 4 °C on a rotator. See the attached chart below for appropriate antibody dilutions. PBS-T and PBS-BT steps were repeated on the third day before addition of fluorescent secondary antibodies, in which embryos were incubated O/N at 4 °C. On the final day, PBS-T washes were repeated, embryos were dehydrated using an ethanol series (50%, 70%, 90%, 100%, 100% EtOH, each for 5 min), incubated in methyl salicylate for 15 min at RT, and then mounted with methyl salicylate and Permount mounting media (Fisher Scientific, SP15-500). More information about reagents can be found in Supplementary Table 1.

Image acquisition

Confocal z-stacks were obtained with the 63X NA 1.24 oil objective on the Leica SP8 image format greater than or equal to 2048x2048, pinhole size 0.7AU, and system optimized z-step sizes of approximately 0.2 um. Images were subsequently deconvolved using Leica HyVolution software with a Huygens Essential Automatic setting. All quantification was performed on the resulting images.

Adult survival calculations

In order to determine the relative viability of btl>DrICE WT on control vs lipid-depleted food, we set up and equal number of adult btl>Gal4 virgin females with UAS-DrICE^{WT}/CyOYFP male flies. The number of flies that hatched were scored for the CyO phenotype (indicating a genotype of btl>Gal4/ CyOYFP) vs straight wings (btl>Gal4/ UAS-DrICE^{WT}) and counted. To determine the expected number of flies of each genotype, the total number of flies was multiplied by 0.5. To determine the overall survival, the observed number of progeny for each genotype was divided by the resulting expected value.

Tracheal lengths were determined by tracing the length of the dorsal trunk by hand through 3D in Volocity Demo 5.5.1.

V. Contributions

SM and GJB conceived and designed the experiments. James Kwon generated the *SREBP*$^{\Delta ORF}$ CRISPR allele. SM performed all other experiments. SM and GJB analyzed the data.

CHAPTER 4: Conclusions and future directions

Study the past if you would define the future.
–Confucius

I. Contributions to knowledge about tube size control and non-apoptotic caspase function

Size control of organs and tissues is critical to ensuring their proper function—without establishment and maintenance of proper size, devastating and currently incurable diseases can occur. One particular challenge to our understanding of size control is that of biological tubes. The countless tubes that comprise our organs must be precisely sized in order to ensure proper organ function. In light of this challenge, our lab uses the developing *Drosophila* tracheal system as a model to study the mechanisms by which epithelial tube size is controlled.

Here, we have investigated the role played by the executioner Caspase-3 homolog, DrICE, in promoting the elongation of the embryonic trachea without causing cell death. Prior to recent years, caspases had almost exclusively been described as the executioners of cell death. Lately, however, many new non-apoptotic caspase functions have been discovered. This work describes our discovery of one such novel non-apoptotic role of DrICE in regulating intracellular trafficking during the morphological changes that accompany tracheal size control.

In Chapter 2, we show that DrICE acts downstream of the Hippo Network to regulate endocytic trafficking of cell polarity, cell junction and apical extracellular matrix proteins involved in tracheal tube size control. We further show that tracheal cells are competent to undergo apoptosis, even though developmentally-regulated DrICE function rarely kills tracheal cells. My results reveal a novel developmental role for caspases, and a previously unidentified pool of DrICE that colocalizes with endocytic markers. We also show for the first time a mechanism by which the Hippo Network controls intracellular trafficking through regulation of caspases. Given recently published reports of *in vitro* regulation of endocytosis by mammalian

caspases during apoptosis, we propose that caspase-mediated regulation of trafficking is an evolutionarily conserved function of caspases that can be co-opted during morphogenesis. When considered together with *in vitro* mammalian results implicating caspases in trafficking in both apoptotic and pathological conditions, our results suggest that caspase regulation of trafficking can be deployed during morphogenesis or inappropriately activated in pathologic conditions like ischemia and cancer.

Our discoveries regarding the functions of caspases and the Hippo Network in regulating intracellular trafficking have implications that are broadly relevant to the fields of developmental biology, cell biology, cell death, and medicine. Importantly, this is the first report of an executioner caspase regulating endocytic trafficking in normal development rather than in apoptosis. Second, while several large-scale screens have identified proteins that allow the endocytic system to regulate Hippo signaling, this work is the first to identify the converse: Hippo Network regulation of endocytic trafficking. Third, this is the first report to identify a pool of executioner caspase that colocalizes with endocytic compartments in non-apoptotic cells. Fourth, there are profound medical implications for caspase activity altering endocytic routing of junctional, polarity or signaling proteins. In particular, our results provide a mechanistic explanation for the observations that during mammalian ischemic vascular injury, there is substantial activation of caspases in non-apoptotic cells, which causes downregulation of claudin-based tight junctions and a concomitant large and damaging increase in vascular permeability. Sub-apoptotic caspase activation is also common in cancer as well as cancer therapeutics; given that downregulation of junctions and polarity determinants contributes to epithelial-to-mesenchymal transition (EMT), however, the possibility that caspase-activating treatments could contribute to EMT is of significant concern.

Furthermore, in the appendices that follow, I detail additional characterization of DrICE. In the third appendix, I characterize a C-terminally FLAG-tagged DrICE that I generated using CRISPR, and I offer some explanations regarding the mechanisms by which it acts as a loss-of-function allele. In the fourth appendix, I investigate whether the intracellular trafficking of additional molecules aPKC and pSrc may also be regulated by DrICE in the trachea and in another epithelial tube in the developing embryo, the hindgut.

In addition to my results detailing the role of caspases in morphogenesis, I provide contributions to our understanding of how physical forces can contribute to the process of tracheal elongation and morphogenesis. In the first section, from a commentary article we published in *PNAS* in 2015, I evaluate a contemporary paper that discusses the self-assembly of supracellular actin rings during tracheal development. In the second, I explore the model of differential junction dynamics, which attempts to explain the preferentially axial orientation of tracheal cells, using Fluorescence Recovery After Photobleaching (FRAP).

Altogether, my work has contributed significant knowledge to the fields of tube size control and non-apoptotic caspase functions. We show that caspases can affect growth through regulation of intracellular trafficking of select cargo, and consequently that the HN can affect trafficking through regulating caspases, and we explore how physical forces can impact morphogenesis. The conclusions drawn from these results are especially impactful because they have profound implications in diseases such as ischemic vascular injury and cancer, which could pave the way for more effective and life-changing therapeutics.

II. Unanswered questions and future directions

The conclusions drawn from this work raise a number of complex and challenging questions that remain to be experimentally addressed. For example, what are the mechanisms by which cells utilize lethal caspases for vital processes without succumbing to cell death? What are the substrates of DrICE that elongate the trachea? Is dSRBEP one such substrate of DrICE? What approaches can help us identify substrates of DrICE? And finally, what is the evolutionary nature of the involvement of DrICE in intracellular trafficking?

How do cells utilize caspases without dying?

Arguably the chief question that has been asked alongside the growing discoveries of non-apoptotic caspase functions is how cells are able to use caspases without succumbing to cell death. One model is

that cells can buffer a limited abundance of caspase activity such that the activation of some number of molecules, X, results in non-apoptotic functions while a number greater than X results in cell death. A related model predicated on the wide range of caspase substrates (see below), is that the binding affinity of caspases for their non-apoptotic substrates is simply greater than their affinity for apoptotic ones. A third model is that the spatiotemporal activity of caspases is strictly controlled by an unknown mechanism such that vital substrates like DNases are not physically accessible to caspases as non-apoptotic processes are being carried out.

We hypothesize that the association of DrICE with the Clathrin adaptor protein Adaptin (AP47) is key to understanding how cells escape caspase-mediated death. As discussed in Chapter 2, select intracellular cargo are selected for trafficking pathways through their interaction with AP47, which is known to interact with cargo through a specific dileucine motif. Indeed, I identified an evolutionarily conserved dileucine motif in DrICE that is also present in other cell death machinery including the apoptotic activator APAF and the initiator caspase Dronc, yet it is notably absent in the anti-apoptotic protein DIAP1 (Figure 2.9a), which is enriched in the nucleus (Figure A4.1e). In Chapter 2, we present experimental evidence that this dileucine motif is required for the tracheal elongating function of overexpressed DrICE.

Our discovery of the association of caspases with intracellular trafficking machinery including AP47 supports a model that is most similar to the third model of spatiotemporal regulation of caspase activity. We hypothesize that the association of DrICE with the Clathrin adaptor protein AP47 controls its spatiotemporal *activation* in order to limit its apoptotic potential. As the dileucine motif that recruits proteins to AP47 is evolutionarily conserved within caspase activators and initiator caspases, our model proposes that the recruitment of DrICE and its activators results in a localized concentration of these molecules that is likely to result in caspase activation specifically at sites of Clathrin-mediated vesicular trafficking.

Our model provides promising mechanistic insight into the question of how caspases can be used by cells without causing cell death. It also raises numerous, experimentally testable questions including: is the

dileucine motif required for apoptotic and/or other non-apoptotic functions of DrICE? Is the motif is required in all of the apoptotic proteins in which it can be found?

What are the substrates of DrICE that elongate the trachea?

There is now a vast number of experimentally validated caspase substrates, but they are so diverse in their cleavage patterns and cellular contexts in which they are cleaved that it only complicates the matter of identifying the substrates of DrICE that cause tracheal elongation. On the level of primary structure, many descriptions of Caspase-3 substrate specificity often describe its cleavage of a peptide bond after the specific amino acid sequence DEVD, an observation that is derived from the peptide sequence in IAP proteins that is cleaved by Caspase-3. In fact, many caspase reporters rely on the cleavage of that DEVD motif as a readout of their activity. A more thorough examination of experimentally determined caspase substrates, however, shows that those substrates can vary widely in amino acid sequence at the site of cleavage. In other words, there are few amino acid sequence requirements that can accurately predict caspase substrate identification.

One method for assaying substrate preference of a caspase is through assays that couple fluorescent reporters to varied synthetic peptides and calculate the rate of the reaction upon incubation with caspase.[4] Such methods have revealed some interesting data on caspase substrate preference, but they can also contradict findings based on *in vivo* data. Identifying “natural” caspase substrates, however, is a herculean task complicated by the complexities of cell death machinery. Other types of experimental approaches such as mass-spectrometry (MS)-based ones, are also promising. Mass spectrometry also has its challenges, however, such as low abundance or stability of substrates, absence of endogenous substrate expression in the tested cells, or interference with product detection by requisite protein digestion.[311]

Is dSREBP a substrate of DrICE?

In Chapter 3, I explore the tracheal function of a putative substrate of DrICE, the Sterol Regulatory Element Binding Protein (dSREBP). Previous reports implicated DrICE as an activator of SREBP necessary for its transcriptional activation in the absence of its canonical protease, S2P. Here, we expand upon those findings to support that the previously demonstrated DrICE-cleaved residue of dSREBP, Asp386, may be required for the restriction of tracheal overelongation. Althouth it remains unclear whether dSREBP is a substrate of DrICE in tracheal morphogenesis, I demonstrate that there is a difference in the tracheal toxicity of the canonically S2P-cleaved dSREBP (*dSREBP*$^{1\text{-}452}$) and its DrICE-cleaved counterpart (*dSREBP*$^{1\text{-}386}$). These data imply that the 66-amino acid tail of dSREBP between the two sites of proteolysis contributes to its differential output that is potentially due to different transcriptional co-factors. A number of key experiments outlined in Chapter 3 will need to be performed in order to confirm whether there is interplay between dSREBP and DrICE, but the difference in phenotypic output between dSREBP with and without that 66 amino-acid tail implies that one non-apoptotic function of DrICE maybe to change the transcriptional binding partners of dSREBP.

What approaches can help us identify tracheal-elongating substrates of DrICE?

The task of determining the factors that influence whether caspase activity will result in apoptotic vs non-apoptotic outcomes is overwhelming in its breadth. Identifying the substrates of DrICE that elongate the trachea may appear to be a more attainable goal, but the two tasks have many common challenges. For example, a candidate approach to tracheal-elongating substrate identification would be largely expensive in time and resources, given the certainly incomplete but vast list of experimentally identified caspase substrates, and has so far led to inconclusive results with *dSREBP*.

One possible experimental approach to identify tracheal-elongating substrates of DrICE is to perform a forward genetic screen in which *DrICE*- or *yorkie*- loss of function mutants are screened against the

deletions in the genome for enhancers and suppressors of their trafficking-mediated tracheal elongation phenotype. Of course, the major limitation of this approach is its time-intensive nature; screening the thousands of multi-gene deficiencies of the *Drosophila* genome that are presently available would not yield quick or simple results. Although this classic approach may provide valuable information, it would also be complicated by classic limitations: because the exact downstream vs parallel nature of genetic relationships is not clear through epistasis data alone. Additionally, because it's likely that DrICE has multiple substrates that contribute to its effects on tracheal length rather than just one, we anticipate that this method is unlikely to yield definitive substrates. Altogether, this approach would therefore require extensive further characterization on top of the myriad genetic crosses.

One alternative to using a genetic screen to identify caspase substrates is to use mass-spectrometry (MS)-based approaches. For example, an immunoprecipitation assay with the DrICE antibody in embryos followed by MS could help generate a list of candidate substrates. This approach may be less time-intensive than a genetic screen, but it also has limitations in the limited availability of embryonic tracheal tissue, the potentially transient or low-signal interactions between caspase and substrate, as well as the standard limitations of MS as discussed above.

It is possible, if not likely, that DrICE acts on multiple substrates in order to drive tracheal elongation, which may complicate any attempt to experimentally determine the identities of its substrates. Given what we were able to conclude based on detailed and thorough analysis of $DrICE^{17}$ and $yorkie^{B5}$ mutant embryos, however, we now have an idea that it acts through its interactions with the Clathrin adaptor protein AP47. Subsequently, because of the strong evolutionary conservation of DrICE and Caspase-3, MS in mammalian cell lines could be used to differentiate between the substrates of Caspase-3 with and without a dileucine motif, thereby generating a list of putative endocytic caspase substrates.

Non-apoptotic caspase function—chicken or egg?

It is tempting to speculate that the cell death functions of caspases arose before non-apoptotic functions because of the evolutionary advantages conferred by the ability of a cell to die. In multicellular organisms, for example, cell death provides an evolutionary advantage by providing a mechanism of micro-evolution within developing tissues—apoptosis can allow a kind of rivalry among cells that can result in establishment of a complex network with minimal errors, as is the case in mammalian brain development or T-cell maturation. As with evolution, the specification of extra cells that are phenotypically or genetically diverse allows innovation by providing a tool to eliminate dangerous errors—caspases provide a metaphorical eraser in the sketch of life. Even though excessive cell death can be devastating to an organism, such a valuable tool gives organisms greater freedom to gain complexity through evolutionary time.

The evolutionary record, however, may favor a model in which the death -dependent and -independent roles of caspases arose simultaneously. Caspases are members of a broad family of proteins that can be found across evolutionary time in select prokaryotes, unicellular eukaryotes, and multicellular eukaryotes. Known metacaspases in single-celled organisms were mostly identified in screens for death related functions, but they also have critical non-death related ones. For example, the yeast caspase-like protein Yca1 is required for breaking up protein aggregates and preventing cell death.[312] These common roles of metacaspases and caspases supports two models (i) concurrent evolution of death-dependent and -independent caspase functions, or (ii) a protein quality control function of caspases arose before their cell-death related functions. One caveat to these speculations, however, is that the metacaspases present in single-celled organisms, are evidence of a shared ancestor with caspases, since they have some divergent properties including mechanisms of activation and sites of cleavage.[313] Indeed, Bell and Megeney make the excellent point that a functional substitution experiment would be necessary to validate the evolutionary relationship between caspases and metacaspases.

III. Concluding remarks

Potential application to human disease

The ultimate goal of our lab is to contribute knowledge to the field of tube size control in order to understand the pathology of currently incurable diseases. This work is potentially applicable to human disease because it suggests that caspases may drive tube size control by contributing to cargo selection during intracellular trafficking. This is related to multiple human tube size pathologies including polycystic kidney disease, vascular ischemic injury, and cancer and metastasis.

Summary

As D'Arcy Thompson sagely suspected over a hundred years ago: *size of the body is no mere accident*. The work we present in this document supports the concepts proposed by Thompson and other early 20th century biologists: there are mechanisms in place to dictate organismal and tissue size. We do so through our discovery of an unexpected role of the executioner caspase DrICE in promoting cell growth by regulating intracellular trafficking, and we explore the potential of the fascinating transcription factor required for lipid synthesis, dSREBP, as a putative tracheal-size determining substrate of DrICE. Altogether, this investigation has identified novel biology and has yielded a promising list of specific future experimental approaches to better understand the molecular mechanisms of tube size control and non-apoptotic caspase function.

REFERENCES

1. Ditzel, M. *et al.* Inactivation of effector caspases through nondegradative polyubiquitylation. *Molecular cell* **32**, 540-553 (2008).
2. Baer, M.M. *et al.* The role of apoptosis in shaping the tracheal system in the Drosophila embryo. *Mechanisms of development* **127**, 28-35 (2010).
3. Samakovlis, C. *et al.* Development of the Drosophila tracheal system occurs by a series of morphologically distinct but genetically coupled branching events. *Development* **122**, 1395-1407 (1996).
4. Poreba, M., Strozyk, A., Salvesen, G.S. & Drag, M. Caspase substrates and inhibitors. *Cold Spring Harbor perspectives in biology* **5**, a008680 (2013).
5. Robbins, R.M., Gbur, S.C. & Beitel, G.J. Non-canonical roles for Yorkie and Drosophila Inhibitor of Apoptosis 1 in epithelial tube size control. *PloS one* **9**, e101609 (2014).
6. Molina, D.K. & DiMaio, V.J. Normal organ weights in men: part II-the brain, lungs, liver, spleen, and kidneys. *The American journal of forensic medicine and pathology* **33**, 368-372 (2012).
7. Cooper, A.D., Campeau, N.G. & Meissner, I. Susceptibility-weighted imaging in familial cerebral cavernous malformations. *Neurology* **71**, 382 (2008).
8. Faguer, S. *et al.* Massively enlarged polycystic kidneys in monozygotic twins with TCF2/HNF-1beta (hepatocyte nuclear factor-1beta) heterozygous whole-gene deletion. *American journal of kidney diseases : the official journal of the National Kidney Foundation* **50**, 1023-1027 (2007).
9. Harris, P.C. & Torres, V.E. Polycystic kidney disease. *Annual review of medicine* **60**, 321-337 (2009).
10. Wilson, P.D. Polycystic kidney disease. *The New England journal of medicine* **350**, 151-164 (2004).
11. Amarneh, B., Matthews, K.A. & Rawson, R.B. Activation of sterol regulatory element-binding protein by the caspase Drice in Drosophila larvae. *The Journal of biological chemistry* **284**, 9674-9682 (2009).
12. Rawlins, E.L. The building blocks of mammalian lung development. *Developmental dynamics : an official publication of the American Association of Anatomists* **240**, 463-476 (2011).
13. West, J.B. Marcello Malpighi and the discovery of the pulmonary capillaries and alveoli. *Am J Physiol Lung Cell Mol Physiol* **304**, L383-390 (2013).
14. Silva, D.M., Nardiello, C., Pozarska, A. & Morty, R.E. Recent advances in the mechanisms of lung alveolarization and the pathogenesis of bronchopulmonary dysplasia. *Am J Physiol Lung Cell Mol Physiol* **309**, L1239-1272 (2015).
15. Yin, Y., Wang, F. & Ornitz, D.M. Mesothelial- and epithelial-derived FGF9 have distinct functions in the regulation of lung development. *Development* **138**, 3169-3177 (2011).
16. Colvin, J.S., White, A.C., Pratt, S.J. & Ornitz, D.M. Lung hypoplasia and neonatal death in Fgf9-null mice identify this gene as an essential regulator of lung mesenchyme. *Development* **128**, 2095-2106 (2001).
17. Glazer, L. & Shilo, B.Z. The Drosophila FGF-R homolog is expressed in the embryonic tracheal system and appears to be required for directed tracheal cell extension. *Genes & development* **5**, 697-705 (1991).
18. Lee, T., Hacohen, N., Krasnow, M. & Montell, D.J. Regulated Breathless receptor tyrosine kinase activity required to pattern cell migration and branching in the Drosophila tracheal system. *Genes & development* **10**, 2912-2921 (1996).
19. Grantham, J.J., Mulamalla, S. & Swenson-Fields, K.I. Why kidneys fail in autosomal dominant polycystic kidney disease. *Nature reviews. Nephrology* **7**, 556-566 (2011).
20. Liu, X. *et al.* Polycystin-2 is an essential ion channel subunit in the primary cilium of the renal collecting duct epithelium. *eLife* **7** (2018).
21. Hooper, K.M. *et al.* Expression of polycystin-1 enhances endoplasmic reticulum calcium uptake and decreases capacitative calcium entry in ATP-stimulated MDCK cells. *American journal of physiology. Renal physiology* **289**, F521-530 (2005).
22. Su, Q. *et al.* Structure of the human PKD1-PKD2 complex. *Science* **361** (2018).

23. Hanaoka, K. *et al.* Co-assembly of polycystin-1 and -2 produces unique cation-permeable currents. *Nature* **408**, 990-994 (2000).
24. Nauli, S.M. *et al.* Polycystins 1 and 2 mediate mechanosensation in the primary cilium of kidney cells. *Nature genetics* **33**, 129-137 (2003).
25. Rodat-Despoix, L., Hao, J., Dandonneau, M. & Delmas, P. Shear stress-induced Ca(2)(+) mobilization in MDCK cells is ATP dependent, no matter the primary cilium. *Cell calcium* **53**, 327-337 (2013).
26. Chebib, F.T., Sussman, C.R., Wang, X., Harris, P.C. & Torres, V.E. Vasopressin and disruption of calcium signalling in polycystic kidney disease. *Nature reviews. Nephrology* (2015).
27. Adeva, M. *et al.* Clinical and molecular characterization defines a broadened spectrum of autosomal recessive polycystic kidney disease (ARPKD). *Medicine (Baltimore)* **85**, 1-21 (2006).
28. Thakur, P., Speer, P. & Rajkovic, A. Novel Mutation in the PKHD1 Gene Diagnosed Prenatally in a Fetus with Autosomal Recessive Polycystic Kidney Disease. *Case Rep Genet* **2014**, 517952 (2014).
29. Torres, V.E., Gansevoort, R.T. & Czerwiec, F.S. Tolvaptan in Later-Stage Polycystic Kidney Disease. *The New England journal of medicine* **378**, 489-490 (2018).
30. Dubois, E.A., Rissmann, R. & Cohen, A.F. Tolvaptan. *Br J Clin Pharmacol* **73**, 9-11 (2012).
31. Weimbs, T., Shillingford, J.M., Torres, J., Kruger, S.L. & Bourgeois, B.C. Emerging targeted strategies for the treatment of autosomal dominant polycystic kidney disease. *Clin Kidney J* **11**, i27-i38 (2018).
32. Muller, R.U. & Benzing, T. Management of autosomal-dominant polycystic kidney disease-state-of-the-art. *Clin Kidney J* **11**, i2-i13 (2018).
33. Berry, K.L., Bulow, H.E., Hall, D.H. & Hobert, O. A C. elegans CLIC-like protein required for intracellular tube formation and maintenance. *Science* **302**, 2134-2137 (2003).
34. Ashley, R.H. Challenging accepted ion channel biology: p64 and the CLIC family of putative intracellular anion channel proteins (Review). *Mol Membr Biol* **20**, 1-11 (2003).
35. Harrop, S.J. *et al.* Crystal structure of a soluble form of the intracellular chloride ion channel CLIC1 (NCC27) at 1.4-A resolution. *The Journal of biological chemistry* **276**, 44993-45000 (2001).
36. Folkman, J. & Haudenschild, C. Angiogenesis in vitro. *Nature* **288**, 551-556 (1980).
37. Jones, S.J. & Baillie, D.L. Characterization of the let-653 gene in Caenorhabditis elegans. *Molecular & general genetics : MGG* **248**, 719-726 (1995).
38. Devine, W.P. *et al.* Requirement for chitin biosynthesis in epithelial tube morphogenesis. *Proceedings of the National Academy of Sciences of the United States of America* **102**, 17014-17019 (2005).
39. Syed, Z.A. *et al.* A luminal glycoprotein drives dose-dependent diameter expansion of the Drosophila melanogaster hindgut tube. *PLoS genetics* **8**, e1002850 (2012).
40. O'Brien, L.E., Zegers, M.M. & Mostov, K.E. Opinion: Building epithelial architecture: insights from three-dimensional culture models. *Nature reviews. Molecular cell biology* **3**, 531-537 (2002).
41. Uv, A., Cantera, R. & Samakovlis, C. Drosophila tracheal morphogenesis: intricate cellular solutions to basic plumbing problems. *Trends in cell biology* **13**, 301-309 (2003).
42. Affolter, M. & Caussinus, E. Tracheal branching morphogenesis in Drosophila: new insights into cell behaviour and organ architecture. *Development* **135**, 2055-2064 (2008).
43. Letizia, A., Sotillos, S., Campuzano, S. & Llimargas, M. Regulated Crb accumulation controls apical constriction and invagination in Drosophila tracheal cells. *Journal of cell science* **124**, 240-251 (2011).
44. Klose, S., Flores-Benitez, D., Riedel, F. & Knust, E. Fosmid-based structure-function analysis reveals functionally distinct domains in the cytoplasmic domain of Drosophila crumbs. *G3* **3**, 153-165 (2013).
45. Jones, T.A. & Metzstein, M.M. A novel function for the PAR complex in subcellular morphogenesis of tracheal terminal cells in Drosophila melanogaster. *Genetics* **189**, 153-164 (2011).
46. Stewart, R.A., Li, D.M., Huang, H. & Xu, T. A genetic screen for modifiers of the lats tumor suppressor gene identifies C-terminal Src kinase as a regulator of cell proliferation in Drosophila. *Oncogene* **22**, 6436-6444 (2003).

47. Nelson, K.S. *et al.* Drosophila Src regulates anisotropic apical surface growth to control epithelial tube size. *Nature cell biology* **14**, 518-525 (2012).
48. Olivares-Castineira, I. & Llimargas, M. Anisotropic Crb accumulation, modulated by Src42A, is coupled to polarised epithelial tube growth in Drosophila. *PLoS genetics* **14**, e1007824 (2018).
49. Laprise, P. *et al.* Epithelial polarity proteins regulate Drosophila tracheal tube size in parallel to the luminal matrix pathway. *Current biology : CB* **20**, 55-61 (2010).
50. Laprise, P. *et al.* The FERM protein Yurt is a negative regulatory component of the Crumbs complex that controls epithelial polarity and apical membrane size. *Developmental cell* **11**, 363-374 (2006).
51. Wang, S. *et al.* Septate-junction-dependent luminal deposition of chitin deacetylases restricts tube elongation in the Drosophila trachea. *Current biology : CB* **16**, 180-185 (2006).
52. Merzendorfer, H. & Zimoch, L. Chitin metabolism in insects: structure, function and regulation of chitin synthases and chitinases. *The Journal of experimental biology* **206**, 4393-4412 (2003).
53. Luschnig, S., Batz, T., Armbruster, K. & Krasnow, M.A. serpentine and vermiform encode matrix proteins with chitin binding and deacetylation domains that limit tracheal tube length in Drosophila. *Current biology : CB* **16**, 186-194 (2006).
54. Tonning, A. *et al.* A transient luminal chitinous matrix is required to model epithelial tube diameter in the Drosophila trachea. *Developmental cell* **9**, 423-430 (2005).
55. Behr, M., Wingen, C., Wolf, C., Schuh, R. & Hoch, M. Wurst is essential for airway clearance and respiratory-tube size control. *Nature cell biology* **9**, 847-853 (2007).
56. Tsarouhas, V. *et al.* Sequential pulses of apical epithelial secretion and endocytosis drive airway maturation in Drosophila. *Developmental cell* **13**, 214-225 (2007).
57. Dong, B., Hannezo, E. & Hayashi, S. Balance between apical membrane growth and luminal matrix resistance determines epithelial tubule shape. *Cell reports* **7**, 941-950 (2014).
58. Olivares-Castineira, I. & Llimargas, M. EGFR controls Drosophila tracheal tube elongation by intracellular trafficking regulation. *PLoS genetics* **13**, e1006882 (2017).
59. Goulev, Y. *et al.* SCALLOPED interacts with YORKIE, the nuclear effector of the hippo tumor-suppressor pathway in Drosophila. *Current biology : CB* **18**, 435-441 (2008).
60. Ren, F., Zhang, L. & Jiang, J. Hippo signaling regulates Yorkie nuclear localization and activity through 14-3-3 dependent and independent mechanisms. *Developmental biology* **337**, 303-312 (2010).
61. Dong, J. *et al.* Elucidation of a universal size-control mechanism in Drosophila and mammals. *Cell* **130**, 1120-1133 (2007).
62. Oh, H. & Irvine, K.D. In vivo regulation of Yorkie phosphorylation and localization. *Development* **135**, 1081-1088 (2008).
63. Justice, R.W., Zilian, O., Woods, D.F., Noll, M. & Bryant, P.J. The Drosophila tumor suppressor gene warts encodes a homolog of human myotonic dystrophy kinase and is required for the control of cell shape and proliferation. *Genes & development* **9**, 534-546 (1995).
64. Rock, J.M. *et al.* Activation of the yeast Hippo pathway by phosphorylation-dependent assembly of signaling complexes. *Science* **340**, 871-875 (2013).
65. Weiss, E.L. Mitotic exit and separation of mother and daughter cells. *Genetics* **192**, 1165-1202 (2012).
66. Xu, T., Wang, W., Zhang, S., Stewart, R.A. & Yu, W. Identifying tumor suppressors in genetic mosaics: the Drosophila lats gene encodes a putative protein kinase. *Development* **121**, 1053-1063 (1995).
67. Udan, R.S., Kango-Singh, M., Nolo, R., Tao, C. & Halder, G. Hippo promotes proliferation arrest and apoptosis in the Salvador/Warts pathway. *Nature cell biology* **5**, 914-920 (2003).
68. Harvey, K.F., Pfleger, C.M. & Hariharan, I.K. The Drosophila Mst ortholog, hippo, restricts growth and cell proliferation and promotes apoptosis. *Cell* **114**, 457-467 (2003).
69. Lai, Z.C. *et al.* Control of cell proliferation and apoptosis by mob as tumor suppressor, mats. *Cell* **120**, 675-685 (2005).
70. Sudol, M. Yes-associated protein (YAP65) is a proline-rich phosphoprotein that binds to the SH3 domain of the Yes proto-oncogene product. *Oncogene* **9**, 2145-2152 (1994).

71. Huang, J., Wu, S., Barrera, J., Matthews, K. & Pan, D. The Hippo signaling pathway coordinately regulates cell proliferation and apoptosis by inactivating Yorkie, the Drosophila Homolog of YAP. *Cell* **122**, 421-434 (2005).
72. Moya, I.M. & Halder, G. Discovering the Hippo pathway protein-protein interactome. *Cell research* **24**, 137-138 (2014).
73. Kwon, Y. *et al.* The Hippo signaling pathway interactome. *Science* **342**, 737-740 (2013).
74. Couzens, A.L. *et al.* Protein interaction network of the mammalian Hippo pathway reveals mechanisms of kinase-phosphatase interactions. *Science signaling* **6**, rs15 (2013).
75. Wang, W. *et al.* Defining the protein-protein interaction network of the human hippo pathway. *Molecular & cellular proteomics : MCP* **13**, 119-131 (2014).
76. Weiss, E.L. Hippo unleashed! Proteome-scale analysis reveals new views of Hippo pathway biology. *Science signaling* **6**, pe36 (2013).
77. Enderle, L. & McNeill, H. Hippo gains weight: added insights and complexity to pathway control. *Science signaling* **6**, re7 (2013).
78. Hergovich, A., Stegert, M.R., Schmitz, D. & Hemmings, B.A. NDR kinases regulate essential cell processes from yeast to humans. *Nature reviews. Molecular cell biology* **7**, 253-264 (2006).
79. Rouleau, G.A. *et al.* Alteration in a new gene encoding a putative membrane-organizing protein causes neuro-fibromatosis type 2. *Nature* **363**, 515-521 (1993).
80. Trofatter, J.A. *et al.* A novel moesin-, ezrin-, radixin-like gene is a candidate for the neurofibromatosis 2 tumor suppressor. *Cell* **72**, 791-800 (1993).
81. Pu, J. *et al.* FERM domain containing protein 7 interacts with the Rho GDP dissociation inhibitor and specifically activates Rac1 signaling. *PloS one* **8**, e73108 (2013).
82. Li, Y. *et al.* Angiomotin binding-induced activation of Merlin/NF2 in the Hippo pathway. *Cell research* (2015).
83. Pearson, M.A., Reczek, D., Bretscher, A. & Karplus, P.A. Structure of the ERM protein moesin reveals the FERM domain fold masked by an extended actin binding tail domain. *Cell* **101**, 259-270 (2000).
84. Li, Q. *et al.* Self-masking in an intact ERM-merlin protein: an active role for the central alpha-helical domain. *Journal of molecular biology* **365**, 1446-1459 (2007).
85. Gonzalez-Agosti, C., Wiederhold, T., Herndon, M.E., Gusella, J. & Ramesh, V. Interdomain interaction of merlin isoforms and its influence on intermolecular binding to NHE-RF. *The Journal of biological chemistry* **274**, 34438-34442 (1999).
86. Badouel, C. *et al.* The FERM-domain protein Expanded regulates Hippo pathway activity via direct interactions with the transcriptional activator Yorkie. *Developmental cell* **16**, 411-420 (2009).
87. Oh, H., Reddy, B.V. & Irvine, K.D. Phosphorylation-independent repression of Yorkie in Fat-Hippo signaling. *Developmental biology* **335**, 188-197 (2009).
88. Gaspar, P., Holder, M.V., Aerne, B.L., Janody, F. & Tapon, N. Zyxin antagonizes the FERM protein expanded to couple F-actin and Yorkie-dependent organ growth. *Current biology : CB* **25**, 679-689 (2015).
89. Bennett, F.C. & Harvey, K.F. Fat cadherin modulates organ size in Drosophila via the Salvador/Warts/Hippo signaling pathway. *Current biology : CB* **16**, 2101-2110 (2006).
90. Yu, J. *et al.* Kibra functions as a tumor suppressor protein that regulates Hippo signaling in conjunction with Merlin and Expanded. *Developmental cell* **18**, 288-299 (2010).
91. Genevet, A., Wehr, M.C., Brain, R., Thompson, B.J. & Tapon, N. Kibra is a regulator of the Salvador/Warts/Hippo signaling network. *Developmental cell* **18**, 300-308 (2010).
92. Baumgartner, R., Poernbacher, I., Buser, N., Hafen, E. & Stocker, H. The WW domain protein Kibra acts upstream of Hippo in Drosophila. *Developmental cell* **18**, 309-316 (2010).
93. Grzeschik, N.A., Parsons, L.M., Allott, M.L., Harvey, K.F. & Richardson, H.E. Lgl, aPKC, and Crumbs regulate the Salvador/Warts/Hippo pathway through two distinct mechanisms. *Current biology : CB* **20**, 573-581 (2010).
94. Wodarz, A., Grawe, F. & Knust, E. CRUMBS is involved in the control of apical protein targeting during Drosophila epithelial development. *Mechanisms of development* **44**, 175-187 (1993).

95. Wodarz, A., Hinz, U., Engelbert, M. & Knust, E. Expression of crumbs confers apical character on plasma membrane domains of ectodermal epithelia of Drosophila. *Cell* **82**, 67-76 (1995).
96. Hurd, T.W., Gao, L., Roh, M.H., Macara, I.G. & Margolis, B. Direct interaction of two polarity complexes implicated in epithelial tight junction assembly. *Nature cell biology* **5**, 137-142 (2003).
97. Nam, S.C. & Choi, K.W. Interaction of Par-6 and Crumbs complexes is essential for photoreceptor morphogenesis in Drosophila. *Development* **130**, 4363-4372 (2003).
98. Sotillos, S., Diaz-Meco, M.T., Caminero, E., Moscat, J. & Campuzano, S. DaPKC-dependent phosphorylation of Crumbs is required for epithelial cell polarity in Drosophila. *The Journal of cell biology* **166**, 549-557 (2004).
99. Wei, Z., Li, Y., Ye, F. & Zhang, M. Structural basis for the phosphorylation-regulated interaction between the cytoplasmic tail of cell polarity protein crumbs and the actin-binding protein moesin. *The Journal of biological chemistry* **290**, 11384-11392 (2015).
100. Ling, C. *et al.* The apical transmembrane protein Crumbs functions as a tumor suppressor that regulates Hippo signaling by binding to Expanded. *Proceedings of the National Academy of Sciences of the United States of America* **107**, 10532-10537 (2010).
101. Robinson, B.S., Huang, J., Hong, Y. & Moberg, K.H. Crumbs regulates Salvador/Warts/Hippo signaling in Drosophila via the FERM-domain protein Expanded. *Current biology : CB* **20**, 582-590 (2010).
102. Herz, H.M. *et al.* vps25 mosaics display non-autonomous cell survival and overgrowth, and autonomous apoptosis. *Development* **133**, 1871-1880 (2006).
103. Zhu, Y. *et al.* Brahma regulates the Hippo pathway activity through forming complex with Yki-Sd and regulating the transcription of Crumbs. *Cellular signalling* **27**, 606-613 (2015).
104. Humbert, P.O. *et al.* Control of tumourigenesis by the Scribble/Dlg/Lgl polarity module. *Oncogene* **27**, 6888-6907 (2008).
105. Grzeschik, N.A., Amin, N., Secombe, J., Brumby, A.M. & Richardson, H.E. Abnormalities in cell proliferation and apico-basal cell polarity are separable in Drosophila lgl mutant clones in the developing eye. *Developmental biology* **311**, 106-123 (2007).
106. Parsons, L.M., Grzeschik, N.A., Allott, M.L. & Richardson, H.E. Lgl/aPKC and Crb regulate the Salvador/Warts/Hippo pathway. *Fly* **4**, 288-293 (2010).
107. Parsons, L.M., Grzeschik, N.A. & Richardson, H.E. lgl Regulates the Hippo Pathway Independently of Fat/Dachs, Kibra/Expanded/Merlin and dRASSF/dSTRIPAK. *Cancers* **6**, 879-896 (2014).
108. Das Thakur, M. *et al.* Ajuba LIM proteins are negative regulators of the Hippo signaling pathway. *Current biology : CB* **20**, 657-662 (2010).
109. Abe, Y., Ohsugi, M., Haraguchi, K., Fujimoto, J. & Yamamoto, T. LATS2-Ajuba complex regulates gamma-tubulin recruitment to centrosomes and spindle organization during mitosis. *FEBS letters* **580**, 782-788 (2006).
110. Rauskolb, C., Sun, S., Sun, G., Pan, Y. & Irvine, K.D. Cytoskeletal tension inhibits Hippo signaling through an Ajuba-Warts complex. *Cell* **158**, 143-156 (2014).
111. Sun, G. & Irvine, K.D. Ajuba family proteins link JNK to Hippo signaling. *Science signaling* **6**, ra81 (2013).
112. Mahoney, P.A. *et al.* The fat tumor suppressor gene in Drosophila encodes a novel member of the cadherin gene superfamily. *Cell* **67**, 853-868 (1991).
113. Cho, E. *et al.* Delineation of a Fat tumor suppressor pathway. *Nature genetics* **38**, 1142-1150 (2006).
114. Mao, Y. *et al.* Dachs: an unconventional myosin that functions downstream of Fat to regulate growth, affinity and gene expression in Drosophila. *Development* **133**, 2539-2551 (2006).
115. Strutt, H. & Strutt, D. Long-range coordination of planar polarity in Drosophila. *BioEssays : news and reviews in molecular, cellular and developmental biology* **27**, 1218-1227 (2005).
116. Hale, R., Brittle, A.L., Fisher, K.H., Monk, N.A. & Strutt, D. Cellular interpretation of the long-range gradient of Four-jointed activity in the Drosophila wing. *eLife* **4** (2015).
117. Willecke, M., Hamaratoglu, F., Sansores-Garcia, L., Tao, C. & Halder, G. Boundaries of Dachsous Cadherin activity modulate the Hippo signaling pathway to induce cell proliferation. *Proceedings of the National Academy of Sciences of the United States of America* **105**, 14897-14902 (2008).

118. Rauskolb, C., Pan, G., Reddy, B.V., Oh, H. & Irvine, K.D. Zyxin links fat signaling to the hippo pathway. *PLoS biology* **9**, e1000624 (2011).
119. Hirata, H., Tatsumi, H. & Sokabe, M. Zyxin emerges as a key player in the mechanotransduction at cell adhesive structures. *Communicative & integrative biology* **1**, 192-195 (2008).
120. Hirata, H., Tatsumi, H. & Sokabe, M. Mechanical forces facilitate actin polymerization at focal adhesions in a zyxin-dependent manner. *Journal of cell science* **121**, 2795-2804 (2008).
121. Emoto, K. *et al.* Control of dendritic branching and tiling by the Tricornered-kinase/Furry signaling pathway in Drosophila sensory neurons. *Cell* **119**, 245-256 (2004).
122. Geng, W., He, B., Wang, M. & Adler, P.N. The tricornered gene, which is required for the integrity of epidermal cell extensions, encodes the Drosophila nuclear DBF2-related kinase. *Genetics* **156**, 1817-1828 (2000).
123. Cornils, H., Kohler, R.S., Hergovich, A. & Hemmings, B.A. Human NDR kinases control G(1)/S cell cycle transition by directly regulating p21 stability. *Molecular and cellular biology* **31**, 1382-1395 (2011).
124. Zhang, L. *et al.* NDR functions as a physiological YAP1 kinase in the intestinal epithelium. *Current biology : CB* **25**, 296-305 (2015).
125. Lucas, E.P. *et al.* The Hippo pathway polarizes the actin cytoskeleton during collective migration of Drosophila border cells. *The Journal of cell biology* **201**, 875-885 (2013).
126. Vassilev, A., Kaneko, K.J., Shu, H., Zhao, Y. & DePamphilis, M.L. TEAD/TEF transcription factors utilize the activation domain of YAP65, a Src/Yes-associated protein localized in the cytoplasm. *Genes & development* **15**, 1229-1241 (2001).
127. Harvey, K. & Tapon, N. The Salvador-Warts-Hippo pathway - an emerging tumour-suppressor network. *Nature reviews. Cancer* **7**, 182-191 (2007).
128. Peng, H.W., Slattery, M. & Mann, R.S. Transcription factor choice in the Hippo signaling pathway: homothorax and yorkie regulation of the microRNA bantam in the progenitor domain of the Drosophila eye imaginal disc. *Genes & development* **23**, 2307-2319 (2009).
129. Nolo, R., Morrison, C.M., Tao, C., Zhang, X. & Halder, G. The bantam microRNA is a target of the hippo tumor-suppressor pathway. *Current biology : CB* **16**, 1895-1904 (2006).
130. Thompson, B.J. & Cohen, S.M. The Hippo pathway regulates the bantam microRNA to control cell proliferation and apoptosis in Drosophila. *Cell* **126**, 767-774 (2006).
131. Vogt, P.K. Oncogenes and the revolution in cancer research: homage to hidesaburo hanafusa (1929-2009). *Genes & cancer* **1**, 6-11 (2010).
132. Curtis, A.S. & Seehar, G.M. The control of cell division by tension or diffusion. *Nature* **274**, 52-53 (1978).
133. Huang, S. & Ingber, D.E. The structural and mechanical complexity of cell-growth control. *Nature cell biology* **1**, E131-138 (1999).
134. Schluck, T., Nienhaus, U., Aegerter-Wilmsen, T. & Aegerter, C.M. Mechanical control of organ size in the development of the Drosophila wing disc. *PloS one* **8**, e76171 (2013).
135. Feng, X. *et al.* Hippo-independent activation of YAP by the GNAQ uveal melanoma oncogene through a trio-regulated rho GTPase signaling circuitry. *Cancer cell* **25**, 831-845 (2014).
136. Dupont, S. *et al.* Role of YAP/TAZ in mechanotransduction. *Nature* **474**, 179-183 (2011).
137. Sansores-Garcia, L. *et al.* Modulating F-actin organization induces organ growth by affecting the Hippo pathway. *The EMBO journal* **30**, 2325-2335 (2011).
138. Fernandez, B.G. *et al.* Actin-Capping Protein and the Hippo pathway regulate F-actin and tissue growth in Drosophila. *Development* **138**, 2337-2346 (2011).
139. Aragona, M. *et al.* A mechanical checkpoint controls multicellular growth through YAP/TAZ regulation by actin-processing factors. *Cell* **154**, 1047-1059 (2013).
140. Smythe, E. & Ayscough, K.R. Actin regulation in endocytosis. *Journal of cell science* **119**, 4589-4598 (2006).
141. Yin, F. *et al.* Spatial organization of Hippo signaling at the plasma membrane mediated by the tumor suppressor Merlin/NF2. *Cell* **154**, 1342-1355 (2013).
142. Deng, H. *et al.* Spectrin regulates Hippo signaling by modulating cortical actomyosin activity. *eLife* **4** (2015).

143. Yoshigi, M., Hoffman, L.M., Jensen, C.C., Yost, H.J. & Beckerle, M.C. Mechanical force mobilizes zyxin from focal adhesions to actin filaments and regulates cytoskeletal reinforcement. *The Journal of cell biology* **171**, 209-215 (2005).
144. Colombelli, J. *et al.* Mechanosensing in actin stress fibers revealed by a close correlation between force and protein localization. *Journal of cell science* **122**, 1665-1679 (2009).
145. Cordenonsi, M. *et al.* The Hippo transducer TAZ confers cancer stem cell-related traits on breast cancer cells. *Cell* **147**, 759-772 (2011).
146. Basu, S., Totty, N.F., Irwin, M.S., Sudol, M. & Downward, J. Akt phosphorylates the Yes-associated protein, YAP, to induce interaction with 14-3-3 and attenuation of p73-mediated apoptosis. *Molecular cell* **11**, 11-23 (2003).
147. Moleirinho, S., Guerrant, W. & Kissil, J.L. The Angiomotins--from discovery to function. *FEBS letters* **588**, 2693-2703 (2014).
148. Chan, S.W. *et al.* Hippo pathway-independent restriction of TAZ and YAP by angiomotin. *The Journal of biological chemistry* **286**, 7018-7026 (2011).
149. Leung, C.Y. & Zernicka-Goetz, M. Angiomotin prevents pluripotent lineage differentiation in mouse embryos via Hippo pathway-dependent and -independent mechanisms. *Nature communications* **4**, 2251 (2013).
150. Zhao, B. *et al.* Angiomotin is a novel Hippo pathway component that inhibits YAP oncoprotein. *Genes & development* **25**, 51-63 (2011).
151. Dai, X. *et al.* Phosphorylation of angiomotin by Lats1/2 kinases inhibits F-actin binding, cell migration, and angiogenesis. *The Journal of biological chemistry* **288**, 34041-34051 (2013).
152. Miller, E. *et al.* Identification of serum-derived sphingosine-1-phosphate as a small molecule regulator of YAP. *Chemistry & biology* **19**, 955-962 (2012).
153. Yu, F.X. *et al.* Regulation of the Hippo-YAP pathway by G-protein-coupled receptor signaling. *Cell* **150**, 780-791 (2012).
154. Sorrentino, G. *et al.* Metabolic control of YAP and TAZ by the mevalonate pathway. *Nature cell biology* **16**, 357-366 (2014).
155. Gao, Y. *et al.* A hairpin within YAP mRNA 3'UTR functions in regulation at post-transcription level. *Biochemical and biophysical research communications* **459**, 306-312 (2015).
156. Porazinski, S. *et al.* YAP is essential for tissue tension to ensure vertebrate 3D body shape. *Nature* **521**, 217-221 (2015).
157. Mammoto, A., Mammoto, T. & Ingber, D.E. Mechanosensitive mechanisms in transcriptional regulation. *Journal of cell science* **125**, 3061-3073 (2012).
158. Ricca, B.L., Venugopalan, G. & Fletcher, D.A. To pull or be pulled: parsing the multiple modes of mechanotransduction. *Current opinion in cell biology* **25**, 558-564 (2013).
159. Engler, A.J., Sen, S., Sweeney, H.L. & Discher, D.E. Matrix elasticity directs stem cell lineage specification. *Cell* **126**, 677-689 (2006).
160. Renfranz, P.J., Blankman, E. & Beckerle, M.C. The cytoskeletal regulator zyxin is required for viability in Drosophila melanogaster. *Anatomical record* **293**, 1455-1469 (2010).
161. Morin-Kensicki, E.M. *et al.* Defects in yolk sac vasculogenesis, chorioallantoic fusion, and embryonic axis elongation in mice with targeted disruption of Yap65. *Molecular and cellular biology* **26**, 77-87 (2006).
162. Choi, H.J. *et al.* Yes-associated protein regulates endothelial cell contact-mediated expression of angiopoietin-2. *Nature communications* **6**, 6943 (2015).
163. Tian, Y. *et al.* A microRNA-Hippo pathway that promotes cardiomyocyte proliferation and cardiac regeneration in mice. *Science translational medicine* **7**, 279ra238 (2015).
164. Lei, Q.Y. *et al.* TAZ promotes cell proliferation and epithelial-mesenchymal transition and is inhibited by the hippo pathway. *Molecular and cellular biology* **28**, 2426-2436 (2008).
165. Makita, R. *et al.* Multiple renal cysts, urinary concentration defects, and pulmonary emphysematous changes in mice lacking TAZ. *American journal of physiology. Renal physiology* **294**, F542-553 (2008).
166. Nishioka, N. *et al.* The Hippo signaling pathway components Lats and Yap pattern Tead4 activity to distinguish mouse trophectoderm from inner cell mass. *Developmental cell* **16**, 398-410 (2009).

167. Lee, M.J., Ran Byun, M., Furutani-Seiki, M., Hong, J.H. & Jung, H.S. YAP and TAZ regulate skin wound healing. *The Journal of investigative dermatology* **134**, 518-525 (2014).
168. Varelas, X. *et al.* The Hippo pathway regulates Wnt/beta-catenin signaling. *Developmental cell* **18**, 579-591 (2010).
169. Barry, E.R. *et al.* Restriction of intestinal stem cell expansion and the regenerative response by YAP. *Nature* **493**, 106-110 (2013).
170. Sebe-Pedros, A., Zheng, Y., Ruiz-Trillo, I. & Pan, D. Premetazoan origin of the hippo signaling pathway. *Cell reports* **1**, 13-20 (2012).
171. Ameisen, J.C. On the origin, evolution, and nature of programmed cell death: a timeline of four billion years. *Cell death and differentiation* **9**, 367-393 (2002).
172. Cryns, V. & Yuan, J. Proteases to die for. *Genes & development* **12**, 1551-1570 (1998).
173. Guicciardi, M.E. & Gores, G.J. Apoptosis: a mechanism of acute and chronic liver injury. *Gut* **54**, 1024-1033 (2005).
174. Cao, L., Quan, X.B., Zeng, W.J., Yang, X.O. & Wang, M.J. Mechanism of Hepatocyte Apoptosis. *J Cell Death* **9**, 19-29 (2016).
175. Vegran, F., Boidot, R., Solary, E. & Lizard-Nacol, S. A short caspase-3 isoform inhibits chemotherapy-induced apoptosis by blocking apoptosome assembly. *PloS one* **6**, e29058 (2011).
176. Huang, Q. *et al.* Caspase 3-mediated stimulation of tumor cell repopulation during cancer radiotherapy. *Nature medicine* **17**, 860-866 (2011).
177. Donato, A.L. *et al.* Caspase 3 promotes surviving melanoma tumor cell growth after cytotoxic therapy. *The Journal of investigative dermatology* **134**, 1686-1692 (2014).
178. Fianco, G. *et al.* Caspase-8 contributes to angiogenesis and chemotherapy resistance in glioblastoma. *eLife* **6** (2017).
179. Li, S., Yang, Y., Ding, Y., Tang, X. & Sun, Z. Impacts of survivin and caspase-3 on apoptosis and angiogenesis in oral cancer. *Oncol Lett* **14**, 3774-3779 (2017).
180. Coleman, M.L. *et al.* Membrane blebbing during apoptosis results from caspase-mediated activation of ROCK I. *Nature cell biology* **3**, 339-345 (2001).
181. Edinger, A.L. & Thompson, C.B. Death by design: apoptosis, necrosis and autophagy. *Current opinion in cell biology* **16**, 663-669 (2004).
182. Zmasek, C.M. & Godzik, A. Evolution of the animal apoptosis network. *Cold Spring Harbor perspectives in biology* **5**, a008649 (2013).
183. Horvitz, H.R., Shaham, S. & Hengartner, M.O. The genetics of programmed cell death in the nematode Caenorhabditis elegans. *Cold Spring Harb Symp Quant Biol* **59**, 377-385 (1994).
184. Ellis, H.M. & Horvitz, H.R. Genetic control of programmed cell death in the nematode C. elegans. *Cell* **44**, 817-829 (1986).
185. Yuan, J.Y. & Horvitz, H.R. The Caenorhabditis elegans genes ced-3 and ced-4 act cell autonomously to cause programmed cell death. *Developmental biology* **138**, 33-41 (1990).
186. Xue, D., Shaham, S. & Horvitz, H.R. The Caenorhabditis elegans cell-death protein CED-3 is a cysteine protease with substrate specificities similar to those of the human CPP32 protease. *Genes & development* **10**, 1073-1083 (1996).
187. Yuan, J., Shaham, S., Ledoux, S., Ellis, H.M. & Horvitz, H.R. The C. elegans cell death gene ced-3 encodes a protein similar to mammalian interleukin-1 beta-converting enzyme. *Cell* **75**, 641-652 (1993).
188. Thornberry, N.A. *et al.* A novel heterodimeric cysteine protease is required for interleukin-1 beta processing in monocytes. *Nature* **356**, 768-774 (1992).
189. Cerretti, D.P. *et al.* Molecular cloning of the interleukin-1 beta converting enzyme. *Science* **256**, 97-100 (1992).
190. Thornberry, N.A. *et al.* A combinatorial approach defines specificities of members of the caspase family and granzyme B. Functional relationships established for key mediators of apoptosis. *The Journal of biological chemistry* **272**, 17907-17911 (1997).
191. Seaman, J.E. *et al.* Cacidases: caspases can cleave after aspartate, glutamate and phosphoserine residues. *Cell death and differentiation* **23**, 1717-1726 (2016).

192. Kerr, J.F., Wyllie, A.H. & Currie, A.R. Apoptosis: a basic biological phenomenon with wide-ranging implications in tissue kinetics. *Br J Cancer* **26**, 239-257 (1972).
193. Sulston, J.E. & Horvitz, H.R. Post-embryonic cell lineages of the nematode, Caenorhabditis elegans. *Developmental biology* **56**, 110-156 (1977).
194. Sulston, J.E., Schierenberg, E., White, J.G. & Thomson, J.N. The embryonic cell lineage of the nematode Caenorhabditis elegans. *Developmental biology* **100**, 64-119 (1983).
195. Ravichandran, K.S. & Lorenz, U. Engulfment of apoptotic cells: signals for a good meal. *Nat Rev Immunol* **7**, 964-974 (2007).
196. Fraser, A.G., McCarthy, N.J. & Evan, G.I. drICE is an essential caspase required for apoptotic activity in Drosophila cells. *The EMBO journal* **16**, 6192-6199 (1997).
197. Rao, L., Perez, D. & White, E. Lamin proteolysis facilitates nuclear events during apoptosis. *The Journal of cell biology* **135**, 1441-1455 (1996).
198. Walker, P.R., Kokileva, L., LeBlanc, J. & Sikorska, M. Detection of the initial stages of DNA fragmentation in apoptosis. *Biotechniques* **15**, 1032-1040 (1993).
199. Oberhammer, F. *et al.* Apoptotic death in epithelial cells: cleavage of DNA to 300 and/or 50 kb fragments prior to or in the absence of internucleosomal fragmentation. *The EMBO journal* **12**, 3679-3684 (1993).
200. Liu, X., Zou, H., Slaughter, C. & Wang, X. DFF, a heterodimeric protein that functions downstream of caspase-3 to trigger DNA fragmentation during apoptosis. *Cell* **89**, 175-184 (1997).
201. Sun, X.M. *et al.* Caspase activation inhibits proteasome function during apoptosis. *Molecular cell* **14**, 81-93 (2004).
202. Wang, X.H. *et al.* Caspase-3 cleaves specific 19 S proteasome subunits in skeletal muscle stimulating proteasome activity. *The Journal of biological chemistry* **285**, 21249-21257 (2010).
203. Adrain, C., Creagh, E.M., Cullen, S.P. & Martin, S.J. Caspase-dependent inactivation of proteasome function during programmed cell death in Drosophila and man. *The Journal of biological chemistry* **279**, 36923-36930 (2004).
204. Jang, M. *et al.* Caspase-7 mediated cleavage of proteasome subunits during apoptosis. *Biochemical and biophysical research communications* **363**, 388-394 (2007).
205. McIlwain, D.R., Berger, T. & Mak, T.W. Caspase functions in cell death and disease. *Cold Spring Harbor perspectives in biology* **5**, a008656 (2013).
206. Ryoo, H.D., Bergmann, A., Gonen, H., Ciechanover, A. & Steller, H. Regulation of Drosophila IAP1 degradation and apoptosis by reaper and ubcD1. *Nature cell biology* **4**, 432-438 (2002).
207. Yoo, S.J. *et al.* Hid, Rpr and Grim negatively regulate DIAP1 levels through distinct mechanisms. *Nature cell biology* **4**, 416-424 (2002).
208. Hays, R., Wickline, L. & Cagan, R. Morgue mediates apoptosis in the Drosophila melanogaster retina by promoting degradation of DIAP1. *Nature cell biology* **4**, 425-431 (2002).
209. Wing, J.P. *et al.* Drosophila Morgue is an F box/ubiquitin conjugase domain protein important for grim-reaper mediated apoptosis. *Nature cell biology* **4**, 451-456 (2002).
210. Lisi, S., Mazzon, I. & White, K. Diverse domains of THREAD/DIAP1 are required to inhibit apoptosis induced by REAPER and HID in Drosophila. *Genetics* **154**, 669-678 (2000).
211. Wilson, R. *et al.* The DIAP1 RING finger mediates ubiquitination of Dronc and is indispensable for regulating apoptosis. *Nature cell biology* **4**, 445-450 (2002).
212. Li, X., Wang, J. & Shi, Y. Structural mechanisms of DIAP1 auto-inhibition and DIAP1-mediated inhibition of drICE. *Nature communications* **2**, 408 (2011).
213. Boatright, K.M. *et al.* A unified model for apical caspase activation. *Molecular cell* **11**, 529-541 (2003).
214. Kischkel, F.C. *et al.* Cytotoxicity-dependent APO-1 (Fas/CD95)-associated proteins form a death-inducing signaling complex (DISC) with the receptor. *The EMBO journal* **14**, 5579-5588 (1995).
215. Arama, E., Agapite, J. & Steller, H. Caspase activity and a specific cytochrome C are required for sperm differentiation in Drosophila. *Developmental cell* **4**, 687-697 (2003).
216. Kennedy, N.J., Kataoka, T., Tschopp, J. & Budd, R.C. Caspase activation is required for T cell proliferation. *The Journal of experimental medicine* **190**, 1891-1896 (1999).

217. Mathieu, J., Sung, H.H., Pugieux, C., Soetaert, J. & Rorth, P. A sensitized PiggyBac-based screen for regulators of border cell migration in Drosophila. *Genetics* **176**, 1579-1590 (2007).
218. Kuranaga, E. *et al.* Drosophila IKK-related kinase regulates nonapoptotic function of caspases via degradation of IAPs. *Cell* **126**, 583-596 (2006).
219. Muro, I. *et al.* The Drosophila caspase Ice is important for many apoptotic cell deaths and for spermatid individualization, a nonapoptotic process. *Development* **133**, 3305-3315 (2006).
220. Steinhauer, J. Separating from the pack: Molecular mechanisms of Drosophila spermatid individualization. *Spermatogenesis* **5**, e1041345 (2015).
221. Zhou, X. *et al.* Auxilin is required for formation of Golgi-derived clathrin-coated vesicles during Drosophila spermatogenesis. *Development* **138**, 1111-1120 (2011).
222. Geisbrecht, E.R. & Montell, D.J. A role for Drosophila IAP1-mediated caspase inhibition in Rac-dependent cell migration. *Cell* **118**, 111-125 (2004).
223. Zhang, B., Zhang, Y. & Shacter, E. Caspase 3-mediated inactivation of rac GTPases promotes drug-induced apoptosis in human lymphoma cells. *Molecular and cellular biology* **23**, 5716-5725 (2003).
224. Oberoi, T.K. *et al.* IAPs regulate the plasticity of cell migration by directly targeting Rac1 for degradation. *The EMBO journal* **31**, 14-28 (2012).
225. Gorelick-Ashkenazi, A. *et al.* Caspases maintain tissue integrity by an apoptosis-independent inhibition of cell migration and invasion. *Nature communications* **9**, 2806 (2018).
226. Blanc, L., De Gassart, A., Geminard, C., Bette-Bobillo, P. & Vidal, M. Exosome release by reticulocytes--an integral part of the red blood cell differentiation system. *Blood Cells Mol Dis* **35**, 21-26 (2005).
227. Gnanapragasam, M.N. & Bieker, J.J. Orchestration of late events in erythropoiesis by KLF1/EKLF. *Curr Opin Hematol* **24**, 183-190 (2017).
228. Weil, M., Raff, M.C. & Braga, V.M. Caspase activation in the terminal differentiation of human epidermal keratinocytes. *Current biology : CB* **9**, 361-364 (1999).
229. Launay, S. *et al.* Vital functions for lethal caspases. *Oncogene* **24**, 5137-5148 (2005).
230. Tsapras, P. & Nezis, I.P. Caspase involvement in autophagy. *Cell death and differentiation* **24**, 1369-1379 (2017).
231. Meyer, E.L., Gahring, L.C. & Rogers, S.W. Nicotine preconditioning antagonizes activity-dependent caspase proteolysis of a glutamate receptor. *The Journal of biological chemistry* **277**, 10869-10875 (2002).
232. Kumar, S. & Doumanis, J. The fly caspases. *Cell death and differentiation* **7**, 1039-1044 (2000).
233. Gobe, G., Rubin, M., Williams, G., Sawczuk, I. & Buttyan, R. Apoptosis and expression of Bcl-2, Bcl-XL, and Bax in renal cell carcinomas. *Cancer Invest* **20**, 324-332 (2002).
234. Kroemer, G., Nicotera, P. & Melino, G. Cell Death and Disease: a new journal for a central area of pathophysiology. *Cell Death Dis* **1**, e11 (2010).
235. Barcia, C. *et al.* IFN-gamma signaling, with the synergistic contribution of TNF-alpha, mediates cell specific microglial and astroglial activation in experimental models of Parkinson's disease. *Cell Death Dis* **2**, e142 (2011).
236. Whelan, R.S., Kaplinskiy, V. & Kitsis, R.N. Cell death in the pathogenesis of heart disease: mechanisms and significance. *Annu Rev Physiol* **72**, 19-44 (2010).
237. Nagata, S. Autoimmune diseases caused by defects in clearing dead cells and nuclei expelled from erythroid precursors. *Immunol Rev* **220**, 237-250 (2007).
238. Madkaikar, M., Mhatre, S., Gupta, M. & Ghosh, K. Advances in autoimmune lymphoproliferative syndromes. *Eur J Haematol* **87**, 1-9 (2011).
239. Sassone, J. *et al.* Mutant Huntingtin induces activation of the Bcl-2/adenovirus E1B 19-kDa interacting protein (BNip3). *Cell Death Dis* **1**, e7 (2010).
240. Degli Esposti, D. *et al.* Ischemic preconditioning induces autophagy and limits necrosis in human recipients of fatty liver grafts, decreasing the incidence of rejection episodes. *Cell Death Dis* **2**, e111 (2011).

241. Machado, N.G., Alves, M.G., Carvalho, R.A. & Oliveira, P.J. Mitochondrial involvement in cardiac apoptosis during ischemia and reperfusion: can we close the box? *Cardiovasc Toxicol* **9**, 211-227 (2009).
242. Lopez-Neblina, F., Toledo, A.H. & Toledo-Pereyra, L.H. Molecular biology of apoptosis in ischemia and reperfusion. *J Invest Surg* **18**, 335-350 (2005).
243. Martins, I., Galluzzi, L. & Kroemer, G. Hormesis, cell death and aging. *Aging (Albany NY)* **3**, 821-828 (2011).
244. Florentin, A. & Arama, E. Caspase levels and execution efficiencies determine the apoptotic potential of the cell. *The Journal of cell biology* **196**, 513-527 (2012).
245. Galluzzi, L., Kepp, O., Trojel-Hansen, C. & Kroemer, G. Non-apoptotic functions of apoptosis-regulatory proteins. *EMBO reports* **13**, 322-330 (2012).
246. Hengartner, M.O. The biochemistry of apoptosis. *Nature* **407**, 770-776 (2000).
247. McSharry, S.S. & Beitel, G.J. The Caspase-3 homolog DrICE regulates endocytic trafficking during Drosophila tracheal morphogenesis. *Nature communications* **10**, 1031 (2019).
248. Zuo, L., Iordanou, E., Chandran, R.R. & Jiang, L. Novel mechanisms of tube-size regulation revealed by the Drosophila trachea. *Cell Tissue Res* **354**, 343-354 (2013).
249. Beitel, G.J. & Krasnow, M.A. Genetic control of epithelial tube size in the Drosophila tracheal system. *Development* **127**, 3271-3282 (2000).
250. Nelson, K.S., Furuse, M. & Beitel, G.J. The Drosophila Claudin Kune-kune is required for septate junction organization and tracheal tube size control. *Genetics* **185**, 831-839 (2010).
251. Laprise, P. [Identification of novel polarity proteins revealed the temporal regulation of the epithelial phenotype]. *Medecine sciences : M/S* **26**, 19-21 (2010).
252. Woods, D.F. & Bryant, P.J. The discs-large tumor suppressor gene of Drosophila encodes a guanylate kinase homolog localized at septate junctions. *Cell* **66**, 451-464 (1991).
253. de Vreede, G. *et al.* The Scribble module regulates retromer-dependent endocytic trafficking during epithelial polarization. *Development* **141**, 2796-2802 (2014).
254. Boucher, M.J., Laprise, P. & Rivard, N. Cyclic AMP-dependent protein kinase A negatively modulates adherens junction integrity and differentiation of intestinal epithelial cells. *Journal of cellular physiology* **202**, 178-190 (2005).
255. Tepass, U. & Knust, E. Phenotypic and developmental analysis of mutations at thecrumbs locus, a gene required for the development of epithelia inDrosophila melanogaster. *Roux Arch Dev Biol* **199**, 189-206 (1990).
256. Mravec, J. *et al.* Subcellular homeostasis of phytohormone auxin is mediated by the ER-localized PIN5 transporter. *Nature* **459**, 1136-1140 (2009).
257. Yu, F.X., Zhao, B. & Guan, K.L. Hippo Pathway in Organ Size Control, Tissue Homeostasis, and Cancer. *Cell* **163**, 811-828 (2015).
258. Salvesen, G.S. & Duckett, C.S. IAP proteins: blocking the road to death's door. *Nature reviews. Molecular cell biology* **3**, 401-410 (2002).
259. Verghese, S., Bedi, S. & Kango-Singh, M. Hippo signalling controls Dronc activity to regulate organ size in Drosophila. *Cell death and differentiation* **19**, 1664-1676 (2012).
260. Duclos, C., Lavoie, C. & Denault, J.B. Caspases rule the intracellular trafficking cartel. *FEBS J* **284**, 1394-1420 (2017).
261. Silva, E., Tsatskis, Y., Gardano, L., Tapon, N. & McNeill, H. The tumor-suppressor gene fat controls tissue growth upstream of expanded in the hippo signaling pathway. *Current biology : CB* **16**, 2081-2089 (2006).
262. Hay, B.A., Wassarman, D.A. & Rubin, G.M. Drosophila homologs of baculovirus inhibitor of apoptosis proteins function to block cell death. *Cell* **83**, 1253-1262 (1995).
263. Xu, D. *et al.* The effector caspases drICE and dcp-1 have partially overlapping functions in the apoptotic pathway in Drosophila. *Cell death and differentiation* **13**, 1697-1706 (2006).
264. Brand, A.H. & Perrimon, N. Targeted gene expression as a means of altering cell fates and generating dominant phenotypes. *Development* **118**, 401-415 (1993).
265. Shiga, Y., TanakaMatakatsu, M. & Hayashi, S. A nuclear GFP beta-galactosidase fusion protein as a marker for morphogenesis in living Drosophila. *Dev Growth Differ* **38**, 99-106 (1996).

266. Le, T. *et al.* A new family of Drosophila balancer chromosomes with a w- dfd-GMR yellow fluorescent protein marker. *Genetics* **174**, 2255-2257 (2006).
267. Tapon, N. *et al.* salvador Promotes both cell cycle exit and apoptosis in Drosophila and is mutated in human cancer cell lines. *Cell* **110**, 467-478 (2002).
268. Goyal, L., McCall, K., Agapite, J., Hartwieg, E. & Steller, H. Induction of apoptosis by Drosophila reaper, hid and grim through inhibition of IAP function. *The EMBO journal* **19**, 589-597 (2000).
269. Amcheslavsky, A. *et al.* Plasma Membrane Localization of Apoptotic Caspases for Non-apoptotic Functions. *Developmental cell* **45**, 450-464 e453 (2018).
270. Zachariou, A. *et al.* IAP-antagonists exhibit non-redundant modes of action through differential DIAP1 binding. *Embo Journal* **22**, 6642-6652 (2003).
271. Luo, M. *et al.* Nuclear entry of active caspase-3 is facilitated by its p3-recognition-based specific cleavage activity. *Cell research* **20**, 211-222 (2010).
272. Feng, Y. *et al.* Subcellular localization of caspase-3 activation correlates with changes in apoptotic morphology in MOLT-4 leukemia cells exposed to X-ray irradiation. *Int J Oncol* **27**, 699-704 (2005).
273. Kamada, S., Kikkawa, U., Tsujimoto, Y. & Hunter, T. Nuclear translocation of caspase-3 is dependent on its proteolytic activation and recognition of a substrate-like protein(s). *The Journal of biological chemistry* **280**, 857-860 (2005).
274. Schneider, M.R. *et al.* A key role for E-cadherin in intestinal homeostasis and Paneth cell maturation. *PloS one* **5**, e14325 (2010).
275. Shigemura, N. *et al.* Localization of activated caspase-3-positive and apoptotic cells in the developing tooth germ of the mouse lower first molar. *Histochem J* **33**, 253-258 (2001).
276. Iglesias-Guimarais, V. *et al.* Apoptotic DNA degradation into oligonucleosomal fragments, but not apoptotic nuclear morphology, relies on a cytosolic pool of DFF40/CAD endonuclease. *The Journal of biological chemistry* **287**, 7766-7779 (2012).
277. Martin, D.N. & Baehrecke, E.H. Caspases function in autophagic programmed cell death in Drosophila. *Development* **131**, 275-284 (2004).
278. Chen, X. *et al.* Regulation of CED-3 caspase localization and activation by C. elegans nuclear-membrane protein NPP-14. *Nature structural & molecular biology* **23**, 958-964 (2016).
279. Kang, Y., Neuman, S.D. & Bashirullah, A. Tango7 regulates cortical activity of caspases during reaper-triggered changes in tissue elasticity. *Nature communications* **8**, 603 (2017).
280. Tiklova, K., Senti, K.A., Wang, S., Graslund, A. & Samakovlis, C. Epithelial septate junction assembly relies on melanotransferrin iron binding and endocytosis in Drosophila. *Nature cell biology* **12**, 1071-1077 (2010).
281. Peglion, F., Llense, F. & Etienne-Manneville, S. Adherens junction treadmilling during collective migration. *Nature cell biology* **16**, 639-651 (2014).
282. Cox, C.M. *et al.* Endosomal regulation of contact inhibition through the AMOT:YAP pathway. *Molecular biology of the cell* **26**, 2673-2684 (2015).
283. Duclos, C.M. *et al.* Caspase-mediated proteolysis of the sorting nexin 2 disrupts retromer assembly and potentiates Met/hepatocyte growth factor receptor signaling. *Cell Death Discov* **3**, 16100 (2017).
284. Han, M.H. *et al.* The novel caspase-3 substrate Gap43 is involved in AMPA receptor endocytosis and long-term depression. *Molecular & cellular proteomics : MCP* **12**, 3719-3731 (2013).
285. Andrade, D. & Rosenblatt, J. Apoptotic regulation of epithelial cellular extrusion. *Apoptosis* **16**, 491-501 (2011).
286. Green, K.J., Getsios, S., Troyanovsky, S. & Godsel, L.M. Intercellular junction assembly, dynamics, and homeostasis. *Cold Spring Harbor perspectives in biology* **2**, a000125 (2010).
287. Zehendner, C.M., Librizzi, L., de Curtis, M., Kuhlmann, C.R. & Luhmann, H.J. Caspase-3 contributes to ZO-1 and Cl-5 tight-junction disruption in rapid anoxic neurovascular unit damage. *PloS one* **6**, e16760 (2011).
288. Zhou, M. *et al.* Caspase-3 regulates the migration, invasion and metastasis of colon cancer cells. *Int J Cancer* **143**, 921-930 (2018).
289. Gramates, L.S. *et al.* FlyBase at 25: looking to the future. *Nucleic acids research* **45**, D663-D671 (2017).

290. Pai, J.T., Brown, M.S. & Goldstein, J.L. Purification and cDNA cloning of a second apoptosis-related cysteine protease that cleaves and activates sterol regulatory element binding proteins. *Proceedings of the National Academy of Sciences of the United States of America* **93**, 5437-5442 (1996).
291. Wang, X. *et al.* Cleavage of sterol regulatory element binding proteins (SREBPs) by CPP32 during apoptosis. *The EMBO journal* **15**, 1012-1020 (1996).
292. Higgins, M.E. & Ioannou, Y.A. Apoptosis-induced release of mature sterol regulatory element-binding proteins activates sterol-responsive genes. *J Lipid Res* **42**, 1939-1946 (2001).
293. Brown, M.S. & Goldstein, J.L. A proteolytic pathway that controls the cholesterol content of membranes, cells, and blood. *Proceedings of the National Academy of Sciences of the United States of America* **96**, 11041-11048 (1999).
294. Wang, X., Sato, R., Brown, M.S., Hua, X. & Goldstein, J.L. SREBP-1, a membrane-bound transcription factor released by sterol-regulated proteolysis. *Cell* **77**, 53-62 (1994).
295. Horton, J.D. *et al.* Combined analysis of oligonucleotide microarray data from transgenic and knockout mice identifies direct SREBP target genes. *Proceedings of the National Academy of Sciences of the United States of America* **100**, 12027-12032 (2003).
296. Sun, L., Halaihel, N., Zhang, W., Rogers, T. & Levi, M. Role of sterol regulatory element-binding protein 1 in regulation of renal lipid metabolism and glomerulosclerosis in diabetes mellitus. *The Journal of biological chemistry* **277**, 18919-18927 (2002).
297. Ishigaki, N. *et al.* Involvement of glomerular SREBP-1c in diabetic nephropathy. *Biochemical and biophysical research communications* **364**, 502-508 (2007).
298. O'Donnell, M.P., Kasiske, B.L., Kim, Y., Schmitz, P.G. & Keane, W.F. Lovastatin retards the progression of established glomerular disease in obese Zucker rats. *American journal of kidney diseases : the official journal of the National Kidney Foundation* **22**, 83-89 (1993).
299. Sugiyama, H., Kashihara, N., Makino, H., Yamasaki, Y. & Ota, A. Apoptosis in glomerular sclerosis. *Kidney Int* **49**, 103-111 (1996).
300. Eberle, D., Hegarty, B., Bossard, P., Ferre, P. & Foufelle, F. SREBP transcription factors: master regulators of lipid homeostasis. *Biochimie* **86**, 839-848 (2004).
301. Shimabukuro, M., Zhou, Y.T., Levi, M. & Unger, R.H. Fatty acid-induced beta cell apoptosis: a link between obesity and diabetes. *Proceedings of the National Academy of Sciences of the United States of America* **95**, 2498-2502 (1998).
302. Karaskov, E. *et al.* Chronic palmitate but not oleate exposure induces endoplasmic reticulum stress, which may contribute to INS-1 pancreatic beta-cell apoptosis. *Endocrinology* **147**, 3398-3407 (2006).
303. Kong, J.Y. & Rabkin, S.W. Palmitate-induced apoptosis in cardiomyocytes is mediated through alterations in mitochondria: prevention by cyclosporin A. *Biochimica et biophysica acta* **1485**, 45-55 (2000).
304. Chai, W. & Liu, Z. p38 mitogen-activated protein kinase mediates palmitate-induced apoptosis but not inhibitor of nuclear factor-kappaB degradation in human coronary artery endothelial cells. *Endocrinology* **148**, 1622-1628 (2007).
305. Hazegh, K.E. & Reis, T. A Buoyancy-based Method of Determining Fat Levels in Drosophila. *Journal of visualized experiments : JoVE* (2016).
306. Pearce, E.L. & Pearce, E.J. Metabolic pathways in immune cell activation and quiescence. *Immunity* **38**, 633-643 (2013).
307. McCarthy, S.A., Mufson, R.A., Pearce, E.J., Rathmell, J.C. & Howcroft, T.K. Metabolic reprogramming of the immune response in the tumor microenvironment. *Cancer biology & therapy* **14**, 315-318 (2013).
308. O'Neill, L.A., Kishton, R.J. & Rathmell, J. A guide to immunometabolism for immunologists. *Nat Rev Immunol* **16**, 553-565 (2016).
309. Daniels, V.W. *et al.* Cancer cells differentially activate and thrive on de novo lipid synthesis pathways in a low-lipid environment. *PloS one* **9**, e106913 (2014).
310. Munir, R. *et al.* Atypical plasma lipid profile in cancer patients: cause or consequence? *Biochimie* **102**, 9-18 (2014).

311. Kumar, S., van Raam, B.J., Salvesen, G.S. & Cieplak, P. Caspase cleavage sites in the human proteome: CaspDB, a database of predicted substrates. *PloS one* **9**, e110539 (2014).
312. Zalila, H. *et al.* Processing of metacaspase into a cytoplasmic catalytic domain mediating cell death in Leishmania major. *Molecular microbiology* **79**, 222-239 (2011).
313. Bell, R.A.V. & Megeney, L.A. Evolution of caspase-mediated cell death and differentiation: twins separated at birth. *Cell death and differentiation* **24**, 1359-1368 (2017).
314. Gov, N.S., McSharry, S.S. & Beitel, G.J. Three-ring circus without a ringmaster: Self-organization of supracellular actin ring patterns during epithelial morphogenesis. *Proceedings of the National Academy of Sciences of the United States of America* **112**, 8521-8522 (2015).
315. Turing, A.M. The Chemical Basis of Morphogenesis. *Philos T Roy Soc B* **237**, 37-72 (1952).
316. Brouzes, E. & Farge, E. Interplay of mechanical deformation and patterned gene expression in developing embryos. *Curr Opin Genet Dev* **14**, 367-374 (2004).
317. Ingber, D.E. Mechanical control of tissue morphogenesis during embryological development. *Int J Dev Biol* **50**, 255-266 (2006).
318. Driquez, B., Bouclet, A. & Farge, E. Mechanotransduction in mechanically coupled pulsating cells: transition to collective constriction and mesoderm invagination simulation. *Phys Biol* **8**, 066007 (2011).
319. Guillot, C. & Lecuit, T. Mechanics of epithelial tissue homeostasis and morphogenesis. *Science* **340**, 1185-1189 (2013).
320. Heisenberg, C.P. & Bellaiche, Y. Forces in tissue morphogenesis and patterning. *Cell* **153**, 948-962 (2013).
321. Hannezo, E., Dong, B., Recho, P., Joanny, J.F. & Hayashi, S. Cortical instability drives periodic supracellular actin pattern formation in epithelial tubes. *Proceedings of the National Academy of Sciences of the United States of America* **112**, 8620-8625 (2015).
322. Salbreux, G., Charras, G. & Paluch, E. Actin cortex mechanics and cellular morphogenesis. *Trends in cell biology* **22**, 536-545 (2012).
323. Dong, B. & Hayashi, S. Shaping of biological tubes by mechanical interaction of cell and extracellular matrix. *Curr Opin Genet Dev* **32**, 129-134 (2015).
324. Swanson, L.E. & Beitel, G.J. Tubulogenesis: an inside job. *Current biology : CB* **16**, R51-53 (2006).
325. Yonemura, S., Wada, Y., Watanabe, T., Nagafuchi, A. & Shibata, M. alpha-Catenin as a tension transducer that induces adherens junction development. *Nature cell biology* **12**, 533-542 (2010).
326. Friedrich, B.M., Buxboim, A., Discher, D.E. & Safran, S.A. Striated acto-myosin fibers can reorganize and register in response to elastic interactions with the matrix. *Biophys J* **100**, 2706-2715 (2011).
327. Shlomovitz, R. & Gov, N.S. Membrane-mediated interactions drive the condensation and coalescence of FtsZ rings. *Phys Biol* **6**, 046017 (2009).
328. Priess, J.R. & Hirsh, D.I. Caenorhabditis elegans morphogenesis: the role of the cytoskeleton in elongation of the embryo. *Developmental biology* **117**, 156-173 (1986).
329. Costa, M., Draper, B.W. & Priess, J.R. The role of actin filaments in patterning the Caenorhabditis elegans cuticle. *Developmental biology* **184**, 373-384 (1997).
330. Xu, X. & Vogel, B.E. A secreted protein promotes cleavage furrow maturation during cytokinesis. *Current biology : CB* **21**, 114-119 (2011).
331. Xu, K., Zhong, G. & Zhuang, X. Actin, spectrin, and associated proteins form a periodic cytoskeletal structure in axons. *Science* **339**, 452-456 (2013).
332. Liegeois, S., Benedetto, A., Michaux, G., Belliard, G. & Labouesse, M. Genes required for osmoregulation and apical secretion in Caenorhabditis elegans. *Genetics* **175**, 709-724 (2007).
333. Shindo, M. *et al.* Dual function of Src in the maintenance of adherens junctions during tracheal epithelial morphogenesis. *Development* **135**, 1355-1364 (2008).
334. Yamada, S., Pokutta, S., Drees, F., Weis, W.I. & Nelson, W.J. Deconstructing the cadherin-catenin-actin complex. *Cell* **123**, 889-901 (2005).
335. Maiden, S.L. & Hardin, J. The secret life of alpha-catenin: moonlighting in morphogenesis. *The Journal of cell biology* **195**, 543-552 (2011).

336. Shaye, D.D., Casanova, J. & Llimargas, M. Modulation of intracellular trafficking regulates cell intercalation in the Drosophila trachea. *Nature cell biology* **10**, 964-970 (2008).
337. Rapsomaniki, M.A. *et al.* easyFRAP: an interactive, easy-to-use tool for qualitative and quantitative analysis of FRAP data. *Bioinformatics* **28**, 1800-1801 (2012).
338. Francis, D. & Ghabrial, A.S. Compensatory branching morphogenesis of stalk cells in the Drosophila trachea. *Development* **142**, 2048-2057 (2015).
339. Forster, D. & Luschnig, S. Src42A-dependent polarized cell shape changes mediate epithelial tube elongation in Drosophila. *Nature cell biology* **14**, 526-534 (2012).

APPENDIX 1: A three-ring circus without a ringmaster: Self-organization of supra-cellular actin ring patterns during epithelial morphogenesis[314]

Nir Gov[1*], Saoirse S. McSharry[2], Greg J. Beitel[2*]
[1] Department of Chemical Physics, Weizmann Institute of Science, 76100 Rehovot, Israel
[2] Department of Molecular Biosciences and Robert H. Lurie Comprehensive Cancer Center, Northwestern University, Evanston, Illinois 60208, USA.

Formation of patterns during development has been long-standing puzzle. Alan Turing proposed chemical gradients as a solution to the problem [315], and many chemical signals that pattern cells have since been found. However, only recently have roles for mechanical forces in patterning become apparent [316-320]. In this issue, Hannezo *et al* [321] present and test a biophysical model involving three key elements – actin, myosin-II and anisotropic "effective friction" arising from interactions with the extracellular matrix (ECM) – that recapitulates the formation of the periodic subcellular actin bundles that coherently span several cells to form rings in the developing *Drosophila* tracheal (airway) tubes (Fig. 1A). Strikingly, although the mechanism of ring formation was previously unknown, their model predicts that formation of the bundles, as well as their periodicity and orientation, are predicted to arise within each cell through self-organization. Experimental tests of predictions of the model show that it correctly describes multiple unexpected behaviors of the system *in vivo*, including imperfections in the actin rings (Fig. 1B,C) and the formation of only a single actin ring per cell when the ECM is eliminated. This work provides a mechanistic basis for understanding formation of patterned actin ring structures in *Drosophila* and other species, and highlights the potential of the ECM to influence actin organization through mechanical rather than biochemical signaling interactions.

To a large extent, the actin cytoskeleton determines a cell's mechanical properties, and greatly influences its shape, mobility, and intracellular signaling[322]. The actin network at the cell's plasma membrane (referred to as cortical actin) is especially dynamic, as actin nucleators that promote actin polymerization are often recruited to and activated at the plasma membrane. Consequently, cortical actin polymerization drives formation of many sub-cellular structures, the most visible of which are cellular protrusions. Simultaneously, myosin-II molecular motors attach to actin filaments and induce contractile forces and motions that play

crucial roles in cellular polarization, morphogenesis, and cell division. The model reported in Hannezo *et al.* uses the same building blocks of actin polymerization and myosin-II contractility, but also includes interactions with an external substrate, which in this case is a chitin-based ECM that transiently fills the lumen of the trachea during development ([323], reviewed in[324]). Remarkably, a strictly mechanical interaction between the ECM and cortical actin flow, represented as friction in the model, can control the periodicity, orientation and dynamics of the actin patterns, without invoking the biochemical signaling typically induced by cell-matrix interactions.

While the ability of Hannezo's model to reproduce central aspects of the actin bundles in individual tracheal cells is impressive, an even bigger accomplishment of the model is its ability to account for the supra–cellular nature of the actin structures. As seen in Fig. 1B and C, actin bundles appear to seamlessly cross cell-cell junctions, keeping perfect registration despite intervening pairs of cell membranes and adherens junctions. Indeed, in the absence of junctional markers, the location of cell-cell boundaries cannot be discerned (Fig. 1C). Although one might expect such coordination to require molecular feedback loops or specialized junctional complexes, to date no mutations have been described that specifically disrupt continuity of the supra-cellular tracheal rings. Consistent with the lack of an specific "ringmaster", Hannezo *et al.* find that even very small coupling interactions, such as those that would be produced by known ability of some cell-cell junctions to mature in response to stresses[325], are capable of producing correlated patterns. Thus, the model predicates that not only that individual cells can produce periodic linear actin structures using "off the shelf" components found in most epithelial cells, but that groups of cells can spontaneously coordinate their actin patterns using standard junctional components. However, further work is required to test models of coordination, as it remains conceivable that elastic interactions across the ECM core of the tube can give rise to long-range registry [326], as well as interactions involving the curvature of the rings[327].

What is the function of actin rings in tracheal tubes and how do tracheal actin rings correspond to rings observed in other species? During tracheal development, the actin rings template formation of cuticular

ECM ridges that, like the ridges of a vacuum cleaner hose, are thought to serve as circumferential buttresses to prevent tube collapse. In other organisms and tissues, actin rings serve a wide variety of purposes. In *C. elegans*, actin rings form at the epidermal surface just prior to molting, presumably to resist the outward tugor pressure of the worm body that would otherwise be unopposed upon cuticle is shedding[328, 329]. The mechanism by which these actin rings arise has not been determined, but the parallels with the *Drosophila* trachea strongly suggest a common underlying mechanism. Perhaps the best-known example of actin ring formation is that of the single actin ring that forms at the cleavage furrow of all dividing eukaryotic cells. Intriguingly, during division of some cell types, including the *C. elegans* germline and preimplantation mouse embryos, successful cell division requires the ECM protein Hemicentin[330] . The precise role of hemicentins in furrow maturation is unclear, but the results of Hannezo *et al*. suggest that mechanical as well as biochemical signaling from hemicentins to the actomyosin contractile ring could be important. Notably, not all actin rings may utilize the actin-mysoin-EMC assembly model. For example, in the case of the actin rings that were recently identified within mammalian axons, ring formation and periodicity maybe controlled by inter-ring complexes containing the cytoskeletal protein Spectrin [331]. Regardless of whether actin rings form by one or more mechanisms, the work by Hannezo *et al.* makes a critical contribution by proposing the first mechanism by which periodic actin rings form and by creating a detailed biophysical framework for understanding the process.

With the model in hand, what remains to be done in understanding the biology of the actin rings? Further validation of the model in *Drosophila* and other species will be critical. A deeper probing into underlying patterning issues is also needed. In particular, Hannezo *et al.* show that anisotropy in the ECM can orient the actin rings, but how is the anisotropy of the chitin-based matrix created and oriented? And what mechanisms allow chitin fibrils to span many cells and form a supra-cellular structure oriented orthogonally to the actin rings? Another frontier will be to understand how the actin rings pattern the ECM. The tracheal actin rings have been predicted to control secretion of the cuticle, and while there is some evidence for actin rings controlling secretion in *C. elegans*[332], the nature of these mechanisms in trachea remains to be determined. Considerable research will be needed to answer these and other questions, but the work of

Hannezo *et al.* illuminate a new role of mechanical interactions in forming cytoskeletal patterns that span entire tissues.

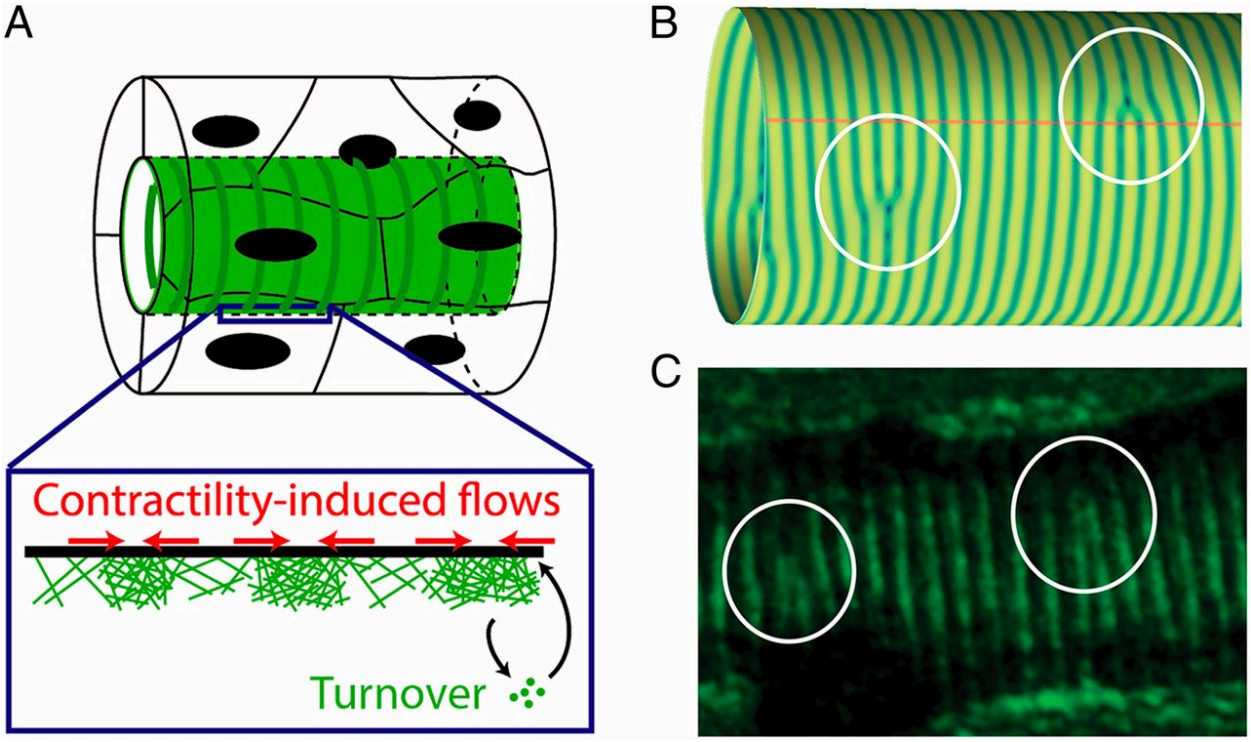

Figure A1.1. A biophysical model of actin, myosin and ECM interactions recapitulates the formation of supra-cellular actin rings in the *Drosophila* tracheal system. (A) Top. The epithelial cells of the Drosophila tracheal system form a tube approximately four cells in diameter. During embryogenesis, the tracheal lumen is filled with a chitin-based extracellular matrix (ECM, lighter green). Cortical actin bundles at the cells' apical surfaces (darker green) form supra-cellular rings that continuously encircle the lumen. Insert. The model predicts that actin rings self-assemble within each cell as a consequence of actin polymerization, myosin-II contractility and anisotropic "effective friction" from interactions with the extracellular matrix. Notably, the influence of the ECM is proposed to be strictly mechanical and does not involve biochemical signaling. Intercellular coupling that aligns actin bundles across cell boundaries requires only small coupling constants that could be achieved by mechanically induced junctional

maturation. (B) An example of actin ring patterns predicted by the biophysical model. Importantly, the model predicts defects in the patterns (white circles) that are remarkably similar to those observed *in vivo* (panel C). (C) Confocal image of actin staining in the tracheal system. Note that actin bundles maintain near perfect registry across cell-cell boundaries (not shown). White circles highlight defects the ring pattern.

APPENDIX 2: Assaying differential junctional remodeling using FRAP

I. Abstract

Several mechanical models now exist to help explain the preferentially axial orientation of tracheal elongation. One such model is that of differential adherens junction dynamics, wherein growing tracheal cells preferentially expand axially due to the increased turnover of axially oriented adherens junctions compared to circumferential ones. In this section, we sought to test the model of differential junctional remodeling using fluorescence recovery after photobleaching (FRAP). We performed preliminary tests of this model to examine whether the rate of axial and circumferential junction turnover varies during tube elongation. The preliminary data presented here do not support this model, as there is not a significant difference in the rate at which axial and circumferential junctions are remodeled.

II. Introduction

One approach to understanding the molecular mechanisms that underlie epithelial tube size control is to adopt a holistic approach by examining the physical mechanics of growth. In this section, we probed whether differential junction stability contributes to the directionality in which tracheal cells elongate. Previous evidence has shown that overall tracheal elongation can be perturbed by the failure of tracheal cells to achieve the correct shape or volume, but an interesting observation is that in Src42A loss of function mutants, the trachea is too short, and there are defects in anisotropic cell growth—tracheal cells grow in the wrong direction.[47] This observation led to the generation of a model for tube growth in which junctions that are oriented in the axial and circumferential directions have different rates and degrees of remodeling. This model predicts that tracheal cells elongate along the axis of the most rapidly remodeled adherens junctions; in a wild type cell, for example, the junctions that run along the axis of the tube remodel faster, and/or to a greater extent than the more stable and less dynamic circumferential junctions, resulting in cells being oriented axially. This model could explain how Src42A, which is known to promote the endocytic

recycling of E-cadherin, could preferentially (a) promote the remodeling of circumferential junctions, or (b) prevent the remodeling of axial junctions, resulting in more dynamic circumferential junctions, and consequently, the observed anisotropic growth defect. We sought to test this model by quantifying the rates of junctional turnover using FRAP.

III. Results and discussion

In these experiments, I used FRAP to assay the rate of axial and circumferential junctional remodeling using a btl>Dα-catenin::GFP at embryonic stage 16. The rates of fluorescence recovery at axial,

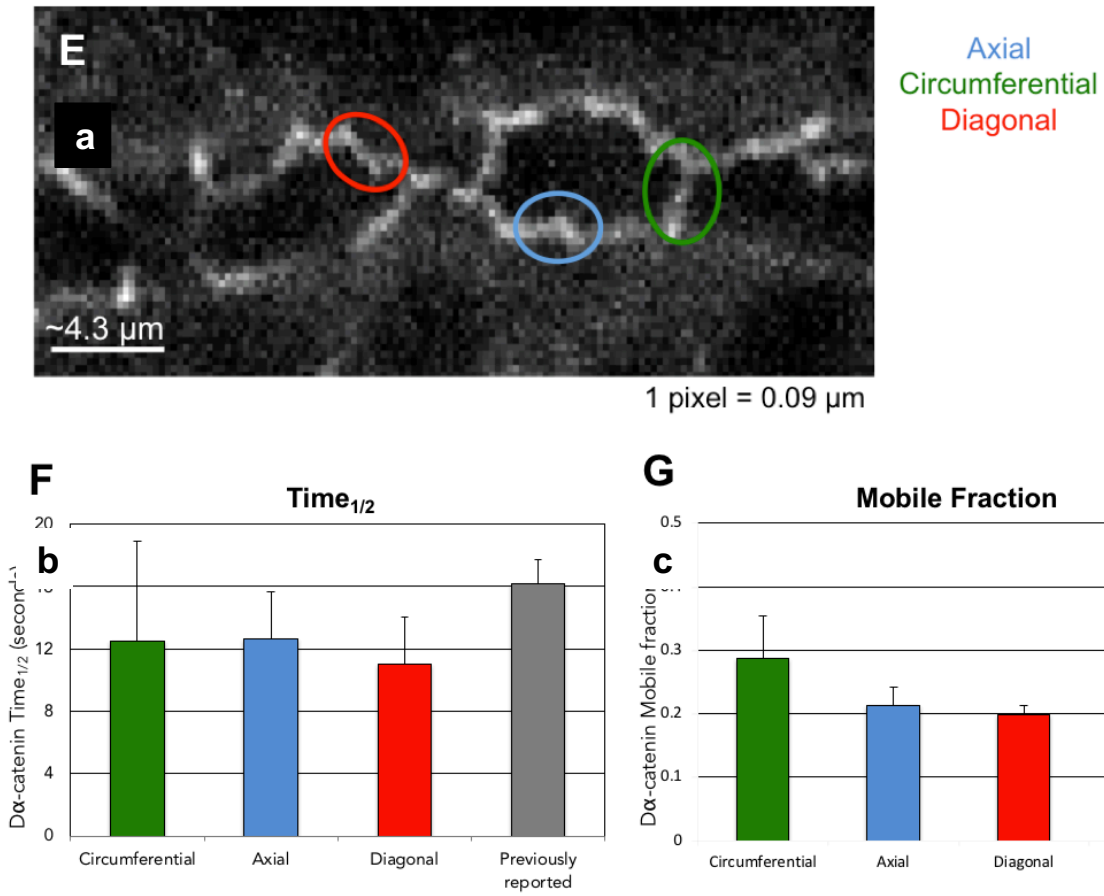

Figure A2.1 The rates of adherens junction remodeling do not vary significantly based on junction orientation at embryonic stage 16. (a) An example image of the FRAP experiment showing α-catenin GFP expression at junctions oriented axially (blue oval), circumferential (green oval), and diagonal (red oval). (b) The amount of time in which half of the fluorescence recovery took place, and (b) the amount of fluorescent a-catenin that is mobile for each junctional orientation are not statistically significantly different from one-another, but they are comparable to previously reported data.

circumferential, and diagonal adherens junctions were similar to the previously reported data on tracheal junction remodeling rates, but there were no significant differences based on junction orientation.[333]

These experiments approached a problem that had not previously been addressed—the model of differential adherens junction dynamics. Future experiments to test this model would benefit from several potential improvements. The main consideration would be repeat these tests at an earlier developmental timepoint, when the trachea undergoes its most significant elongation; by stage 16, *Src42A*$^{26\text{-}1}$ mutant tracheal cells were observed to already have adapted the wrong orientation, meaning it is potentially less likely to display an observable difference in junctional stability.

In addition, tracheal-specific overexpression of Dα-catenin (btl>Dα-catenin::GFP) had previously been used to quantify overall adherens junction (AJ) dynamics in the developing trachea, but Dα-catenin resides in the cytoplasmic side of the junction, and the exact role of Dα-catenin in the AJ remains relatively elusive. Instead, it may be beneficial to perform this experiment by tagging endogenous DE-cadherin with a stronger fluorescent marker. One endogenous potential marker is GFP-tagged DE-cadherin; unfortunately, in our experience, its expression isn't strong enough for tracheal FRAP.[334, 335]

Another possible approach would be to use simultaneous live imaging of DE-cadherin and endosomal activity to detect if there's a greater concentration of DE-cadherin endocytosis circumferentially or axially. [336] This experiment may prove challenging, however, because it would involve the simultaneous live imaging of recycling endocytic vesicles alongside DE-cadherin.

In FRAP data supporting the model of differential adherens junction dynamics, we expect to observe increased AJ dynamics (that is, lower $Time_{1/2}$ and higher Mobile Fraction) as tracheal cells elongate axially earlier in development. My preliminary data studying btl>α-catenin::GFP, however, suggests that there is a minimal difference in junctional dynamics between those oriented axially and circumferentially. Future

experiments at earlier timepoints, however, mI will observe a more uniform rate of junctional dynamics across all developmental times.

IV. Methods

FRAP

In order to test the model of differential adherens junction stability, Fluorescence Recovery After Photobleaching (FRAP) was performed using an Olympus multiphoton FVMPE-RS confocal microscope to examine live embryos at stage 16 of embryonic development. The UAS-Gal4 system was used to specifically drive expression of a fusion protein Dα-catenin::GFP in the embryonic trachea. This transgenic approach was used because previous experiments using overexpression of the transmembrane adhesive protein DE-cadherin caused tracheal defects, and because tagging the endogenous DE-cadherin produced faint levels of fluorescence, which precluded the successful execution of FRAP.[333]

The morning of imaging, staged embryos were collected and dechorionated as in previous chapters. Embryos were then mounted in oxygen-permeable halocarbon oil, and covered with a coverslip. Bleaching was carried out with the 405 nm laser at a power that is capable of bleaching without causing damage. Images will be acquired at approximately 350X200 pixels. Three regions of interest (ROIs) were selected and their intensity recorded throughout the experiment: (1) a bleached junction of interest (2) an unbleached adjacent junction, and (3) an unbleached background area. 10 pre-bleach images preceded a single bleach step, followed by 10 images separated by 2 seconds each, and finally a number of images taken at 10- or 20-second intervals.

Data analysis

Data was exported in .xls format, and the resulting Excel spreadsheet of pixel intensity of each ROI over time was imported into a MATLAB extension called easyFRAP for analysis and generation of normalized

graphs, which will output the intensity of a given junction over time while accounting for intensity of both (a) an adjacent unbleached junction and (b) a background region. [337]

APPENDIX 3: Endogenous DrICE::FLAG is a loss-of-function allele

I. Introduction

In Chapter 2, we show that DrICE has a non-apoptotic function in regulating intracellular trafficking during embryonic tracheal morphogenesis. In that study, we utilized two antibodies to assay the subcellular localization of DrICE; having an endogenously tagged DrICE, however, would be an invaluable tool for future studies. For example, it would be a key reagent to address subcellular localization via live imaging and binding partners via immunoprecipitation. There are no published studies with endogenously-tagged DrICE, so we set out to generate a C-terminally tagged version of DrICE.

We used CRISRP to generate two endogenously tagged alleles of DrICE—DrICE::GFP and DrICE::3XFLAG. The GFP-tagged protein would be especially useful for live-imaging studies, but we anticipated that the 27kDa GFP might interfere with DrICE's normal binding partners and functions since DrICE is a relatively small protein (the ~40kDa zymogen is cleaved into 20 and 10kDa subunits). We therefore also generated a 3XFLAG tagged-DrICE, in which the tag totals only 3kDa, much smaller than GFP and hopefully less likely to interfere with endogenous functions of DrICE.

Interestingly, neither tagged version of DrICE behaved as we expected. Here, we show that the GFP is cleaved from the C-terminus of DrICE, and that *3XFLAG::DrICE* behaves as a loss-of-function allele.

II. Results and discussion

DrICE::GFP is processed to remove GFP

We performed a Western Blot to verify whether the C-terminal GFP tagged allele of DrICE interferes with its normal function, as we had initially anticipated. The heterozygous state produced the predicted series of bands corresponding to the expected cleavage pattern of DrICE. (Figure A3.1) Because DrICE is required for its own cleavage, we hypothesized that if the GFP tag interferes with DrICE function, the only

band would correspond to the zymogen form at 64kDa when DrICE::GFP is homozygous. We were surprised to find, however, that—while there is only one band— that band corresponds to the GFP alone, suggesting that it is cleaved off the fusion protein. The difference between the observed cleavage pattern of DrICE::GFP in a heterozygous vs homozygous state suggests that endogenous untagged DrICE is required for the normal processing of its GFP-tagged counterpart. Curiously, when DrICE::GFP is present in the homozygous state the GFP is invariably cleaved from the caspase. Together, these observations suggest two important consequences: (1) DrICE can be processed at its C-terminus, which is a previously unobserved finding, and (2) the activity of DrICE::GFP is not the same as the untagged protein.

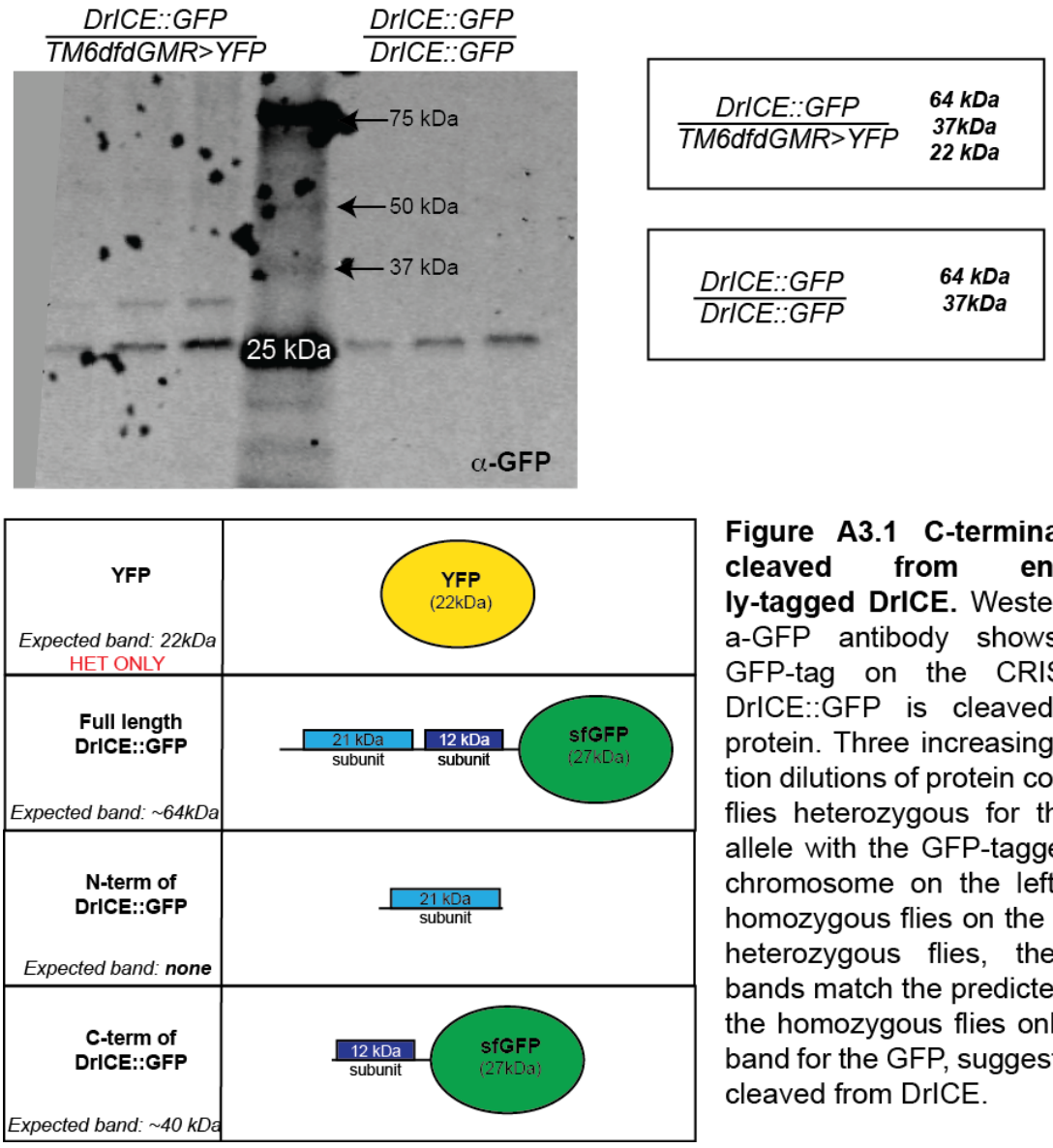

Figure A3.1 C-terminal GFP is cleaved from endogenously-tagged DrICE. Western blot with a-GFP antibody shows that the GFP-tag on the CRISPR allele DrICE::GFP is cleaved from the protein. Three increasing concentration dilutions of protein collected from flies heterozygous for the CRISPR allele with the GFP-tagged balancer chromosome on the left, and from homozygous flies on the right. In the heterozygous flies, the observed bands match the predicted sizes, but the homozygous flies only contain a band for the GFP, suggesting that it is cleaved from DrICE.

3XFLAG::DrICE phenocopies other *DrICE* loss-of-function alleles

We next wished to characterize the phenotype of the *3XFLAG::DrICE* CRISPR allele. It was first obvious that flies homozygous for *3XFLAG::DrICE* were typically not viable—emerging homozygous adults were rarely observed (data not shown). The rare escapers, however, had noticeable phenotypes that were similar to those previously observed in the $DrICE^{\Delta 1}$ deletion allele. (Figure A3.2)

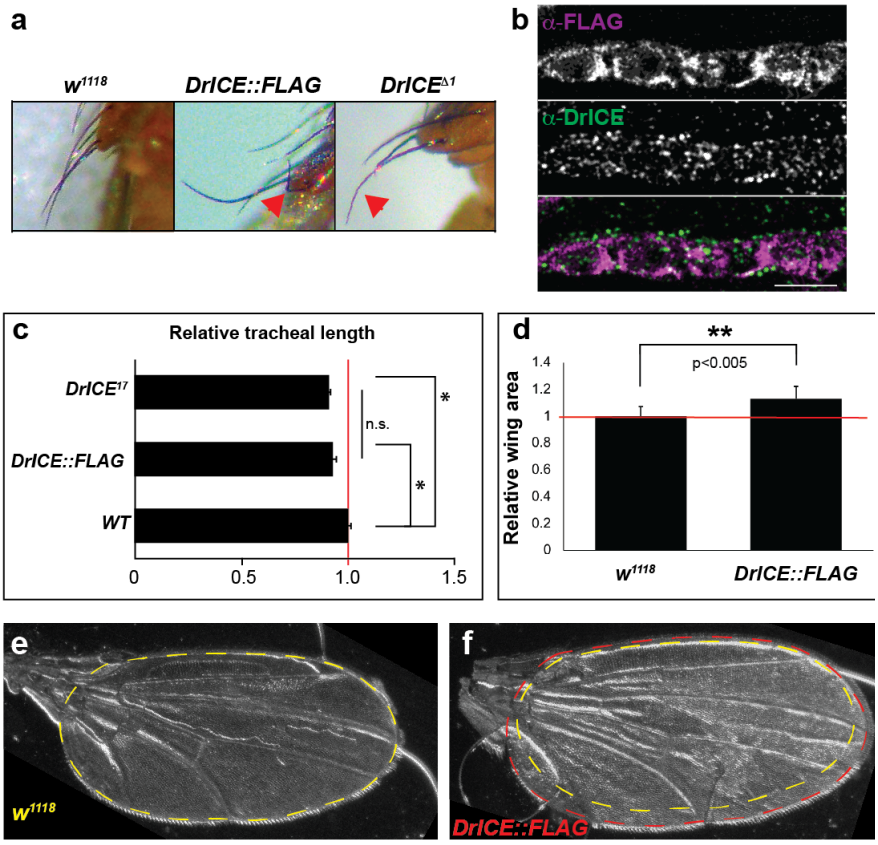

Figure A3.2
Endogenous FLAG-tagged DrICE is a loss-of-function allele (a) *3XFLAG::DrICE* flies have a kinked bristle defect that has been previously been observed in the $DrICE^{\Delta 1}$ allele. **(b)** Immunofluorescence for FLAG shows that *3XFLAG::DrICE* trachea of stage 16 embryos have a more homogenous cytosolic pattern of localization that is more reminiscent of uncleaved DrICE staining (SK31); there is no significant colocalization of DrICE CST9478 with FLAG, suggesting that the FLAG-tagged DrICE may not be fully cleaved and activated. **(c)** Trachea of *3XFLAG::DrICE* embryos are short, as they are in $DrICE^{17}$. **(d-f)** Wing size is greater in *3XFLAG::DrICE* homozygous animals.

For example, *3XFLAG::DrICE* have kinked bristles, which is also present in $DrICE^{\Delta 1}$, and it is associated with an actin-nucleation defect. (Figure A3.2a) The wings also had an overgrowth phenotype, which had previously been attributed to lack of apoptosis in $DrICE^{\Delta 1}$. (Figure A3.2d-f) Finally, the elongation of the trachea of *3XFLAG::DrICE* embryos was also defective to the same extent as the dominant negative $DrICE^{17}$. (Figure A3.2c) FLAG localization in the trachea is more similar to the ubiquitous cytosolic SK31

signal than to signal associated with cleaved DrICE (compare Figure A3.2b to Figure 2.5g), supporting our hypothesis that 3XFLAG::DrICE remains uncleaved.

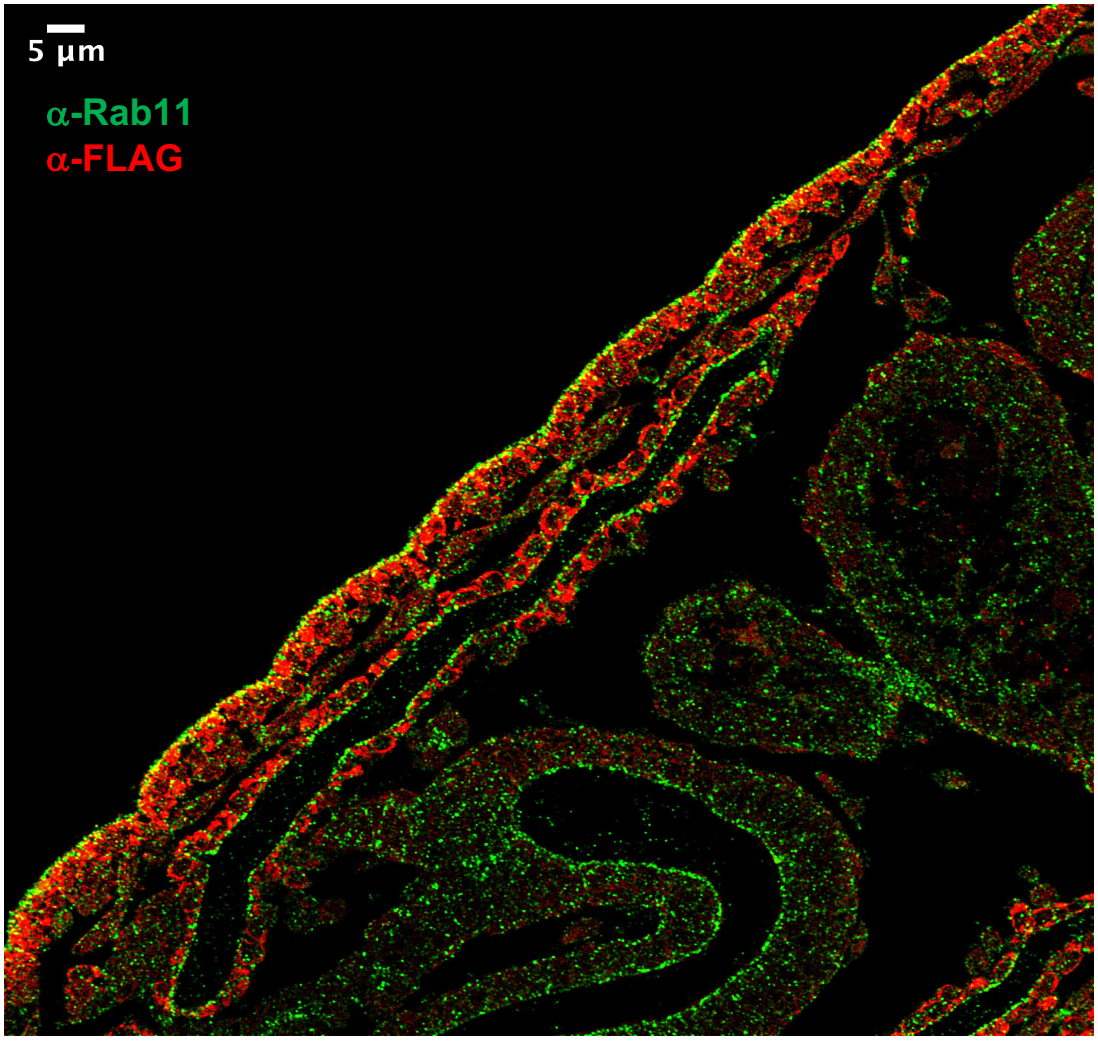

Figure A3.3 FLAG abundance varies in a tissue-specific manner. Homozygous stage 16 3XFLAG::DrICE embryo stained for Rab11 and FLAG shows varied abundance in the trachea / epidermis and the hindgut and midgut.

One interesting observation gained from this investigation, however, is that there appears to be a tissue-specific difference between expression or processing of 3XFLAG::DrICE, as seen in Figure A3.3. The trachea and the epidermis have a much higher abundance of 3XFLAG::DrICE than the hindgut; this could mean that the fusion protein is degraded or otherwise processed to remove the FLAG tag to a greater

extent, or that its transcription is altered, in the hindgut. It is unclear whether this is the case with endogenous non-tagged DrICE, but if so, could explain the differences between tracheal output of DrICE between these tissues. (See Appendix 4)

Concluding remarks

Although an endogenously-tagged allele of DrICE could be immensely helpful for additional experimental approaches that would allow us to use methods like live-imaging to ask more detailed questions about its mechanism of involvement in various processes. We now suspect that the reason there are no currently published studies that utilize an endogenously-tagged version of DrICE or its mammalian homolog Caspase-3 due to the complexity of how adding tags to such a small protein can interfere with its processing and/or activation.

APPENDIX 4: DrICE affects trafficking in non-tracheal epithelia

I. Abstract

We recently showed that DrICE, the *Drosophila* homolog of the executioner Caspase-3, regulates endocytic trafficking during tracheal morphogenesis.[247] Caspase involvement in this vital developmental process is one example of a growing number of examples of non-apoptotic caspase function. Here, we expand upon our previous findings in the trachea to demonstrate that DrICE regulates the trafficking of additional apical signaling molecules pSrc and aPKC, and that its effect on trafficking is not restricted to the trachea. DrICE also regulates the abundance and localization of a number of molecules in other developing epithelial tissues, the epidermis and the hindgut, but not always in the same manner as in the trachea. Together our data suggest that DrICE regulates trafficking in a molecule- and tissue-specific manner.

II. Introduction

Non-apoptotic caspase function is a growing field of knowledge with significant implications for our understanding of cell death and potential related human therapeutics ranging from cancer to immune diseases. In Chapter 2, we described how the majority of known cases of non-apoptotic caspase function, there are morphological changes that are common to cell death; for example, in the terminal differentiation of human keratinocytes, the nucleus is lost in a Caspase-3 dependent fashion. However, we recently demonstrated that during the development of the Drosophila tracheal system, the Caspase-3 homolog, DrICE, is required for a cellular process that isn't immediately associated with apoptosis: altering intracellular trafficking. Indeed, one reason that our previous work was significant is precisely because the involvement of DrICE in altering intracellular trafficking during morphogenesis suggests that there may be some function of trafficking alterations in apoptosis; we hypothesized that the extrusion of a dying cell from an epithelium is one such apoptotic example wherein increased junctional trafficking could be useful.

One remaining question is whether this function of DrICE acts in a tissue-specific manner. The developing trachea is a very dynamic tissue where cellular trafficking plays a critical role in the cell-cell communication as well as intercellular signaling that are necessary for the determination of length. We therefore sought to determine whether DrICE also plays a role in trafficking in other epithelial tissues.

III. Results

DrICE colocalizes with Clathrin in non-tracheal epithelia

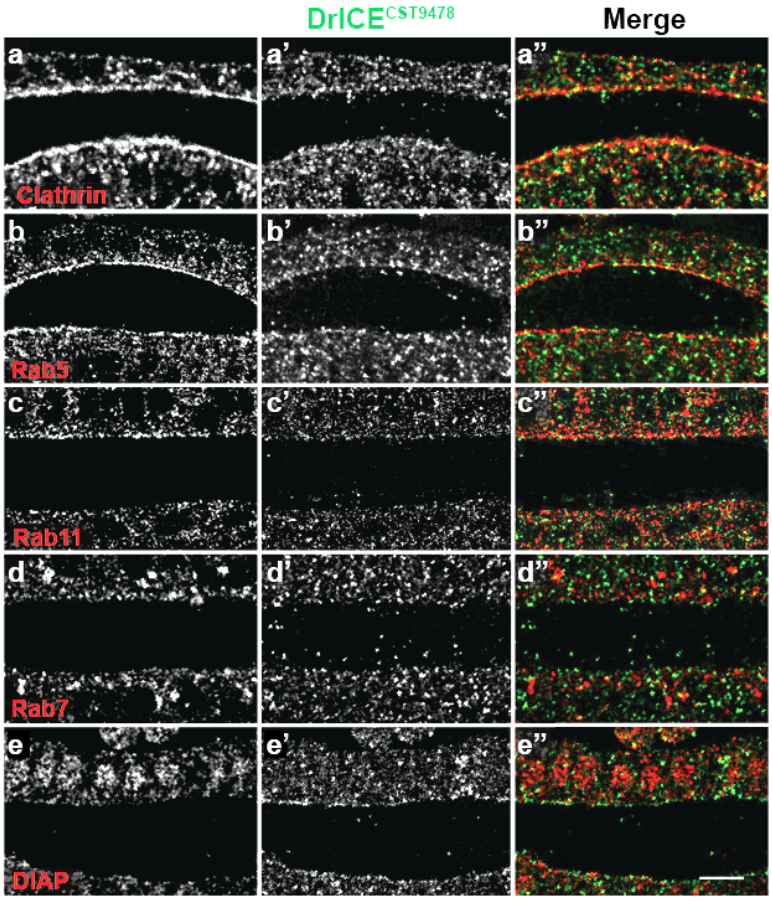

Figure A4.1: DrICE colocalizes with Clathrin in the hindgut,. (a-d") At stage 16, the extent of colocalization of α-DrICE^{CST9478} with endocytic pathway components Clathrin (endocytic vesicles a-a"), Rab5 (early endosome, b-b"), Rab7 (late endosome d-d"), and Rab11 (recycling endosome, c-c") in the hindgut resembles that in the trachea. **(e-e")** DIAP1 localizes predominantly to the nucleus, while α -DrICE^{CST9478} staining in present in both the cytosol and nucleus. Notably, α-DrICE^{CST9478} and DIAP staining rarely co-localize. Scale bar for a-e" in e", 5 μm

Is the endocytic function of DrICE a specialized function that only operates in the trachea? Immunostaining for α-DrICE^{CST9478} reveals a similar punctate pattern and overlap with Clathrin and other Rabs in the hindgut, as in the trachea (Figure A4.1 and Figure 2.6). In our previous findings, we determined that DrICE affects the trafficking of signaling molecules in various intra- and extracellular locations including the apical signaling molecule Crumbs and the septate junction component Kune-kune. We next wished to determine whether there was a

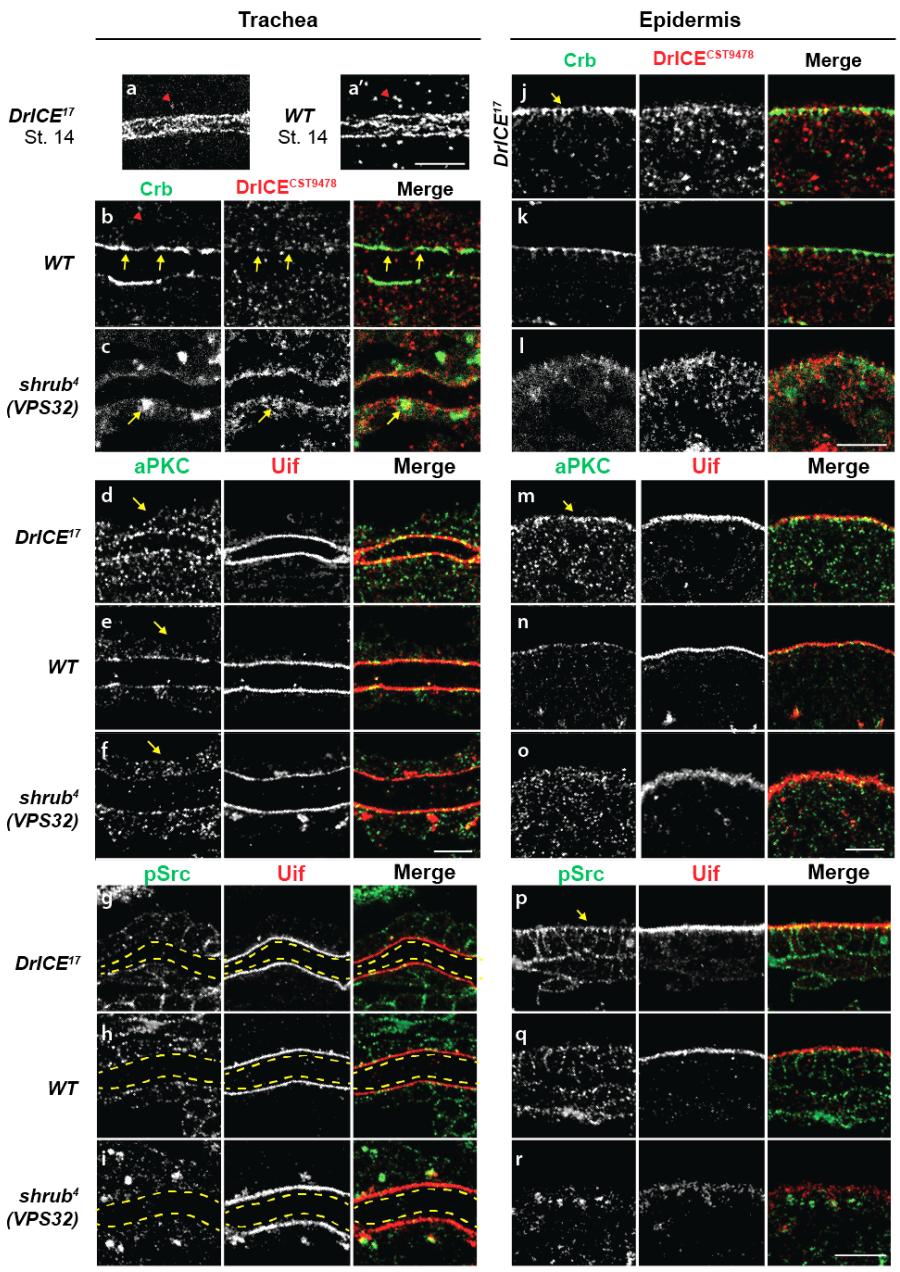

Figure A4.2: DrICE is required for abundance and localization of the size determinants Crb, pSrc and aPKC in both trachea and epidermis (a-i") The number of cytosolic Crb punctae is decreased in *DrICE*^{17} mutants at stage 14 (a', arrowheads) compared to WT (a, and Supplemental Fig. 2A). At stage 16, □-DrICE^{CST9478} signal partially overlaps with Crb at the apical surface in WT trachea (b, arrows), and Crb colocalizes with DrICE in aberrant cytosolic structures in *VPS32/shrub*^{4} trachea (c, arrows). In *DrICE*^{17} mutants, aPKC levels are increased (d), while pSrc levels are decreased, particularly at the apical surface (g, yellow lines). Uif staining marks the apical surface. **(j-r")** *DrICE*^{17} affects the levels and/or localization of Crb, aPKC and pSrc in the epidermis. Crb, aPKC, and pSrc levels are increased in *DrICE*^{17} epidermis, particularly at the apical surface (j,m,p, arrows). Crb, aPKC and pSrc levels and/or localization are also strongly affected by in the endocytic mutant *VPS32/shrub*^{4} (l,o,r).

functional consequence of DrICE affecting trafficking of other signaling molecules in both the trachea and

the hindgut.

Trafficking of aPKC and pSrc are affected by DrICE in the trachea and the epidermis

In order to determine whether DrICE is required for the intracellular trafficking and/or levels of apically localized, non-transmembrane size determinants in addition to Crumbs, we examined the effects of *DrICE*^{17} on the localization and levels of aPKC and phosphorylated Src (pSrc)[47, 338, 339] The number and intensity of

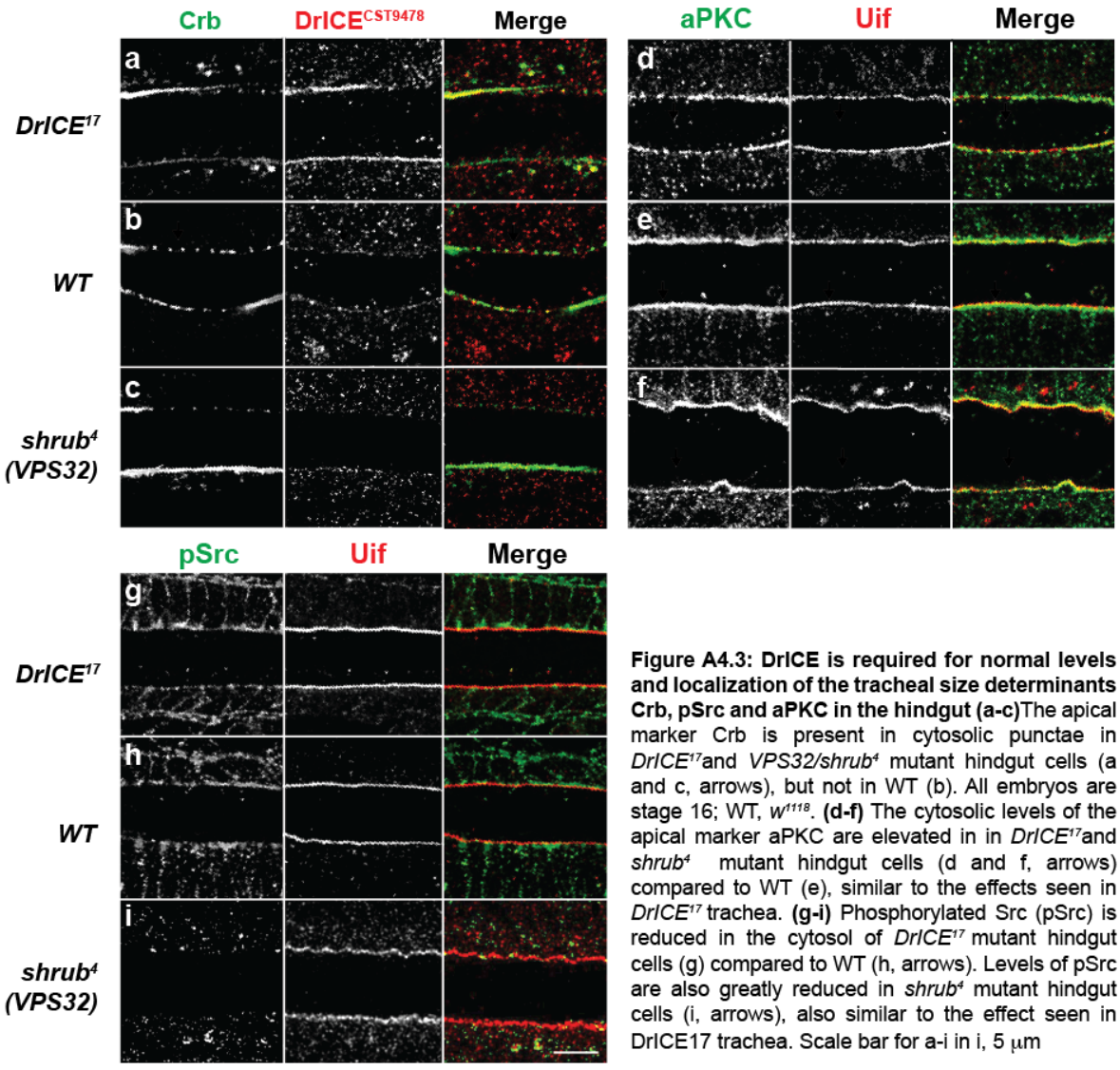

Figure A4.3: DrICE is required for normal levels and localization of the tracheal size determinants Crb, pSrc and aPKC in the hindgut (a-c) The apical marker Crb is present in cytosolic punctae in *DrICE*^{17}and *VPS32/shrub*^{4} mutant hindgut cells (a and c, arrows), but not in WT (b). All embryos are stage 16; WT, *w*^{1118}. **(d-f)** The cytosolic levels of the apical marker aPKC are elevated in in *DrICE*^{17}and *shrub*^{4} mutant hindgut cells (d and f, arrows) compared to WT (e), similar to the effects seen in *DrICE*^{17} trachea. **(g-i)** Phosphorylated Src (pSrc) is reduced in the cytosol of *DrICE*^{17} mutant hindgut cells (g) compared to WT (h, arrows). Levels of pSrc are also greatly reduced in *shrub*^{4} mutant hindgut cells (i, arrows), also similar to the effect seen in DrICE17 trachea. Scale bar for a-i in i, 5 μm

aPKC punctae are dramatically increased in *DrICE*^{17} tracheal cells, similar to the increases seen in *VPS32/shrub*^{4} mutant cells, a mutation which affects trafficking by interfering with the inward budding of the mutivesicular body (arrows, Figure A4.2d-f). pSrc is reduced at the apical membrane in both *DrICE*^{17} and *shrb*^{4} mutant trachea (Figure A4.2g-i). Interestingly, these effects were not limited to the trachea, but were also present in the epidermis (Figure A4.2j-r) and in the hindgut. (Figure A4.3) Together, these results demonstrate that DrICE is required for normal endocytic trafficking of diverse apical membrane size determinants.

Effects of DrICE on trafficking varies by molecule and by tissue

Altogether, we have observed that in both the epidermis and the hindgut, *DrICE*^{17} alters trafficking of apical, lumenal and junctional proteins, including Crb, aPKC, pSrc, Kune, MTf, and Dlg, but this effect was not always in the same as in the trachea. For instance, while abundance of Kune-kune decrease in *DrICE*^{17} and increase *yki*^{B5} trachea (Figure 2.7d-f), they do not appear to be as dramatically affected in the hindgut (Figure A4.4g-i). Importantly, however, some of the significant effects of DrICE on trafficking are maintained—for example, the excess of apical Serp in *yrt*^{65A} mutant trachea (Figure 2.8a-i) is also present in hindgut and epidermis and critically, can also be suppressed by *DrICE*^{17} (Figure A4.4a-f'). DrICE is therefore required for the correct trafficking of apical, secreted, and junctional proteins in multiple developing epithelial tissues.

IV. Discussion

This section highlights additional characterization of the role of DrICE in intracellular trafficking in other epithelial tissues. In Chapter 2, we described the role of DrICE in regulating the trafficking of several important tracheal size determinants including Crumbs, Kune-kune, and Serpentine. Here, we have

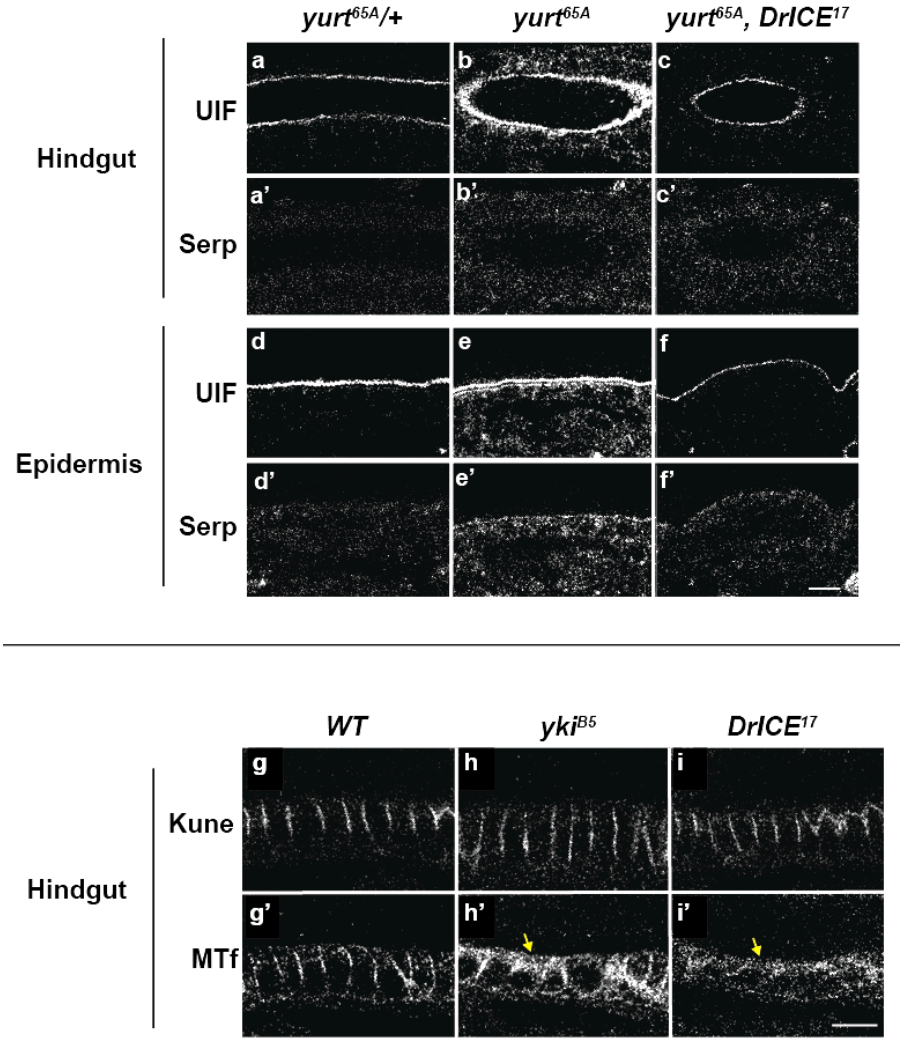

Figure A4.4: As in the trachea, DrICE affects trafficking in non-tracheal epithelia, but not always in the same manner (a-f') In the hindgut (a-c') and in the epidermis (d-f'), a mutation in the basolateral polarity gene *yrt* increases levels of the apical size determinant UIF and the lumenal size determinant Serp (b, b', e and e'). In both tissues, this increase is suppressed by a *DrICE*^{17} mutation (c, c', f and f'). Scale bar for a-f' in f', 5 μm. **(g-i')** In the hindgut, trafficking of the SJ component Kune is largely unaffected in *DrICE*^{17} and *yki*^{B5} mutants (g-i). However, trafficking of MTf in the hindgut is affected (g'-i') with MTf accumulating in *yki*^{B5} mutants (h', arrow) and showing little junctional localization in *DrICE*^{17} (i', arrow). Scale bar for g-i' in i', 5 μm.

expanded upon those findings to show that DrICE also can affect trafficking of these components in the epidermis as well as the hindgut. We also show two additional examples of signaling molecules that are also regulated by DrICE: aPKC and pSrc. Together, these results are significant because they demonstrate that DrICE affects trafficking of at least seven determinants of tissue size, and importantly that its impact on the trafficking of these molecules can vary based on the molecule and based on the tissue.

The findings represented here are significant because they lend some insight into the mechanism of DrICE function. In Chapter 2, we propose that DrICE affects the trafficking of certain molecules through its association with the *Drosophila* Clathrin adaptor protein AP-47. Association of DrICE with AP-47 through its evolutionarily conserved dileucine motif could explain its varied impacts on different molecules and tissues. For example, while the claudin Kune-kune is necessary for the proper elongation and barrier function of the drosophila trachea, its role has not been previously described in hindgut morphogenesis.[250] It is possible, then, that the differential effect of DrICE on Kune-kune abundance in the trachea compared to the hindgut could be due to comparatively differential rate of Clathrin-mediated endocytosis of Kune-kune.

Altogether, the results presented in this section support the hypothesis that DrICE regulates trafficking of various molecules differently in each tissue due to its interactions with AP-47, which can facilitate the sorting of various cargo early in Clathrin-mediated endocytosis. We hypothesize that the sorting protein AP-47 facilitates the recruitment of DrICE to the site of Clathrin-mediated endocytosis. One substantial question that remains, however, is: what is the mechanism by which DrICE influences sorting with AP-47? Although this question remains unanswered, future investigations that focus on uncovering that mechanism may reap the greatest benefits from a proteomic screen in order to determine the substrates of DrICE (see Chapter 4).

V. Methods

See methods section in Chapter 2.

CURRICULUM VITAE

Education

Ph.D. *Molecular Biosciences.* Northwestern University. **June 2019**

B.A. *Biological Sciences*. The University of Chicago. **Dec. 2010**

Publications

S. McSharry and G.J. Beitel. The Caspase-3 homolog DrICE regulates endocytic trafficking during *Drosophila* tracheal morphogenesis. *Nature Communications* **10**, 1031. **March 2019**

N.S. Gov, **S. McSharry**, G.J. Beitel. Three-ring circus without a ringmaster: Self-organization of supracellular actin ring patterns during epithelial morphogenesis. *Proceedings of the National Academy of Science of the United States of America.* **112,** 8251 **July 2015**

A. Osbourne, Calway T, Broman M, **McSharry S.,** Earley J, Kim GJ. Downregulation of Connexin43 by microRNA-130a in cardiomyocytes results in cardiac arrhythmias. *Journal of molecular and cellular cardiology.* **74,** 53 **Sept. 2014**

Research Experience

Graduate research assistant. **April 2014- June 2019**

Lab of Greg J. Beitel, Northwestern University.

- Independent research project studying the roles of key molecular determinants of epithelial tube size in *Drosophila*

Research technician. **Dec. 2012- Aug. 2013**

Lab of Gene H. Kim, The University of Chicago

- Generation and initial characterization of murine transgenic and inducible models of microRNA-130a overexpression
- Maintenance of all mouse colonies

Research technician **Jan. 2009- Dec. 2012**

Lab of Eric C. Svensson, The University of Chicago

- Experimental support to graduate students and post-docs in studying the roles of Ets-1, FOG-2, and MTA-1 in murine heart development.

Conference attendance & presentations during PhD

S. McSharry and Beitel GJ. Regulation of endocytic trafficking by the executioner caspase DrICE in *Drosophila* tracheal morphogenesis — **August 2018**
Gordon Research Conference: Cell Death. Newry, ME

S. McSharry and Beitel GJ. Non-apoptotic caspase activity is required for endosomal trafficking and tracheal elongation — **April 2018**
Genetics Society of America Drosophila Research Conference. Philadelphia, PA

S. McSharry, Beitel GJ. Non-apoptotic function of the caspase DrICE regulates *Drosophila* tracheal size downstream of Hippo Signaling. — **April 2017**
Genetics Society of America Drosophila Research Conference. San Diego, CA

S. McSharry and M. Paulsen. RSG Science Communication Training & Outreach Programs. *American Society of Biochemistry and Molecular Biology Research Conference. Chicago, IL* — **April 2017**

ComSciCon science communication conference, *Chicago IL* — **August 2017**

Awards & Grants

- **Cellular and Molecular Basis of Disease Training Grant** — **June 2015- June 2017**
- **Neil Welker IBiS Teaching Assistant Excellence Award** — **Sept. 2015**

Teaching Experience

Instructor — **April - June 2018**
Northwestern University
BIOL_SCI 164: Genetics & Evolution
- Undergraduate general education course for non-majors
- Designed all curriculum and all course materials. *Course evaluations available upon request*.

New TA Conference Peer Leader — **June - Sept. 2018**
Searle Center for Advancing Learning and Teaching
- Developed and led training sessions for participants designing discipline-specific and cross-disciplinary workshops for Northwestern's New TA Conference.

RSG Graduate Assistant **May - Sept. 2018**

Northwestern University

- Consulted on revising RSG training program course materials and implementation
- Attended weekly professional development meetings, journal clubs, and act as teaching assistant for The Graduate School's research communication course, RSG

Private Tutor

- Four hours/ week one-on-one sessions with a Northwestern undergraduate student enrolled in Human Genetics course **Jan. - April 2018**

AP Biology Tutor **Oct. 2016- May 2017**

- Weekly one-on-one sessions with a high school junior preparing for the AP Biology exam

Teaching Assistant **March - June 2016**

Northwestern University

BIOL_SCI 222: Investigative Laboratory

- Undergraduate laboratory course optional for biology majors
- Third quarter of a three-quarter lab sequence
- Only instructor in the room at most times; classroom management, grading, generating assessments, holding office hours, etc

Teaching Assistant **Sept. - Dec. 2014**

Northwestern University

BIOL 220: Genetics and Molecular Processes Laboratory

- Undergraduate laboratory course required for biology majors; first of a three-quarter lab sequence
- Only instructor in the room at most times; classroom management, grading, generating assessments, holding office hours, etc.

<u>Professional Development at Northwestern University</u>

Teaching Consultant **Sept. 2015 - June 2019**

Searle Center for Advancing Learning and Teaching

- At instructors' request, facilitate focus groups with undergraduates regarding their learning experiences in a specific course.
- Report feedback to the instructor, enabling them to make improvements to teaching

Teaching-As-Research Project 2018 **June 2018**

Familiar media sources increase biology self-efficacy scores in non-major students

- In conjunction with BIOL164 course
  With guidance from CIRTL at Searle Center for Advancing Learning and Teaching at Northwestern University

Teaching Certificate Program **Sept. 2017- June 2018**

Searle Center for Advancing Teaching and Learning

- Year-long sequence of seminars, workshops and peer and faculty mentorship focused on improving student learning
- Analyze and reflect on disciplinary commitment to teaching through in-depth discussions of intercultural pedagogy, assessment methods, evaluation techniques, etc.

Teaching-As-Research Project 2016 **March - June 2016**

Classroom Assessment Techniques (CATs) may improve undergraduate students' confidence in choosing experimental methods in a lab course

- In conjunction with BIOL222 course
- With guidance from CIRTL at Searle Center for Advancing Learning and Teaching at Northwestern University

New TA Conference Workshop Leader **June 2016 & 2015**

Searle Center for Advancing Learning and Teaching

- Design and lead a total of two discipline-specific workshops and one cross-disciplinary workshop to prepare new TAs at Northwestern's New TA Conference in 2015 and again in 2016

RSG Leadership Team **June - Sept. 2016**

- Provide student perspective for restructuring and act as a teaching assistant for The Graduate School's RSG research communication course

Professional Development Chair **Jan. 2016-June 2017**

IBiS Student Organization

- Design and implement professional development activities for graduate students, including "IBiS Career Day" as well as recruitment of off-campus seminar speakers

Standardized Test Scores

- **GRE** **Oct. 2011**
  Verbal: 164 (94th percentile) | Quantitative: 156 (74th percentile) | Analytical Writing: 4.5 (72nd percentile)